

# **New Synthetic Applications of Galactose Oxidase and *Candida* *Antarctica* Lipase B**

A thesis submitted to the University of Manchester  
for the degree of Doctor of Philosophy  
in the Faculty of Engineering and Physical Sciences

**2011**

**Bo Yuan**

**School of Chemistry**

## Table of Contents

<b>Table Index .....</b>	<b>5</b>
<b>Abbreviations .....</b>	<b>6</b>
<b>Abstract .....</b>	<b>9</b>
<b>Declaration .....</b>	<b>10</b>
<b>Copyright Statement .....</b>	<b>11</b>
<b>Preface .....</b>	<b>12</b>
<b>Acknowledgements .....</b>	<b>13</b>
<b>1. Introduction .....</b>	<b>15</b>
<b>1.1 Galactose oxidase (GOase) .....</b>	<b>15</b>
1.1.1 The enzyme galactose oxidase (GOase) .....	15
1.1.2 History of directed evolution of GOase .....	20
1.1.3 Applications of GOase .....	23
1.1.4 Summary .....	24
<b>1.2 Resolution and asymmetric synthesis methods .....</b>	<b>25</b>
1.2.1 Kinetic resolution .....	26
1.2.2 Dynamic kinetic resolution (DKR) .....	27
1.2.3 Desymmetrisation .....	35
1.2.4 Deracemisation by tandem transformation .....	37
1.2.5 Summary .....	44
<b>2. Results and Discussion – Application of GOase in the Deracemisation of Secondary Alcohols .....</b>	<b>45</b>
<b>2.1 Production of GOase .....</b>	<b>46</b>
2.1.1 Expression and purification of GOase .....	46
2.1.2 Activity assay of GOase M <sub>3-5</sub> .....	47
<b>2.2 Deracemisation employing chemical reducing agents .....</b>	<b>47</b>
<b>2.3 Deracemisation employing transfer hydrogenation (TH) and asymmetric transfer hydrogenation (ATH) .....</b>	<b>50</b>

2.3.1 Optimisation of the oxidation step.....	53
2.3.2 Optimisation of the reduction step.....	57
2.3.3 Deracemisation reactions employing optimised reaction conditions .....	62
<b>2.4 Summary and outlook .....</b>	<b>68</b>
<b>3. Results and Discussion - Application of GOase in the Production of Single Atropisomers.....</b>	<b>70</b>
<b>3.1 Introduction.....</b>	<b>70</b>
3.1.1 Synthesis of single atropisomers by chemical methods .....	70
3.1.2 Synthesis of single atropisomers by enzymatic methods.....	72
3.1.3 Applications of atropisomers .....	75
<b>3.2 Asymmetric synthesis of diaryl ethers .....</b>	<b>76</b>
3.2.1 HPLC method development .....	77
3.2.2 Optimisation of reaction conditions .....	78
3.2.3 Enzymatic production of methyl <i>tert</i> -butyl diaryl ethers.....	81
3.2.4 Absolute configuration assignment of the atropisomers.....	88
3.2.5 Complementary approaches for the production of single atropisomers .	89
3.2.6 Enzymatic production of methyl isopropyl diaryl ethers.....	92
3.2.7 Summary.....	95
<b>3.3 Asymmetric synthesis of biaryls .....</b>	<b>96</b>
3.3.1 HPLC method development .....	96
3.3.2 Enzymatic production of naphthyl-substituted biaryls .....	98
3.3.3 Enzymatic production of phenanthryl-substituted biaryls .....	104
3.3.4 Enzymatic production of halogen-substituted biaryls .....	108
3.3.5 Summary and outlook.....	113
<b>4. Results and Discussion - Application of CALB (Novozym<sup>®</sup> 435) in the Production of Erucamide.....</b>	<b>116</b>
<b>4.1 Introduction.....</b>	<b>116</b>
4.1.1 The enzyme <i>Candida antarctica</i> Lipase B (CALB) .....	116
4.1.2 Lipase catalysed amidation of fatty acids in organic solvents.....	118
4.1.3 Solvent-free lipase catalysed amidation of fatty acids.....	120

---

<b>4.2 Lipase catalysed amidation of fatty acids in organic solvents .....</b>	<b>121</b>
<b>4.3 Solvent-free lipase catalysed amidation of fatty acids .....</b>	<b>122</b>
4.3.1 Optimisation of evacuation.....	123
4.3.2 Optimisation of the enzymatic concentration .....	125
4.3.3 Enzyme recycling .....	126
4.3.4 Enzyme support .....	128
4.3.5 Optimisation of the ammonia concentration.....	129
<b>4.4 Summary and outlook .....</b>	<b>130</b>
<b>5. Conclusions and Future Outlook .....</b>	<b>132</b>
<b>6. Materials and Methods .....</b>	<b>134</b>
<b>6.1 Materials.....</b>	<b>134</b>
6.1.1 Chemicals .....	134
6.1.2 Media.....	134
6.1.3 Buffers and Solutions .....	135
<b>6.2 Methods .....</b>	<b>136</b>
6.2.1 Protein preparation .....	136
6.2.2 Procedures for production of single atropisomers .....	139
6.2.3 Procedures for the deracemisation of secondary alcohols .....	142
6.2.4 Procedures for the lipase catalysed solvent-free amidation.....	143
6.2.5 Analytical techniques.....	143
Appendix 1: IUPAC three and one letter code for amino acids.....	153
Appendix 2: Biocatalytic Desymmetrisation of an Atropisomer with both an Enantioselective Oxidase and Ketoreductases.....	154
<b>References .....</b>	<b>158</b>

This thesis contains 29,680 words.

## Table Index

Table 1. Mutations of major variants of GOase. ....	23
Table 2. Screening of reducing agents for deracemisation. ....	48
Table 3. Deracemisation of <b>46</b> with GOase M <sub>3-5</sub> and <b>50</b> . ....	49
Table 4. Oxidation of <b>64</b> by GOase M <sub>3-5</sub> in the presence of Ir-TsCYDN. ....	55
Table 5. Oxidation of <b>64</b> by GOase M <sub>3-5</sub> in the presence of HCOONa. ....	56
Table 6. Side reaction: O <sub>2</sub> inhibition of the reduction step. ....	57
Table 7. Oxidation of <b>62</b> catalysed by ( <i>S</i> )-selective Rh-TsDPEN. ....	58
Table 8. Optimisation of concentration and ligands for the reducing agents. ....	59
Table 9. Optimisation of metal catalyst concentration. ....	61
Table 10. Deracemisation of <b>63</b> by GOase M <sub>3-5</sub> and ( <i>rac.</i> ) Ir-TsCYDN. ....	63
Table 11. Deracemisation starting with the oxidation step. ....	64
Table 12. Deracemisation with 4 g/L enzymatic concentration. ....	65
Table 13. Deracemisation of a range of secondary alcohols. ....	66
Table 14. Enzymatic oxidative couplings of 2-naphthol derivatives. <sup>133-134</sup> ....	73
Table 15. Reduction of <b>91c</b> by KREDs. ....	91
Table 16. Acetylation of diol <b>91a</b> by Novozym <sup>®</sup> 435. ....	92
Table 17. Reduction of dialdehyde <b>92c</b> by KREDs. ....	94
Table 18. Enzymatic oxidation of diol <b>93a</b> by GOase M <sub>3-5</sub> (30 °C). ....	99
Table 19. Enzymatic oxidation of diol <b>93a</b> by GOase M <sub>3-5</sub> (20 °C). ....	100
Table 20. Ketoreduction of dialdehyde <b>93c</b> by KREDs. ....	101
Table 21. Enzymatic oxidation of diol <b>94a</b> by GOase M <sub>3-5</sub> . ....	105
Table 22. Ketoreduction of dialdehyde <b>94c</b> by KREDs. ....	106
Table 23. Enzymatic production of monoaldehydes <b>95b/96b</b> . ....	110
Table 24. Slope of the best fit trend line of equations of standard curves (y = mx) of substrates and products of biotransformations. ....	151

---

**Abbreviations**

2M2B	2-methyl-2-butanol
aa	amino acid
ADH - 'A'	ADH from <i>Rhodococcus ruber</i>
BINAP	2,2'-bis(diphenylphosphino)-1,1'-binaphthyl
<i>ca</i>	<i>circa</i> , approximately
CALB	<i>Candida antarctica</i> Lipase B
CASTing	Combinatorial Active Site Testing
CD	circular dichroism
CFE	cell free extract
CIP	Cahn–Ingold–Prelog priority rules
CRL	<i>Candida rugosa</i> lipase
CuSO <sub>4</sub>	copper sulphate
Da	Dalton
D-AAO	D-amino acid oxidase
L-AAO	L-amino acid oxidase
DCM	dichloromethane
dH <sub>2</sub> O	demineralised water
DKR	dynamic kinetic resolution
DMF	dimethylformamide
DNA	deoxyribonucleic acid
d.r.	diastereomeric ratio
<i>E.coli</i>	<i>Escherichia coli</i>
EDTA	ethylenediaminetetraacetic acid
<i>ee</i>	enantiomeric excess
eq.	equivalents
GlcNAc	N-acetylglucosamine
Glc	glucose

---

Gal	galactose
GOase	galactose oxidase
GOase WT	wild type galactose oxidase
HPLC	high performance liquid chromatography
HRP	horse radish peroxidase
h	hour (s)
IPA	propan-2-ol
IPE	diisopropyl ether
ISM	Iterative Saturation Mutagenesis
KPi	potassium phosphate buffer
KRED	ketoreductase
LB	Luria-Bertani medium
LK-ADH	ADH from <i>Lactobacillus kefir</i>
Man	mannose
MAO-N	monoamine oxidase from <i>Aspergillus niger</i>
MIBK	methyl isobutyl ketone
min	minute
mL	millilitre
MTBE	methyl <i>tert</i> -butyl ether
NaBH <sub>4</sub>	sodium borohydride
NAD(P)	nicotinamide adenine dinucleotide (phosphate)
NaH <sub>2</sub> PO <sub>4</sub>	monosodium phosphate
Na <sub>2</sub> HPO <sub>4</sub>	disodium hydrogen phosphate
NaPi	sodium phosphate buffer
NBP	N-bromophthalimide
No.	number
OD <sub>600</sub>	optical density at 600 nm
OTf/triflate	trifluoromethanesulfonate
PCL	<i>Pseudomonas cepacia</i> lipase

---

PED	1-phenyl-1, 2-ethanediol
PMSF	phenylmethyl sulfonyl fluoride
PFL	<i>Pseudomonas fluorescens</i> lipase
PLE	pig liver esterase
PPL	porcine pancreas lipase
<i>rac.</i>	racemic
rpm	revolutions per minute
SDS-PAGE	sodium dodecylsulphate polyacrylamide gel electrophoresis
Tal	talose
TB-ADH	ADH from <i>Thermoanaerobium brockii</i>
TBD	1,5,7-triazabicyclo[4.4.0]dec-5-ene
TEMPO	(2,2,6,6-Tetramethylpiperidin-1-yl)oxyl
TMS-DM	trimethylsilyldiazomethane
TsCYDN	( <i>p</i> -toluenesulfonyl)-1,2-cyclohexanediamine
TsDPEN	<i>n</i> -( <i>p</i> -toluenesulfonyl)-1,2-diphenylethylenediamine
VOC	volatile organic compound
v/v	volume by volume
wt	weight



## Abstract

Increasing demand for chiral technology in industry has led to the rapid development of catalysts for enantioselective processes. In this respect biocatalysts are of particular interest due to their excellent regio- and stereo-selectivity and their ability to work under mild conditions.

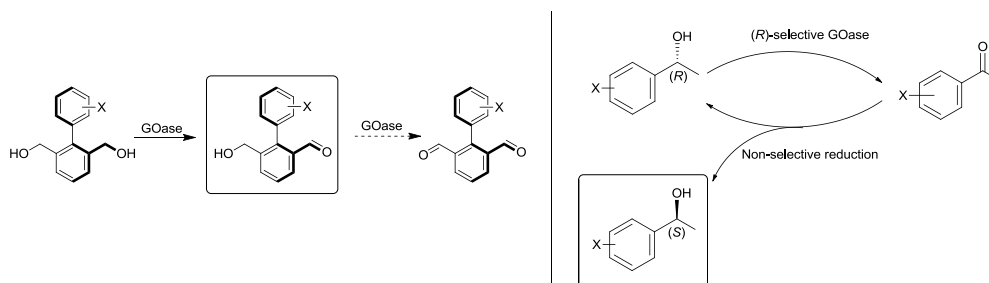
The development of catalysts for the selective oxidation of alcohols to aldehydes and ketones represents a major challenge in organic synthesis. Previous work showed that a variant of the enzyme galactose oxidase (GOase) was capable of oxidising a wide range of chiral secondary alcohols with high enantioselectivity.<sup>1</sup> The aim of this work is to develop new applications for this variant.

Two new stereoselective processes have been developed employing this variant:

1. Enzymatic desymmetrisation of proatropisomeric diaryl ethers and biaryls. Atropisomers are stereoisomers resulting from restricted rotation about an axis, where the rotational barrier is high enough for isolation of the conformers. Desymmetrisation by GOase has allowed the production of atropisomers with enantiomeric excess (*ee*) up to 99% in good yields. An alternative approach based upon asymmetric reduction of the corresponding dialdehyde using ketoreductases (KREDs) has also been explored.

2. Deracemisation of racemic secondary alcohols by a combination of enzyme and transition metal catalysts. Deracemisation is a method for the production of enantiopure compounds starting from racemic substrates. Combination of the enzyme GOase and a transition metal catalyst has allowed the production of a single enantiomer of a number of secondary alcohols from the corresponding racemic mixture (*ee* > 99%, yield > 98%).

Primary amides are widely applied in the polymer industry. They are produced in large quantities each year. An efficient solvent-free process (yield > 90%) for the production of erucamide has been developed employing immobilised *Candida antarctica* Lipase B (CALB, Novozym<sup>®</sup> 435) under mild conditions (solid ammonia source, 90 °C).



## **Declaration**

No portion of the work referred to in this thesis has been submitted in support of an application of another degree or qualification of this or any other university, or other institution of learning.

## Copyright Statement

- i. The author of this thesis (including any appendices and/or schedules to this thesis) owns certain copyright or related rights in it (the “Copyright”) and she has given The University of Manchester certain rights to use such Copyright, including for administrative purposes.
- ii. Copies of this thesis, either in full or in extracts and whether in hard or electronic copy, may be made only in accordance with the Copyright, Designs and Patents Act 1988 (as amended) and regulations issued under it or, where appropriate, in accordance with licensing agreements which the University has from time to time. This page must form part of any such copies made.
- iii. The ownership of certain Copyright, patents, designs, trade marks and other intellectual property (the “Intellectual Property”) and any reproductions of copyright works in the thesis, for example graphs and tables (“Reproductions”), which may be described in this thesis, may not be owned by the author and may be owned by third parties. Such Intellectual Property and Reproductions cannot and must not be made available for use without the prior written permission of the owner(s) of the relevant Intellectual Property and/or Reproductions.
- iv. Further information on the conditions under which disclosure, publication and commercialisation of this thesis, the Copyright and any Intellectual Property and/or Reproductions described in it may take place is available in the University IP Policy (see <http://www.campus.manchester.ac.uk/medialibrary/policies/intellectual-property.pdf>), in any relevant Thesis restriction declarations deposited in the University Library, The University Library’s regulations (see <http://www.manchester.ac.uk/library/aboutus/regulations>) and in The University’s policy on presentation of Theses.

## Preface

Three projects were conducted during the course of this PhD. The first one was entitled “Application of galactose oxidase (GOase) in the deracemisation of secondary alcohols”; the second project was entitled “Application of GOase in the production of single atropisomers”, which can be divided into two sections: in the first section diaryl ethers were employed as substrates, and biaryls were employed in the second section; the third project was entitled “Application of *Candida antarctica* lipase B in the production of erucamide”. This thesis is arranged accordingly, in six chapters. The first chapter is a general introduction to the enzyme GOase and an introduction to techniques for the production of enantiopure compounds. The next three chapters describe the three major projects, respectively. In addition, other than the introduction to deracemisation that is included in the first chapter, introductions to the second and third chapters are included in each chapter. The fifth chapter discussed conclusions and future outlook for this research and the last chapter contains information on materials and experimental methods.

## Acknowledgements

First of all, I would like to express my profound gratitude to my supervisor Professor Nicholas J. Turner for providing me the precious opportunity to study in the UK as an overseas PhD student. He has always been patient to me and meetings with him are always helpful, pleasant and encouraging. Thanks to him I have genuinely enjoyed my PhD and if I can choose again I would not hesitate to make the same choice.

I would also like to acknowledge Croda Enterprises Ltd., and my industrial supervisors Dr. Kim Carmichael, Dr. Dass Chahal and Dr. Damian Kelly. During my placement as a visiting scientist at Croda, they have been very helpful to me and I enjoyed everyday working with them.

I would like to thank everyone I have collaborated with during my PhD: Dr. Abigail Page, Michael Tait and Professor Jonathan Clayden from the University of Manchester; Dr. Xiaofeng Wu and Professor Jianliang Xiao from the University of Liverpool. They have all contributed significantly to my PhD projects. They have been very effective and efficient during our collaborations and I'm honoured to have the opportunity to work with them.

I would like to thank all the colleagues and also friends from the Turner/Flitsch group. Especially Dr. Franck Escalettes and Dr. Avgousta Ioannou, who guided me through the beginning of my PhD; Dr. Julie Rannes, who not only helped me with biology, but also is my dearest friend and one of the most intelligent person I know; and Dr. Valentin Koehler, who guided me with great patience and gave me ideas that benefitted my PhD significantly.

I would also like to thank Dr. Martina Austeri, Dr. Anthony Green, Dr. Claire Doherty, my soul mate Jie Gao, Hua Tian, and Diego Ghislieri for proof reading this thesis, despite the short notices I gave them. Special thanks to the Jar For Bo – which was made by Dominique Richardson and I have to put one pound in it for each day I did not write. I have obeyed the rules religiously and will use all the 18 pounds from the Jar to buy every one

drinks.

I would like to thank my country China. Without travelling abroad, I would never realise how deeply I love my country.

Finally, I would like to thank my mother Fangli Shang and my father Fuqiang Yuan, who love and support me unconditionally. 爸爸妈妈我永远爱你们!

# 1. Introduction

## 1.1 Galactose oxidase (GOase)

### 1.1.1 The enzyme galactose oxidase (GOase)

Galactose oxidase (GOase, EC 1.1.3.9) is a monomeric copper-containing enzyme of fungal origin with a molecular mass of 68.5 kDa and composed of 639 amino acids (aa). Cooper *et al.* first isolated the enzyme in 1959 from the fungus *Polyporus circinatus*.<sup>2</sup> It was later reclassified as *Dactylium dendroides*;<sup>3-4</sup> however, further classification studies demonstrated that the enzyme was an isolate of the fungus *Fusarium graminearum*.<sup>5</sup>

Wild-type GOase (GOase WT) catalyses the oxidation of galactose (Gal) **1** to the aldehyde **2** coupled with reduction of molecular oxygen to hydrogen peroxide ( $\text{H}_2\text{O}_2$ ) according to the reaction scheme in Figure 1.<sup>1,6</sup>

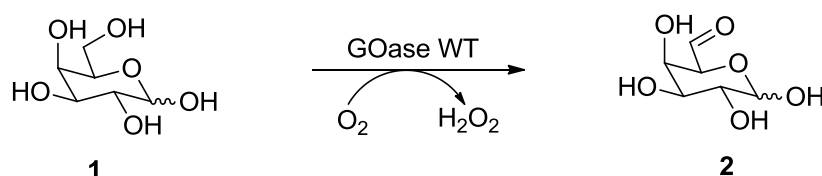


Figure 1. Oxidation of **1** catalysed by GOase WT.<sup>1</sup>

GOase WT has a relatively narrow substrate specificity, catalysing only the oxidation of simple primary alcohols and a few sugars other than **1**.<sup>7-8</sup>

#### 1.1.1.1 GOase structure

Ito *et al.* determined the crystal structure of mature GOase in 1991.<sup>3</sup> It was shown that GOase contains three domains. A  $\beta$ -sandwich structure was found in the first domain. The second and largest domain consists of twenty eight  $\beta$ -strands and a short  $\alpha$ -helix, on which the active site including the copper ion is situated. The third domain is the C-terminal domain, which lies on top of the

second domain, and contains seven  $\beta$ -strands.

A thioether bond between Tyr272 and Cys228 in the mature form of the protein was also revealed and this is a remarkable feature. It is also heavily involved in the redox chemistry of GOase (mechanism see §1.1.1.2). The GOase gene was found to include an N-terminal leader peptide sequence, which is cleaved off and results in the mature protein of 639 aa.<sup>4,9-12</sup> It was shown that the precursor form converts to the mature GOase by a self-processing mechanism.<sup>9,12</sup> The thioether bond is also formed during this process under either aerobic or anaerobic conditions.<sup>12</sup> Figure 2 shows the mature form and the precursor form of GOase as well as the structural difference between them. Five regions of main chain and some key residues of the active site were identified to differ dramatically.

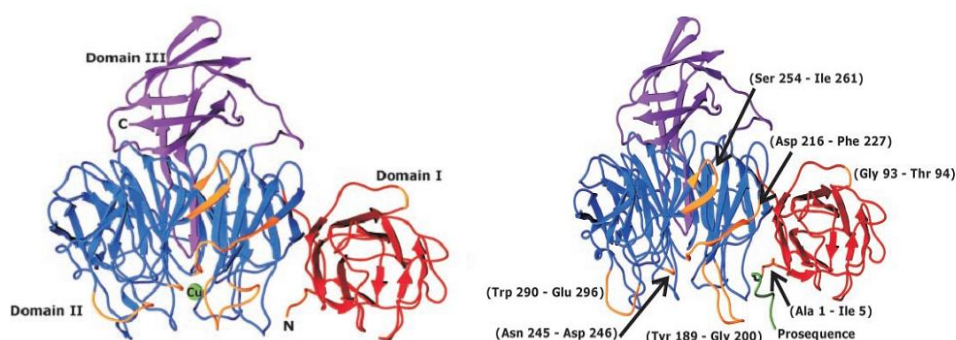


Figure 2. Structures of the mature GOase (*left*) and the precursor (*right*).<sup>10</sup> The complete molecule is coloured according to domains (the first domain in red, the second blue, the third purple). The regions with more than 2Å structural differences are shown in yellow.

Figure 3a is a schematic presentation of the square pyramidal coordination of the copper active site,<sup>3</sup> which is derived from the crystal structure of the active site of GOase shown in Figure 3b.<sup>13</sup> An almost perfect square is formed by His496, His581, Tyr272, and an acetate ion; the fifth ligand, Tyr 495, is at the axial position of the copper, completing the square pyramidal shape. When acetate ion is replaced by a water molecule, the structure is essentially the same. From Figure 3b, the stacking of Trp 290 over the thioether bond between Tyr272 and Cys228 can be seen, which is believed



to affect the substrate binding and redox potential.<sup>14</sup>

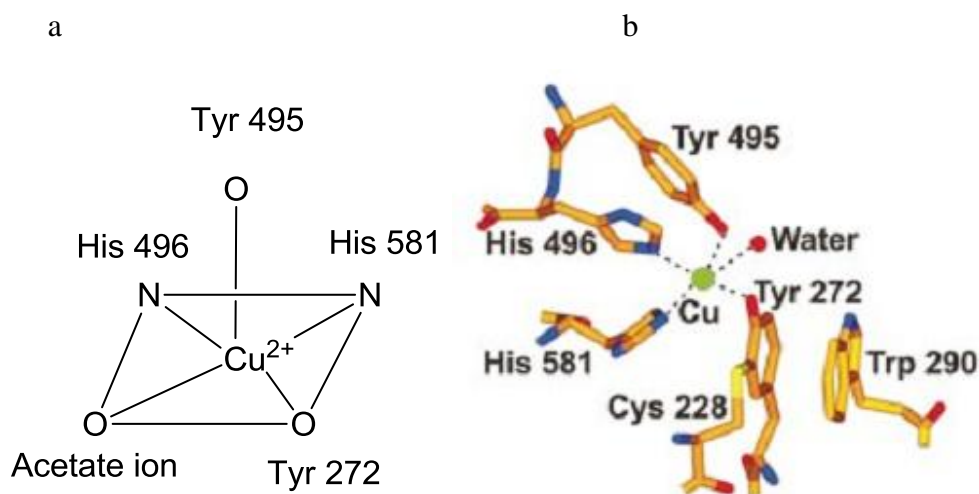


Figure 3. a, Schematic representation of the square pyramidal coordination of copper;<sup>3</sup> b, crystal structure of the active site of GOase.<sup>13</sup>

#### 1.1.1.2 GOase mechanism

The mechanisms for the substrate oxidation and regeneration of the enzyme have been reported by several groups.<sup>10,15-20</sup> It has been proposed that GOase operates by a free radical mechanism, and contains two one-electron redox centres: the copper atom and Tyr272, which is crosslinked with Cys228. A stable free-radical is formed in the Tyr-Cys site, leading to the redox-active site in the protein.

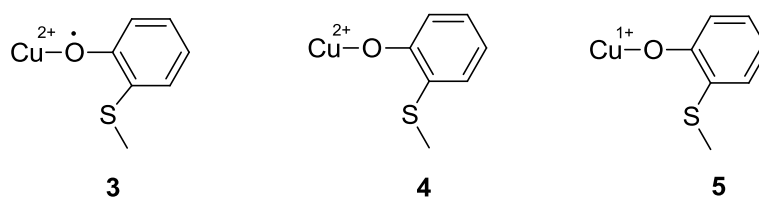


Figure 4. Oxidised **3**, semi-reduced **4** and reduced **5** forms of copper complex in active site of GOase.<sup>18</sup>

GOase has three different oxidation forms: oxidised **3**, semi-reduced **4** and reduced **5** as shown in Figure 4.<sup>18</sup> The catalytic process involves a ping-pong turnover mechanism,<sup>15,21</sup> which consists of two half reactions. Figure 5A shows the first half reaction, where the alcohol substrate binds to the oxidised

copper.<sup>17</sup> There are three steps involved in this half reaction: proton transfer from substrate to Tyr 495 which acts as a general base, hydrogen atom transfer to the cofactor-based radical centre and electron transfer to produce the  $\text{Cu}^{\text{I}}$ .

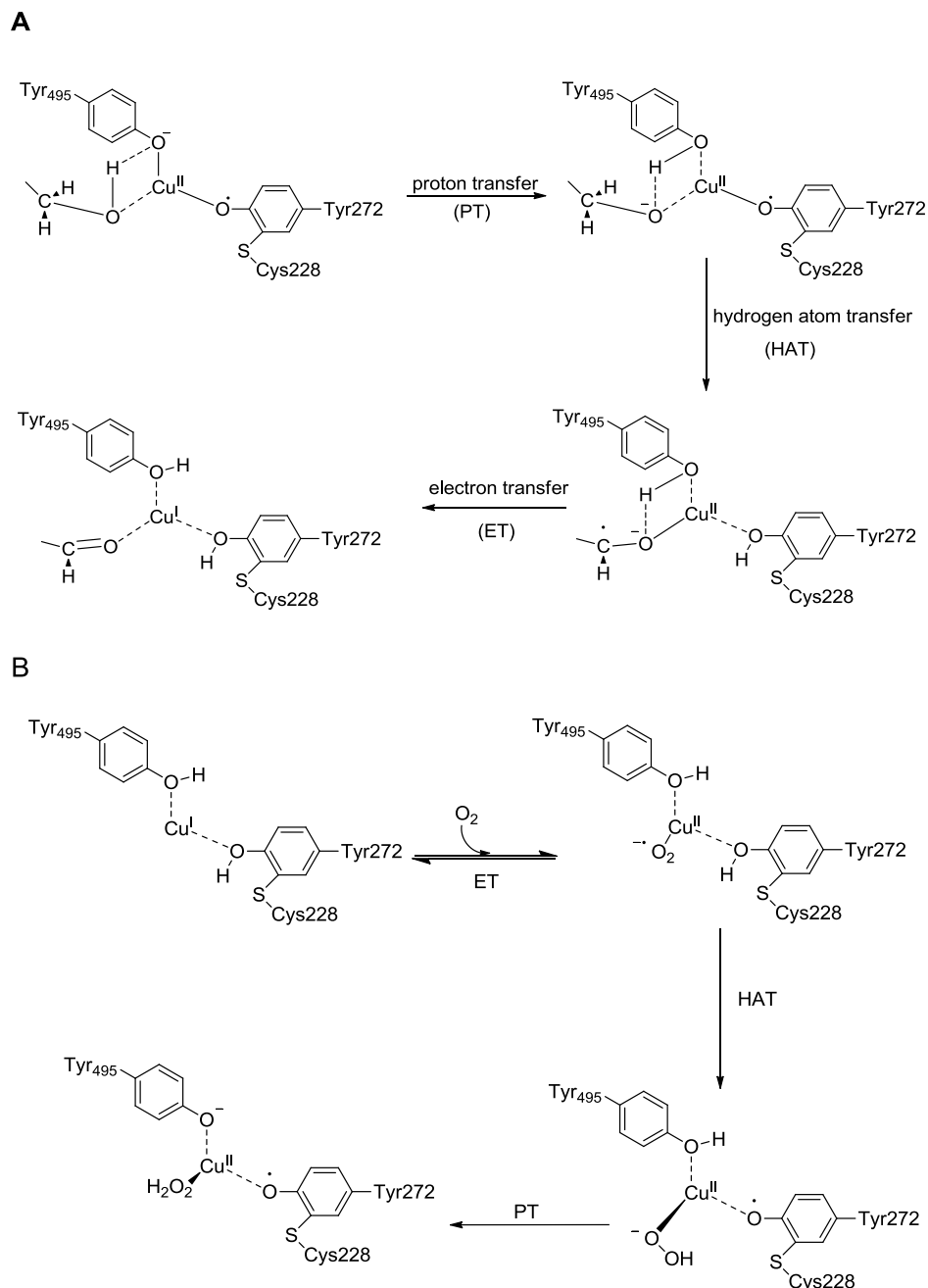


Figure 5. Mechanisms of GOase (A), the first half reaction and (B), the second half reaction.<sup>16-17,22</sup>

The second half-reaction involves the binding of the  $\text{Cu}^{\text{I}}$ -tyrosine site to  $\text{O}_2$ . The  $\text{O}_2$  is reduced to  $\text{H}_2\text{O}_2$  by the  $\text{Cu}^{\text{I}}$  (Figure 5B).<sup>22</sup> The initial  $\text{Cu}^{\text{II}}$ -tyrosyl radical state is thus regenerated. The mechanism of the second half reaction is

proposed to consist of three steps; firstly, the metal-bound superoxide is generated by electron transfer from  $\text{Cu}^{\text{I}}$  to coordinated oxygen; then a hydrogen atom transfers from the Tyr-Cys cofactor centre to the metal bound superoxide to produce hydroperoxide and a radical at the Tyr-Cys cofactor centre; finally, hydrogen peroxide is produced by proton transfer from Tyr495 to the metal bound hydroperoxide and the enzyme is fully reoxidised.

The crystal structure with substrate bound in the active site has not yet been reported.<sup>16</sup> One of the possible reasons is that the substrate binding in the crystal is inefficient, as indicated by the high Michaelis constant,  $K_{\text{M}}$  value (70-100 mM for **1**).<sup>23</sup> On the other hand, molecular modeling studies have constructed the binding model of **1** in the active site of GOase WT (Figure 6).<sup>23-24</sup>

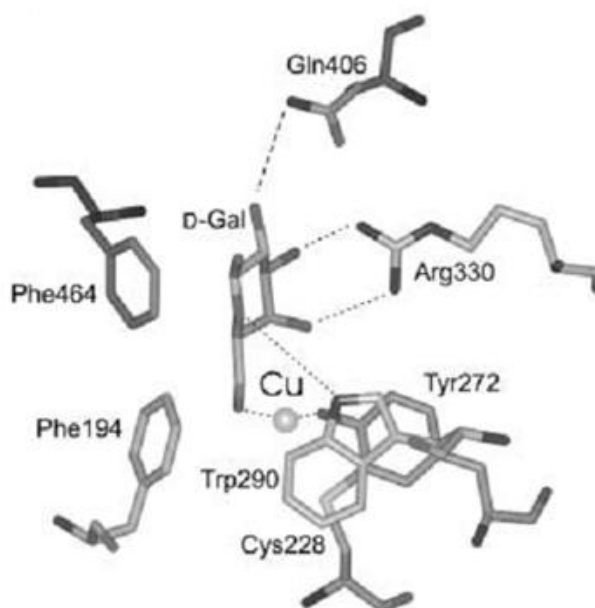


Figure 6. Model of **1** in the active site showing the proposed hydrogen bond interactions.<sup>23</sup>

As shown in Figure 6, the O(6) atom of **1** coordinated to the copper directly. Hydrogen bonds between O(3) and O(4) and Arg330 were also proposed. In addition, the O(2) and O(5) atoms may form hydrogen bonds with Gln406 and Trp290, respectively. This model provides convincing explanations of substrate specificity of GOase towards **1**.

### 1.1.2 History of directed evolution of GOase

A number of variants of GOase have been produced via directed evolution. These variants exhibit various properties, such as altered substrate specificity, better expression and higher activity.

Sun *et al.* achieved functional expression of GOase in *E. coli* and generated a GOase mutant (A3.E7) with improved thermostability by combining random mutagenesis and staggered extension process (StEP).<sup>25-26</sup> Later, attempts to introduce D-glucose (D-Glc) activity (GOase WT shows almost no activity towards D-Glc<sup>27</sup>) by random mutagenesis achieved little success.<sup>28</sup> Therefore, based on the published crystal structures and substrate binding models,<sup>3,29</sup> key residues, Arg330, Gln406, Phe464, Phe194, Trp290, were identified (Figure 7) and site saturation mutagenesis libraries of these residues in GOase mutant A3.E7 were constructed.<sup>28</sup>

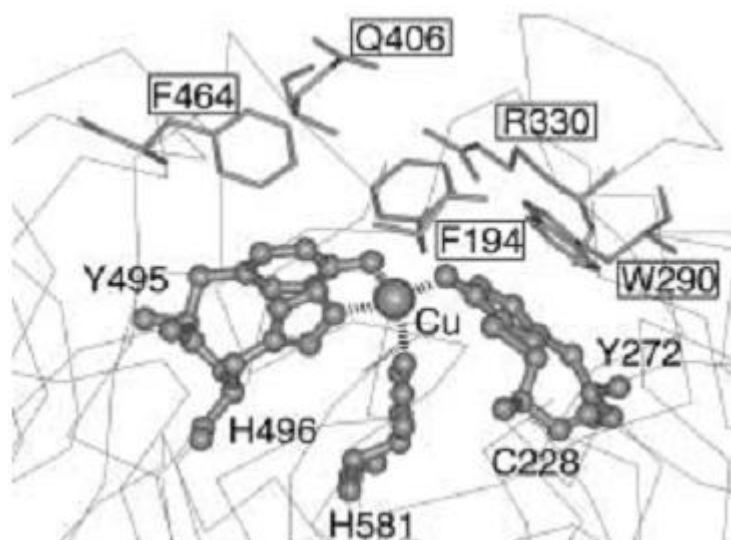


Figure 7. The location of key residues Arg330, Gln406, Phe464, Phe194, and Trp290, which were targeted for saturation mutagenesis (in stick form), and key active site residues Tyr495, His496, His581, Cys228, and Tyr272 (in ball and stick form) in the GOase crystal structure.<sup>28</sup>

A mutant (M-RQW) with 100 fold increased activity towards D-Glc compared to the parent mutant A3.E7 was generated. Three mutations were identified: Trp290Phe, Arg330Lys, and Gln406Thr.<sup>28</sup>

Deacon *et al.* generated a GOase mutant with enhanced fructose oxidase activity.<sup>23</sup> They demonstrated that the Arg330Lys variant showed an 8.2-fold increase in activity towards fructose compared to the wild-type enzyme.

Later Escalettes *et al.* used the mutants (A3.E7) and (M-RQW), renamed M<sub>1</sub> and M<sub>3</sub>, respectively, as the starting point for further rounds of directed evolution for the purpose of generating mutants with high activity towards secondary alcohols.<sup>1</sup> A high throughput solid phase assay<sup>30</sup> was employed to screen approximately 80,000 colonies generated by error-prone PCR. One mutant M<sub>3-5</sub> with a single mutation Lys330Met from its parent mutant M<sub>3</sub> was found to show a significant improvement in activity and enantioselectivity towards a wide range of secondary alcohols. The *ee* for kinetic resolution reactions of a range of secondary alcohols catalysed by this mutant are shown in Figure 8.<sup>1</sup> In this thesis, the mutant M<sub>3-5</sub> was applied to the desymmetrisation of a series of atropisomers and the deracemisation of secondary alcohols (see §2 and §3).

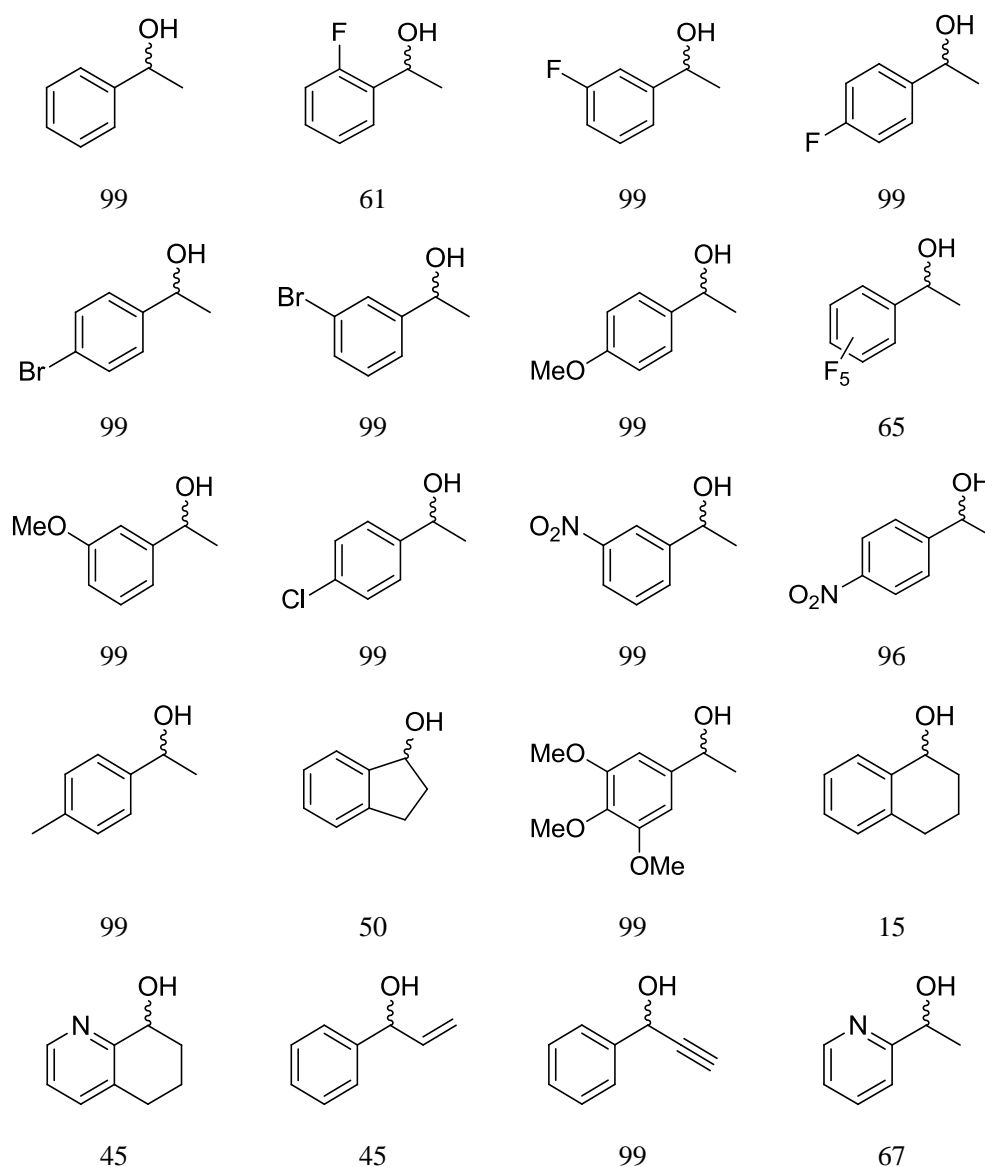


Figure 8. Kinetic resolution of a range of secondary alcohols using the GOase M<sub>3-5</sub> variant (*ee* values shown under the structures).<sup>1</sup>

Also employing M<sub>1</sub> and M<sub>3</sub> as starting points, Rannes *et al.*<sup>31</sup> generated site saturation libraries based upon the principle of Combinatorial Active Site Testing (CASTing) reported by Reetz *et al.*<sup>32</sup> Five initial residues (Phe194, Trp290, Arg330, Gln406 and Phe464) were identified and eight saturation libraries were constructed. Five mutants (H<sub>1</sub>, E<sub>1</sub>, E<sub>2</sub>, F<sub>1</sub>, F<sub>2</sub>) were identified and for the first time GOase activity towards D-mannose (Man) and D-N-acetyl glucosamine (GlcNAc) was obtained. These mutants were then used for the chemoenzymatic labelling of glycoproteins.

Major mutants mentioned above with their mutations are listed in Table 1.

Table 1. Mutations of major variants of GOase.

GOase Variants	Mutations	Reference
<b>M<sub>1</sub> (A3.E7)</b>	Ser10Pro/Met70Val/Pro136/Gly195Glu/ Val494Ala/Asn535Asp	<b>26</b>
<b>M<sub>3</sub> (M-RQW)</b>	Trp290Phe/Arg330Lys/Gln406Thr in M <sub>1</sub>	<b>28</b>
<b>M<sub>3-5</sub></b>	Trp290Phe/Arg330Met/Gln406Thr in M <sub>1</sub>	<b>1</b>
<b>Arg330Lys</b>	Arg330Lys	<b>23</b>
<b>H<sub>1</sub></b>	Arg330Lys in M <sub>1</sub>	<b>31</b>
<b>E<sub>1</sub></b>	W290F R330K Q406T P463I in M <sub>1</sub>	<b>31</b>
<b>E<sub>2</sub></b>	Trp290Phe/Arg330Lys/Gln406Tyr/Tyr463Val in M <sub>1</sub>	<b>31</b>
<b>F<sub>1</sub></b>	Trp290Phe/Arg330Lys/Gln406Tyr/Tyr405Phe in M <sub>1</sub>	<b>31</b>
<b>F<sub>2</sub></b>	Trp290Phe/Arg330Lys/Gln406Glu/Tyr405Phe in M <sub>1</sub>	<b>31</b>

### 1.1.3 Applications of GOase

GOase has found numerous applications in a broad range of areas including biosensors,<sup>33</sup> cancer detection<sup>34</sup> and chemical synthesis.<sup>35</sup>

Joen *et al.* used GOase in biosensors for the detection of glycoproteins, especially antibodies.<sup>33</sup> GOase catalyses the oxidation of galactosyl residues on glycoproteins including antibodies. This reaction is coupled with the reduction of molecular oxygen to H<sub>2</sub>O<sub>2</sub>. The H<sub>2</sub>O<sub>2</sub> produced from this reaction is then electrochemically oxidised and quantified using DC amperometry at a platinum or gold electrode.

In the area of cancer detection, GOase is widely applied in the galactose oxidase-Schiff (GOS) assay, which is used to detect carbohydrate markers on glycoproteins. Carter *et al.* reported cancer detection by exploiting the selectivity of GOase towards **1** among other hexoses to modify D-galactose-β[1, 3]-N-acetylgalactosamine [Gal-β[1, 3]-GalNAc], an important tumour marker. Strong correlation has been found between this protein-bound disaccharide and certain cancers, in particular colon cancer.<sup>34</sup>

Bulter *et al.* reported the application of GOase in the enzymatic oxidation of uridine 5'-diphospho- $\alpha$ -D-galactose (UDP-Gal) and uridine 5'-diphospho-N-acetyl- $\alpha$ -D-galactosamine (UDP-GalNAc).<sup>35</sup> It provides a technique which is capable of introducing a label at a unique site in the oligosaccharide chain of the relevant glycoproteins and glycolipids. A chemical biotinylation step was conducted after the enzymatic oxidation of UDP-Gal and UDP-GalNAc on a 100 mg scale. The biotinylated products could then be applied as donor substrates for human recombinant galactosyltransferases.

#### **1.1.4 Summary**

In summary, GOase is one of the most extensively studied enzymes and it has broad applications in a variety of research areas. In particular, the unique and excellent activity for the oxidation of secondary alcohols from the mutant M<sub>3-5</sub> is potentially important and worth further investigation. In the following chapters studies towards applications of this mutant will be discussed in detail. In §2 results for the desymmetrisation of atropisomers will be discussed followed by results and discussion for deracemisation of secondary alcohols in §3.



## 1.2 Resolution and asymmetric synthesis methods

A chiral molecule is defined as a molecule without an internal plane of symmetry and thus it is non-superimposable with its mirror image. Ever since the first observation of chirality in salts of tartaric acid by Louis Pasteur in 1948, research efforts have made significant progress on this subject. Especially since 1992 the United States Food and Drug Administration (FDA) and the European Committee for Proprietary Medicinal Products approved the guidelines requiring stricter testing of drugs that were to be marketed as racemates.<sup>36</sup> As a result, the need for enantiomerically pure compounds has grown substantially in the past ten years. The global sales of chiral technology products reached \$4.3 billion in 2008 and \$4.5 billion in 2009. This market is expected to exceed \$5.1 billion by 2014.<sup>37</sup>

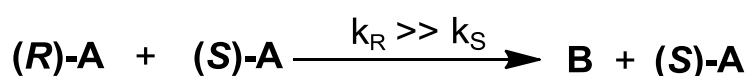
Production of enantiopure compounds can be achieved by either resolution methods or asymmetric synthesis. Resolution methods include physical separations such as crystallisation; and chemical reactions such as kinetic resolution. Asymmetric synthesis, on the other hand, differs from resolutions for the reason that one or more chirality element is formed in a substrate during the process. As a result, desymmetrisation belongs to the category of asymmetric synthesis.

The two most common chemical processes to produce enantiopure products are: (1) kinetic resolution of a racemate, giving a product and a substrate enantiomer, each in 50% maximum theoretical yield; (2) desymmetrisation of a prochiral or *meso*-compound to yield a single enantiomeric product in 100% yield.<sup>38</sup> Since only one enantiomer is generally needed for synthesis, with the other regarded as “waste”, an arduous separation method is needed for the isolation of the product from the substrate.<sup>39</sup> Although (2) seems to be more efficient than (1), most biotransformations employ the less efficient kinetic resolution. The reason is that the availability of racemates

is higher than prochiral or *meso*-compounds.<sup>38</sup> As a result, more advantageous methods such as dynamic kinetic resolution (DKR) and deracemisation, which allow the complete transformation of both enantiomers into a single stereoisomeric product in 100% theoretical maximum yield, have been developed. These four methods will be discussed in detail in §1.2.1-1.2.4.

### 1.2.1 Kinetic resolution

Kinetic resolution is a reaction of racemic starting materials (Figure 9, (*R*)-**A** and (*S*)-**A**), in which one of the enantiomers (Figure 9, (*R*)-**A** or (*S*)-**A**) forms a product (**B**) (Figure 9) more rapidly than the other. With vastly different reaction rates ( $k_R \gg k_S$ ) the product and the substrate enantiomer remaining can be obtained with a 50% theoretical maximum yield.<sup>38,40-41</sup> The product **B** can be either achiral or chiral.



(*R*)-**A**, (*S*)-**A** = substrate enantiomers

**B** = product

$k_R$ ,  $k_S$  = reaction rates of substrate enantiomers

Figure 9. General concept of kinetic resolution.<sup>41</sup>

An example of the kinetic resolution of the pharmaceutically important amino alcohols **6** to produce the ketone **7** is shown in Figure 10.<sup>42</sup> A chiral enantiopure copper complex was used as a bio-mimetic model of GOase, and molecular oxygen as the sole oxidant. Kinetic resolution is based on the difference in reaction rates  $k_R$  and  $k_S$  of the enantiomers. The chiral copper complex is readily available from  $\text{Cu}(\text{OTf})_2$  and *R*-BINAM (**8**). TEMPO was also used in the reaction, and it was suspected to act as a hydrogen acceptor during the catalytic cycle.<sup>43</sup>

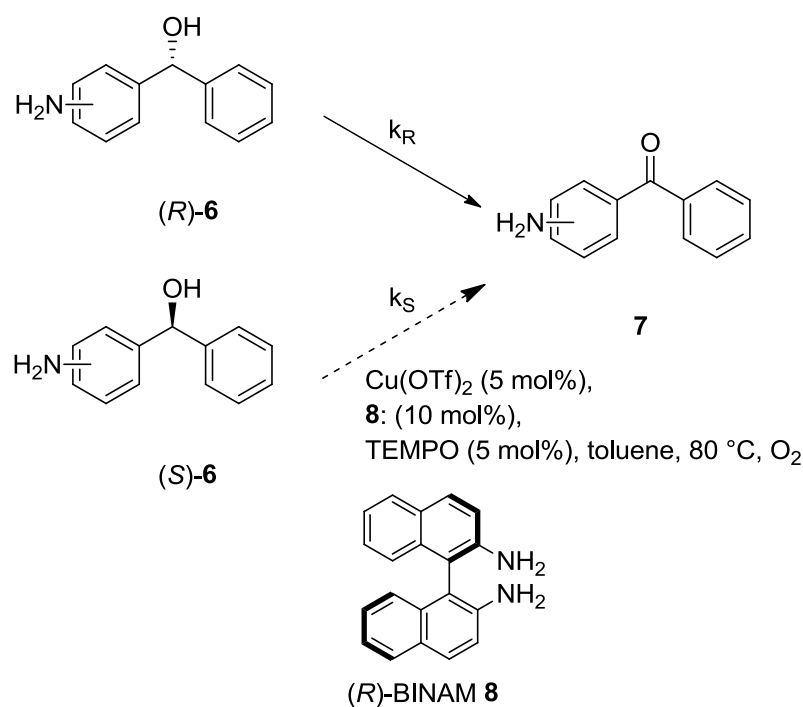
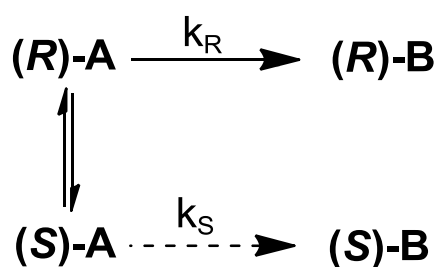


Figure 10. Kinetic resolution of amino alcohols.<sup>42</sup>

A number of ortho- and para-substituted amino alcohols were resolved with good *ee* (71-93%).

### 1.2.2 Dynamic kinetic resolution (DKR)

To overcome the limitation of a 50% theoretical maximum yield from kinetic resolution, DKR processes have been developed. The resolution step of kinetic resolution is combined with an *in situ* racemisation of chiral racemate substrates (Figure 11, (R)-**A** and (S)-**A**).<sup>38,44</sup> It is important that the rate of racemisation is faster than that of the slower reacting enantiomer in reaction with the chiral enantiopure catalyst.



$(R)\text{-A}$ ,  $(S)\text{-A}$  = substrate enantiomers

$(R)\text{-B}$ ,  $(S)\text{-B}$  = product enantiomers

$k_R$ ,  $k_S$  = reaction rates of enantiomers

Figure 11. General concept of DKR.<sup>38,44</sup>

DKR can be achieved by combining enzymes and transition metal catalysts, non-enzymatic methods and enzymatic methods.<sup>44</sup> In particular, DKR by the combination of enzymes and transition metal catalysts showed impressive results. As proof of concept, it demonstrated the feasibility of combining enzymes and transition metal catalysts. Other than DKR, there is also potential for the application of this approach in deracemisation.

In the following sections (§1.2.2.1-1.2.2.3), DKR by a combination of enzymes and transition metal catalysts, non-enzymatic methods and enzymatic methods will be reviewed.

#### 1.2.2.1 DKR by a combination of enzymes and transition metal catalysts

DKR by enzymes and transition metal catalysts combines the advantages of the high enantioselectivity arising from the enzymes and the racemising ability of transition metal catalysts. The scope of DKR has been extended dramatically since the first report of this method.<sup>44-49</sup> However, it is not always straightforward for enzymes and metals to work together. Other than the requirement for the enzymes and transition metal catalysts to be active enough to facilitate both the kinetic resolution and racemisation, there is one extra important consideration, which is to develop a system where the enzymes and the transition metal catalysts are not affected adversely by each

other.

The first example of DKR involving an enzyme/metal was reported by Williams *et al.* in 1996. Combination of a hydrolase (lipase) and a palladium catalyst was described using allyl acetate as the acyl donor (Figure 12).<sup>50-51</sup>

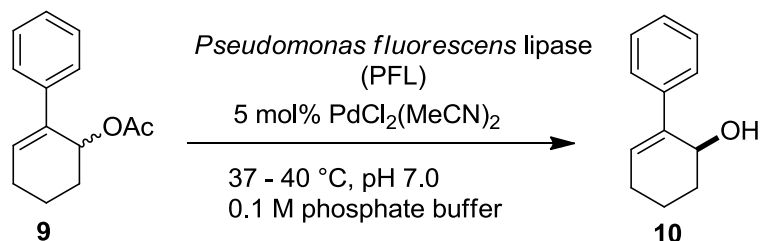


Figure 12. DKR by a combination of a lipase and a palladium catalyst.<sup>50</sup>

Ideally, the enzyme *Pseudomonas fluorescens* lipase (PFL) and the palladium catalyst should not affect each other. The enzyme would enantioselectively hydrolyse the allyl acetate (**9**) while the palladium catalyst racemises the starting material (but not the product). Indeed, when the kinetic resolution was performed by itself, the *ee* of the alcohol product **10** was 80%; when the two reactions were performed together, the *ee* was 96% with a yield of 87%, indicating that the tandem *in situ* racemisation and resolution were compatible under the reaction conditions.

Subsequently, DKR with enzymes and transition metal catalysts was applied to produce a broad range of substrates in optically pure forms, including secondary alcohols,<sup>52-57</sup>  $\beta$ -amino esters,<sup>58-59</sup> and amines.<sup>60</sup>

For the DKR of secondary alcohols with enzymes and transition metal catalysts, one of the earliest examples was reported by Larsson *et al.* in 1997.<sup>55</sup> They developed a method for DKR at 70 °C using Shvo's catalyst **11a**<sup>61</sup> and CALB under an argon atmosphere (Figure 13). Later, this method was applied to a variety of substrates with good to excellent results (13 examples, yield 63% - 88%, *ee* over 90% with one exception).<sup>54</sup>

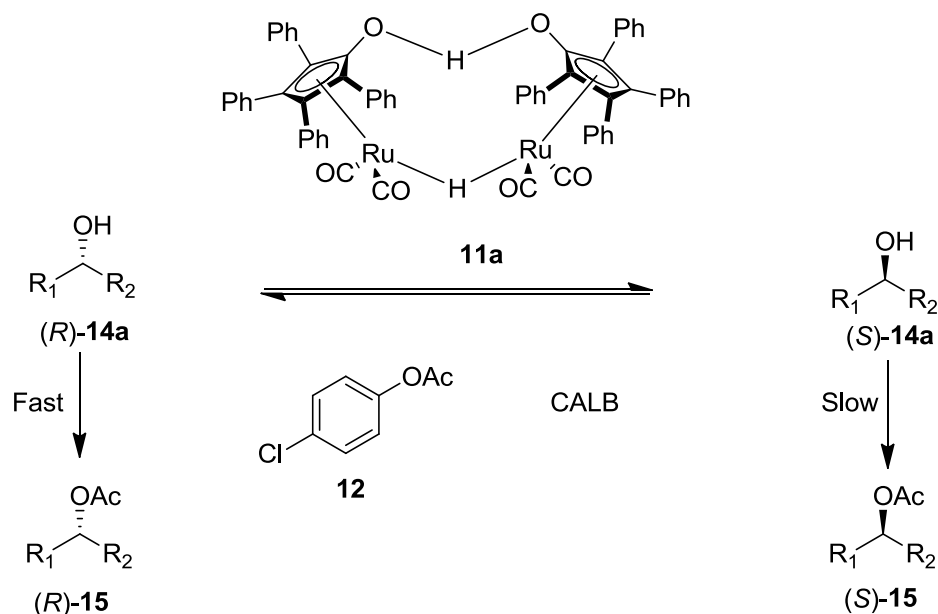


Figure 13. DKR of secondary alcohols using the Shvo's catalyst **11a** and CALB.<sup>54-55</sup> (*R*, *S* were assigned to **14** and **15** when  $R_1 > R_2$  in CIP priority rules)

Nevertheless, the unreacted *p*-chlorophenyl acetate **12** often leads to difficulties in separation of the DKR products; and catalyst **11a** is not compatible with alkenyl acetate. Choi *et al.* reported an effective racemising ruthenium catalyst **13**, which is compatible with the acyl donor isopropenyl acetate and the enzyme CALB.<sup>56-57</sup> This catalyst was subsequently applied in the DKR of a range of aliphatic and benzylic secondary alcohols (**14**), and satisfactory results were obtained (10 selected examples are shown in Figure 14).

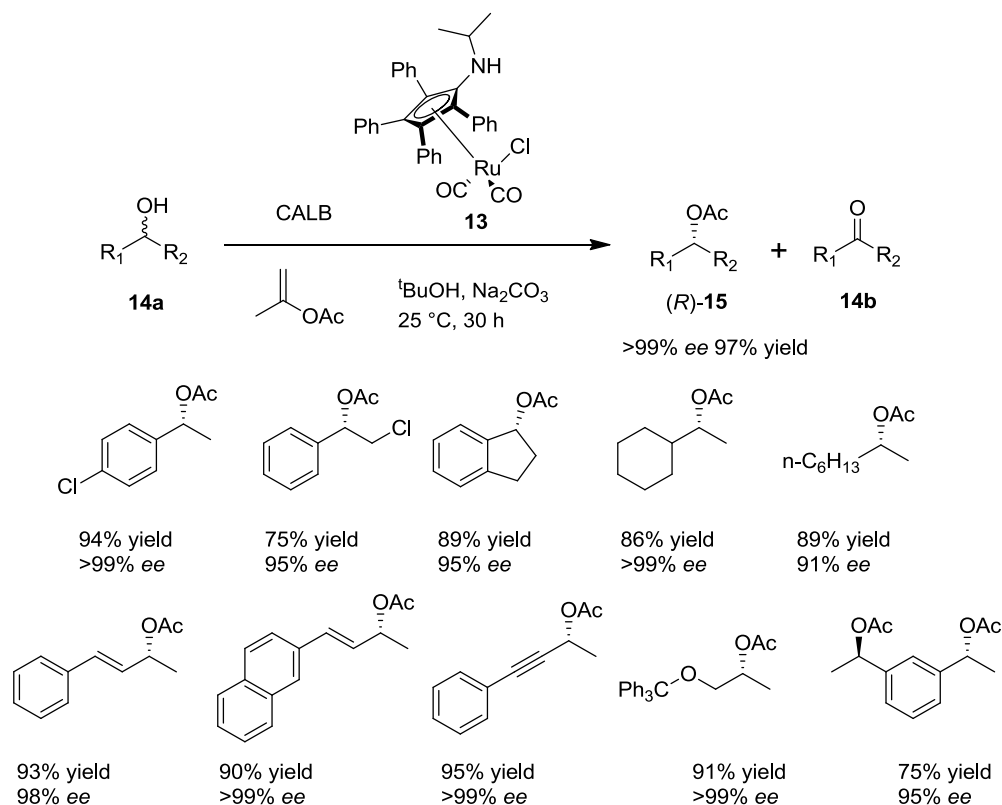


Figure 14. DKR of secondary alcohols employing ruthenium catalyst **13** and CALB.<sup>56-57</sup> The enantiopure products below the reaction scheme represent those obtained from the DKR of the corresponding alcohols.

Although the above examples showed outstanding efficiency in the DKR of secondary alcohols by the combination of enzymes and transition metal catalysts, most of the alcohols produced were (*R*)-configuration due to the selectivity of CALB. Recently, Engstrom *et al.* reported an (*S*)-selective DKR employing the (*S*)-selective CALB W104A, in combination with a ruthenium catalyst **16** (Figure 15).<sup>52</sup> With this method, 3 acetate products of benzylic secondary alcohols (**15**) were obtained in high optical purities (*ee* > 90%), and the conversions were also good (with less than 10% of the ketone product and 1% of the starting material left in the system).

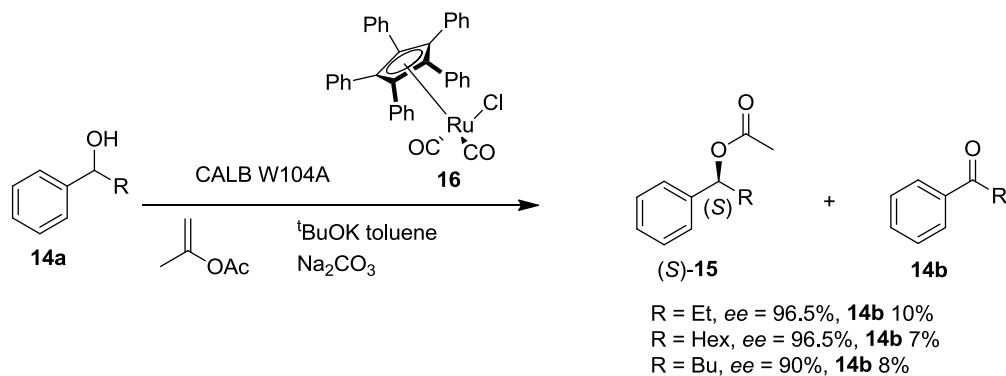


Figure 15. DKR of secondary alcohols employing (S)-selective CALB W104A.<sup>52</sup>

For the DKR of amines with enzymes and transition metal catalysts, typically, harsher reaction conditions, including higher temperatures, are required. One of the reasons is that amines can act as strong ligands for active metal intermediates. In addition, it can be problematic to hydrolyse the amide products obtained from the DKR to the desired amines. In 1996, Reetz *et al.* reported the first example of the DKR of amines by using palladium on carbon with CALB.<sup>62</sup> Although the optical purity was excellent, only a moderate yield (64%) of 1-phenylethylamine was obtained after a long reaction time (8 days). The major reason is due to the poor performance of the racemisation catalyst and the requirement for very harsh reaction conditions.<sup>46</sup> More effective metal catalysts were developed later and a considerable improvement demonstrated using these catalysts.

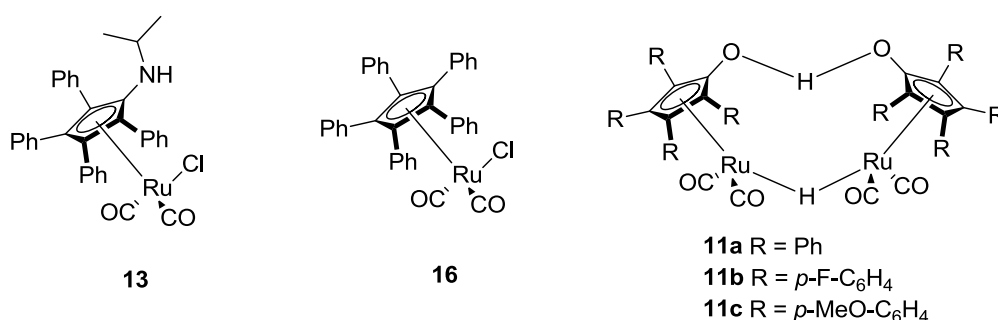


Figure 16. Transition metal catalysts employed for DKR of amines by Paetzold *et al.*<sup>63</sup>

Paetzold *et al.* examined a number of transition metal catalysts and found that catalysts **13** and **16** (Figure 16), which show high racemising activity



towards secondary alcohols, showed only modest rates towards amines.<sup>63</sup> Under optimised conditions, the Shvo type catalyst **11c** was found to be the most efficient. 93-99% *ee* was obtained with various primary amines in 45-95% yields. Subsequently, opposed to chiral amide products obtained by using common acyl donors such as isopropyl acetate, Hoben *et al.* employed dibenzyl carbonate as the acyl donor, which leads to the product of carbamates. It allows subsequent release of the free amine under very mild conditions, and thus circumvents the problems created by the chiral amide products, which require harsh reaction conditions to liberate the free amine. High enantioselectivity was obtained in the kinetic resolution of primary amines catalysed by CALB. Various primary amines were subjected to DKR and the resulting yields range from 60% to 95% and *ee* 90% to 99%.<sup>64-65</sup>

#### 1.2.2.2 DKR by non-enzymatic methods

For DKR by non-enzymatic methods, the kinetic resolution step can be catalysed by either organocatalysts or transition metal catalysts. Gustafson *et al.* reported the DKR of axially chiral biaryls,<sup>66</sup> where resolution was induced by a tripeptide **17** catalysed asymmetric triple bromination by *N*-bromophthalimide (NBP) (Figure 17). The racemisation was a result of interconverting atropisomeric substrates with rotation barriers as low as *ca.* 7 kcal/mol.

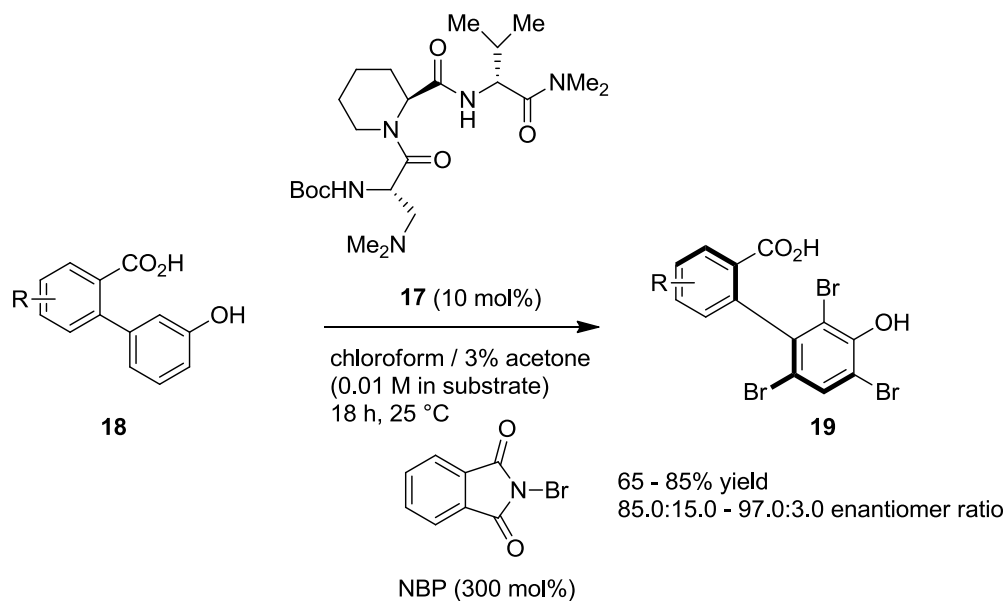


Figure 17. DKR of axially chiral biaryls employing peptide catalysed asymmetric bromination.<sup>66</sup>

An enantiomeric ratio (e.r.) as high as 97:3 was obtained with an 80% isolated yield. This method was applied to 10 biaryl substrates with various substituents at the upper phenyl ring and very good e.r. (higher than 85:15) and yields (higher than 70%) were obtained. The rotation barrier of the triply-brominated product **19** was estimated to be approximately 30 kcal/mol. This is higher than that of the substrate and is enough to allow the separation of optically enriched products at room temperature.

### 1.2.2.3 DKR by non-metal based enzymatic methods

DKR by enzymatic methods could offer advantages in terms of the high enantio- and regio-selectivity of enzymes possible compared to chemical methods. Pietruszka *et al.* employed CALB in the DKR of methyl 2,3-dihydro-1*H*-indene-1-carboxylate **20** (Figure 18).<sup>67</sup> The base, 1,5,7-triazabicyclo[4.4.0]dec-5-ene (TBD) was used as the racemising catalyst. A preparative scale DKR was performed and enantio-enriched product **21** (*ca.* 97% *ee*) was obtained with an outstanding yield (95%). The product could then serve as a starting material for the preparation of biaryl indanyl ketone

(*R*)-**22**, which is a lead compound for novel inhibitors of peptidyl-prolyl-*cis/trans*-isomerases.

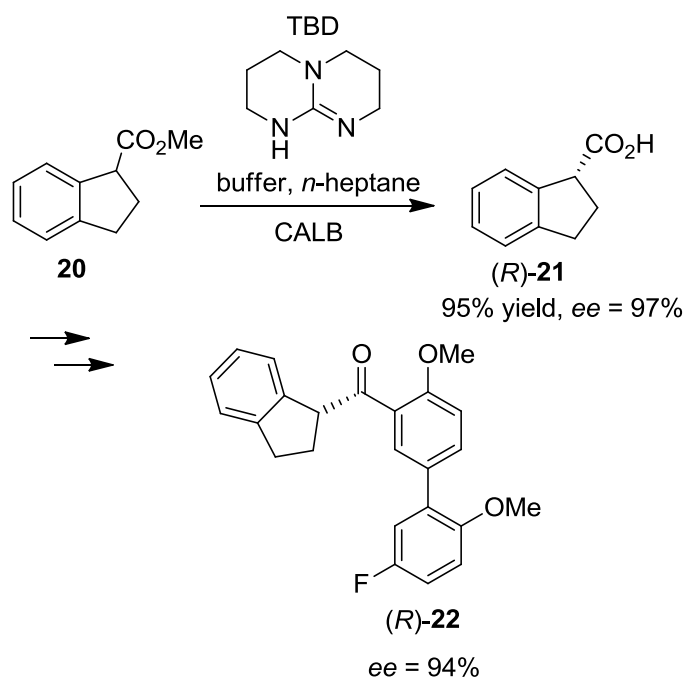
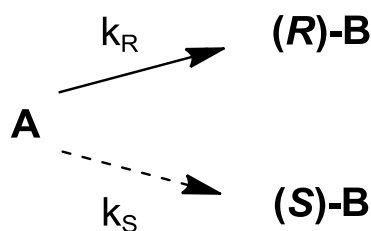


Figure 18. DKR of methyl 2,3-dihydro-1*H*-indene-1-carboxylate **20** by enzymatic methods.<sup>67</sup>

### 1.2.3 Desymmetrisation

Desymmetrisation is the chemical reaction that converts prochiral or *meso*-substrates into product enantiomers (Figure 19, (*R*)-**B** and (*S*)-**B**) at different reaction rates (Figure 19,  $k_R \gg k_S$ ). One or more elements of symmetry of the substrate are eliminated by the desymmetrisation.<sup>68</sup> A theoretical 100% yield of a single enantiomer could be obtained from desymmetrisation.<sup>69</sup>



**A** = prochiral or *meso*-substrate

**(R)-B**, **(S)-B** = product enantiomers

$k_R$ ,  $k_S$  = stereodivergent reaction rates

Figure 19. General concept of desymmetrisation.<sup>38</sup>

A recent example reported by Kohler *et al.*, showed that by employing a variant of monoamine oxidase (D5, MAO-N from *Aspergillus niger*), oxidative desymmetrisation of a range of unprotected pyrrolidines can be achieved (Figure 20).<sup>70</sup> Biotransformations were carried out at a 20 mM substrate concentration with *E. coli* cells expressing MAO-N in aqueous phosphate buffer (100 mM).

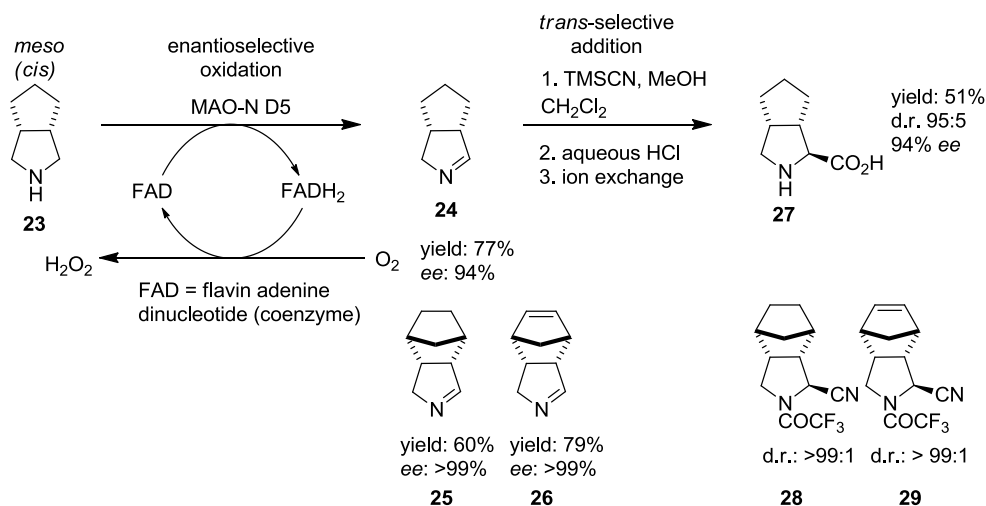


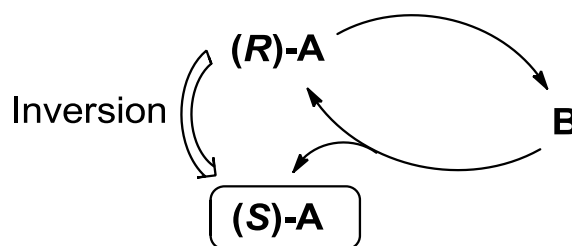
Figure 20. Oxidative desymmetrisation of pyrrolidines.<sup>70</sup> The chiral products below the reaction scheme represent those obtained from the enantioselective oxidation and *trans*-selective addition.

Outstanding *ee* values (94% - 99%) for the imine products (**24** - **26**) were obtained as shown in Figure 20. The oxidation reaction can be conducted in presence of HCN and this gives the corresponding  $\alpha$ -amino nitriles (**28** - **29**) in high diastereomeric excess. However, it was found that epimerisation

occurred after addition of HCN in buffered conditions; therefore, reaction of the imine products with TMSCN/MeOH in  $\text{CH}_2\text{Cl}_2$  was conducted and good results were obtained (d.r. > 99:1). Later, hydrolysis in aqueous HCl gives the free amino acid (**27**) in high d.r. (95:5).

### 1.2.4 Deracemisation by tandem transformation

Deracemisation is the technique to obtain only 1 enantiomer ((*S*)-**A** in the case shown in Figure 21) starting from a racemic mixture (Figure 21, (*R*)-**A** and (*S*)-**A**). It involves a cyclic sequence of 2-steps; first step: only 1 enantiomer ((*R*)-**A**) of the starting material is transformed to an achiral intermediate (**B**); second step: this intermediate is non-selectively converted to a racemic mixture of the starting material. The sequence is repeated a number of times and eventually 100% theoretical yield can be achieved.



(*R*)-**A**, (*S*)-**A** = Substrate enantiomers

**B** = achiral product

Figure 21. General concept of deracemisation.

Consideration of the kinetics of the cyclic deracemisation process reveals that a five-fold repetition of the oxidation-reduction sequence gives an *ee* of 97% as shown in Figure 22. There are two important parameters to consider, which are determined by the enantioselectivity of the catalyst: the maximum *ee* that can be obtained after an infinite number of cycles and the number of cycles required to reach a certain desired *ee*. However, in practice the cycles are not as defined as the theoretical model. Instead of the oxidation-reduction sequence, the oxidation and the reduction steps usually proceed in parallel.

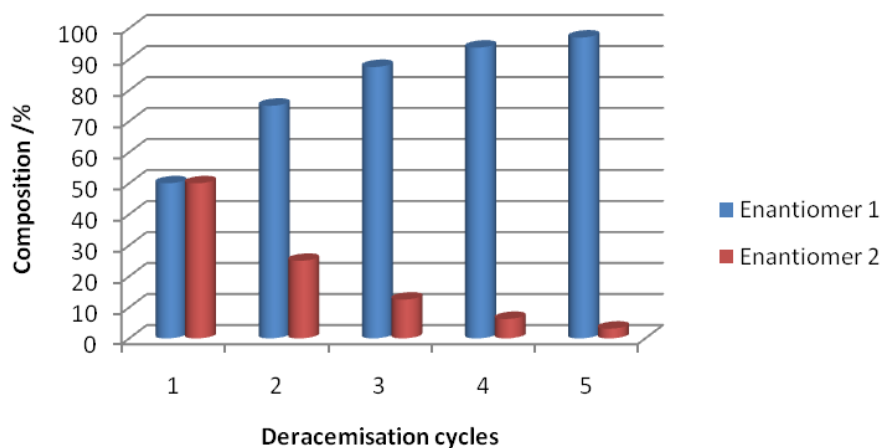


Figure 22. Composition of the enantiomers during a cyclic oxidation-reduction sequence with perfect selectivity towards oxidation.<sup>38</sup>

In order to achieve deracemisation, chemical reduction can be combined with biocatalytic oxidation. The chemoenzymatic deracemisation of DL-lactate (DL-**30**) has been achieved in a one-pot, two-step process by Oikawa *et al.* in 2001 (Figure 23).<sup>71</sup> Enantioselective biocatalytic oxidation of L-**30** was combined with non-selective reduction of pyruvate (**31**) by sodium borohydride ( $\text{NaBH}_4$ ). Full conversion of the racemate to the D-enantiomer was observed in 90 minutes at a relatively low substrate concentration (5 mM).

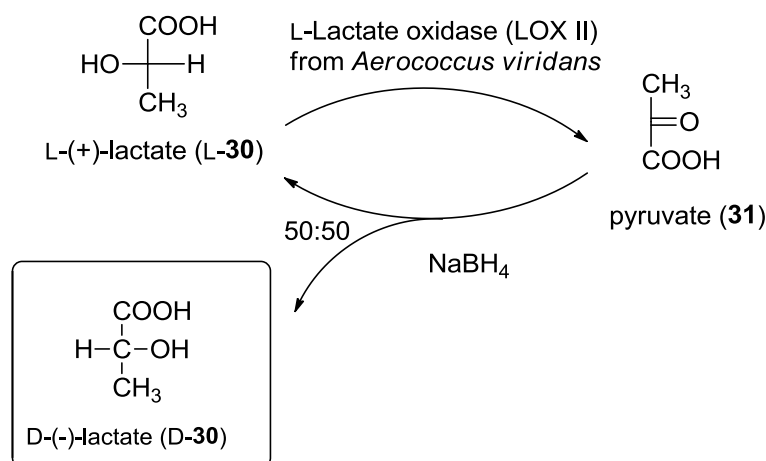


Figure 23. Deracemisation of DL-**30** by a chemoenzymatic method.<sup>71</sup>

Deracemisation of amino acids, amines and secondary alcohols has been studied extensively previously. They are discussed in §1.2.4.1 and §1.2.4.2.

### 1.2.4.1 Deracemisation of secondary alcohols

Deracemisation of secondary alcohols can be achieved by employing transition metal catalysts,<sup>72-73</sup> enzymes<sup>74-75</sup> or a combination of enzymes and transition metal catalysts.<sup>76</sup>

For deracemisation employing only metal catalysts, Adair *et al.* have reported in 2005 the deracemisation of a range of secondary alcohols with moderate *ee* employing a ruthenium catalysed non-selective oxidation and an enantioselective hydrogenation (Figure 24).<sup>72</sup> In 2007, they reported optimised deracemisation conditions with up to 99% *ee*.<sup>73</sup>

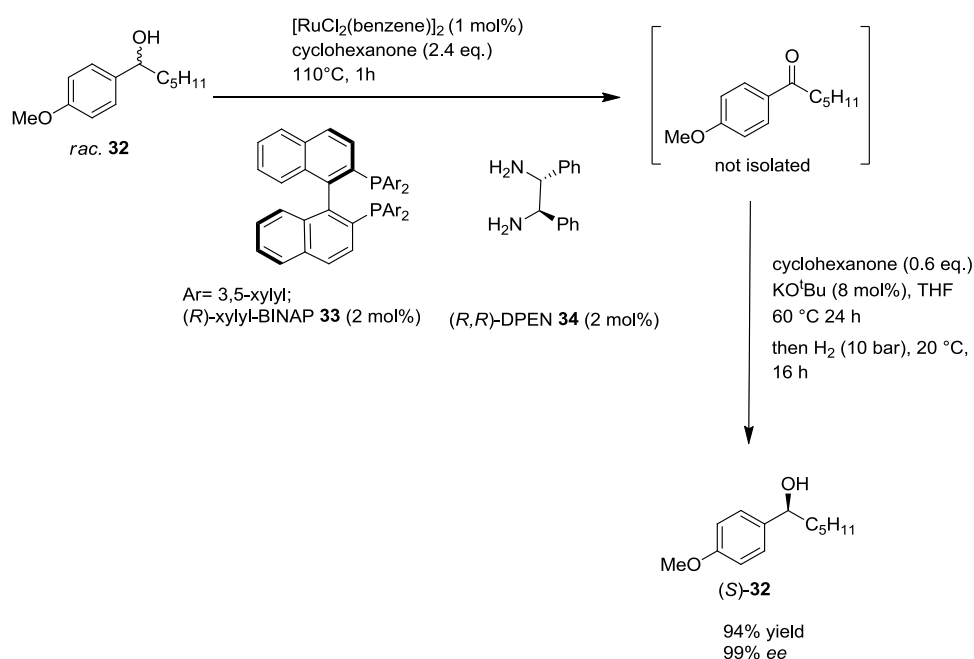


Figure 24. Deracemisation of secondary alcohols employing a ruthenium catalysed oxidation and hydrogenation.<sup>72-73</sup>

A ruthenium complex was generated by treating  $[\text{RuCl}_2(\text{benzene})]_2$  with ligands *(R)*-xylyl-BINAP **33** and *(R,R)*-DPEN **34** *in situ*. This ruthenium complex catalysed the non-selective oxidation and hydrogenation with hydrogen (10 bar). The alcohol **32** was then recovered yielding the *(S)*-enantiomer with 99% *ee*.

Other than employing only one metal catalyst for both of the oxidation and reduction, Shimada *et al.* have reported the deracemisation of secondary

alcohols **14** by a two-step process through the combination of two ruthenium complexes (Figure 25). A combination of (*S*)-selective oxidation catalysed by the Noyori ruthenium complex  $[\text{RuCl}\{(\text{S,S})\text{-tsDPEN}\}(\eta^6\text{-mesitylene})]$  (Figure 25, **35**) and (*R*)-selective reduction by  $[\text{RuCl}_2(\text{PPh}_3)(\text{ip-FOXAP})]$  (ip-FOXAP = isopropylferrocenyloxazolinylphosphine) (Figure 25, **36**) gives high yields and up to 95% *ee* of a range of benzylic alcohol substrates.<sup>77</sup>

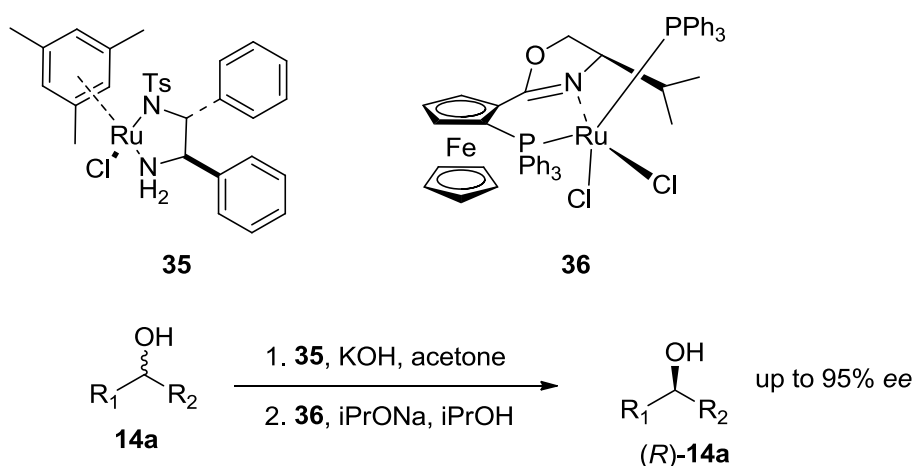


Figure 25. Deracemisation of secondary alcohols catalysed by a combination of two ruthenium metal complexes.<sup>77</sup>

For deracemisation employing only enzymes, the group of Kroutil and Faber have conducted a number of studies.<sup>38,74-75</sup> In one study deracemisation was achieved by employing enantioselective enzymatic oxidation by *Alcaligenes faecalis* and stereoselective reduction by an alcohol dehydrogenase (ADH from *Rhodococcus ruber*: ADH-A, or ADH from *Lactobacillus kefir*: LK-ADH).<sup>74</sup> A range of secondary alcohols were deracemised in 4-22 h with both *ee* and yields of up to 99%.

Later, both of these alcohol dehydrogenases were employed in a concurrent deracemisation process (Figure 26).<sup>75</sup> In this one-pot process, for the production of the (*S*)-alcohol, the NADPH-dependent alcohol dehydrogenase (*R*)-LK-ADH and NADH-dependent (*S*)-ADH-'A' were added. Independent cofactor recycling systems were also added to this reaction, including the recycling system for NADPH: YcnD NADPH oxidase; and the recycling



system for NADH: NADH-dependent-formate dehydrogenase FDH and formate. In addition, by using alcohol dehydrogenases with different enantioselectivities ((*S*)-selective TB-ADH: ADH from *Thermoanaerobium brockii*; and (*R*)-selective ADH-PR2: commercial ADH), both the *R* and *S* products of the alcohols were obtained in excellent *ee* and yields. It was demonstrated that successful deracemisation can be achieved by using only enzymes. The recycling systems can be combined without affecting each other.

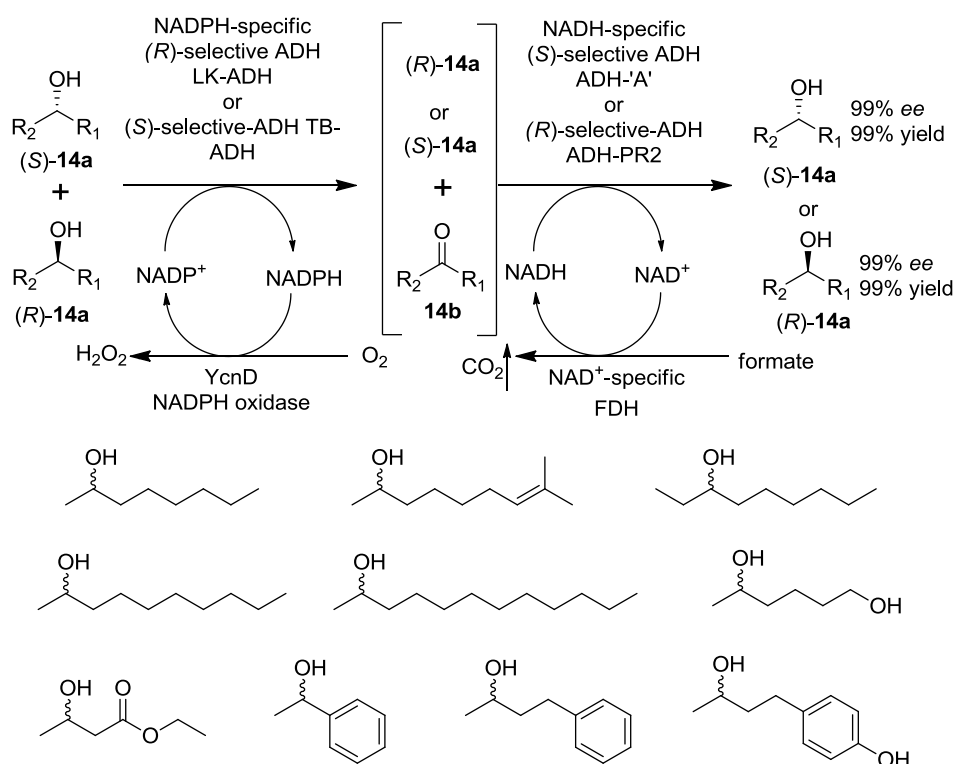


Figure 26. Concurrent deracemisation using a combination of alcohol dehydrogenases.<sup>75</sup> The structures below the reaction scheme represent the substrate alcohols and products in 99% *ee* and 99% yield were obtained for all of these substrates.

In the group of Chadha, deracemisations have been conducted using whole cells. Titu *et al.* reported that *Candida parapsilos* can be applied for the deracemisation of alcohols.<sup>78</sup> Racemic alcohols were converted to (*R*)-alcohol using only this enzyme and water at room temperature. It is believed that possibly an enantioselective oxidation and a complementary enantioselective reduction occurred during the reaction. This is supported by the detection of the ketone intermediate by reverse phase HPLC. Good to excellent *ee* (76%-99%)

and good yields (68%-78%) were obtained.

For deracemisation employing a combination of enzymes and transition metal catalysts, only one example has been reported. Mutti *et al.* employed an iridium metal catalyst **39**, for the non-selective oxidation, with an enzyme, ADH-A, for the asymmetric reduction, to achieve deracemisation of secondary alcohols (Figure 27).<sup>76</sup> They optimised the hydrogen acceptor (**40**) for the metal catalyst and conducted studies to improve the compatibility of the enzyme with the metal catalyst. The final composition of the alcohol (*R*)-**37** reached 99.9%; nevertheless, the maximum *ee* was only 40%.

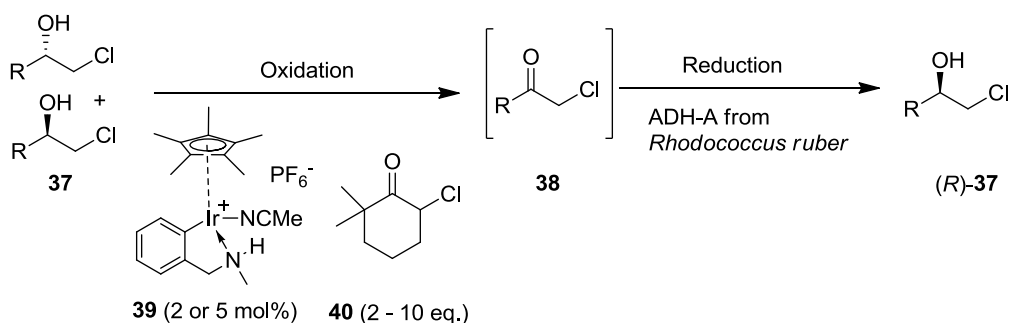


Figure 27. Deracemisation of secondary alcohols employing an iridium metal catalyst and an enzyme.<sup>76</sup>

#### 1.2.4.2 Deracemisation of amino acids and amines

Unnatural amino acids are of increasing importance for pharmaceutical, agrochemical, and other industrial applications, and biocatalysis is used widely next to chemical methods for the industrial-scale manufacture of such chiral compounds.<sup>79</sup> Optimised methods which are applicable for the deracemisation of both amino acids and amines have been extensively investigated in the past few years.

In the Turner group methods employing porcine kidney D-amino acid oxidase (D-AAO) and a hydride reducing agent (Sodium cyanoborohydride ( $\text{NaCNBH}_3$ ) or  $\text{NaBH}_4$ ) to achieve deracemisation have been developed.<sup>80</sup> The deracemisation of DL-amino acids has also been accomplished by using

L-amino acid oxidase (L-AAO) from *Proteus myxofaciens* and amine-boranes as chemical reducing agents.<sup>81</sup> Amine-boranes were shown to have a better reactivity than the hydride reducing agents NaCNBH<sub>3</sub> and NaBH<sub>4</sub>.<sup>79</sup>

Deracemisation of amines has also been extensively studied in the Turner group. Variants of MAO-N were obtained by directed evolution, and these variants were applied in the deracemisation of primary,<sup>82-83</sup> secondary<sup>84</sup> and tertiary amines.<sup>85</sup>

Deracemisation of the primary amine  $\alpha$ -methylbenzylamine (**41**) has been achieved by employing a MAO-N mutant with a single mutation Asn336Ser, and amine-boranes as the non-selective reducing agents (Figure 28).<sup>83</sup> 47-fold improvement in activity and 6-fold in selectivity of the mutant were shown by assaying against **41**, benzylamine and amylamine. When using this mutant in the deracemisation of **41**, 93% *ee* in 77% yield of (*R*)-**41** was obtained.

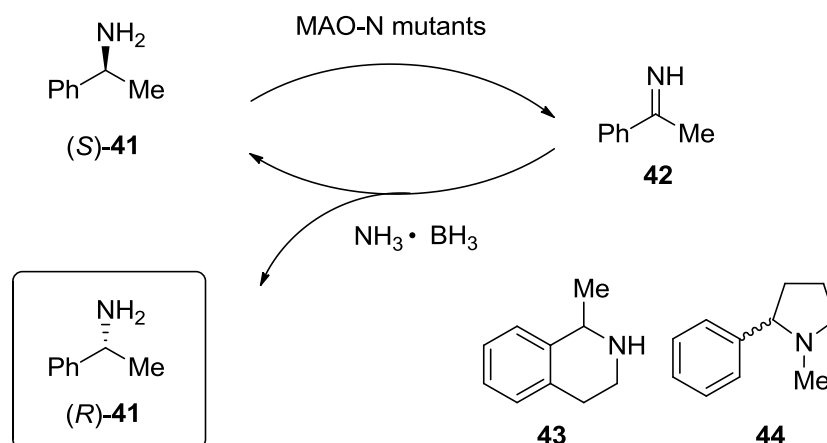


Figure 28. Deracemisation of **41**, **43** and **44** using MAO-N mutants in combination with amine-boranes as the reducing agent.<sup>83</sup>

Later, a broad range of primary and secondary amines (51 examples) were screened for activity with the Asn336Ser MAO-N mutant with an additional mutation Met348Lys.<sup>82</sup> Good activity was obtained with more than half of the substrates (33 out of 51 with more than 5% activity of **41**).

Since the Asn336Ser MAO-N mutant showed only low to moderate activity towards chiral secondary amines, a new MAO-N mutant D3 was generated with one additional important mutation Ile246Met.<sup>84</sup> This mutant

was subsequently applied to preparative deracemisation of the secondary amine 1-methyltetrahydroisoquinoline (Figure 28, **43**) and 71% isolated yield and 99% *ee* were obtained. Furthermore, immobilisation of the enzyme resulted in a higher yield of 95% with 99% *ee*.

Later, the mutant MAO-N D5 with 5 mutations Ile246Met, Asn336Ser, Met348Lys, Thr384Asn and Asp385Ser was found to show high enantioselectivity and activity towards tertiary amines.<sup>85</sup> Preparative deracemisation of N-methyl-2-phenylpyrrolidine (Figure 28, **44**) was carried out and (*R*)-**44** was obtained in 75% isolated yield with 99% *ee*.

Subsequently, the structures of MAO-N D3 and D5 mutants were resolved,<sup>86-87</sup> and further applications of these mutants have been developed in the Turner group.<sup>70,88-89</sup>

### 1.2.5 Summary

In summary, resolution and asymmetric synthesis techniques are very important tools for the production of enantiopure compounds. The novel methods DKR and deracemisation, in particular, have drawn significant research interests during the past decades.

DKR provides an excellent solution to the problem of 50% maximum yield by kinetic resolution. DKR by a combination of enzymes and transition metal catalysts also demonstrates an interesting concept that can be applied to methods other than DKR. For example, deracemisation employing a combination of enzymes and transition metal catalysts will be discussed in §3.

Deracemisation is also an effective method for the synthesis of optically pure compounds in 100% theoretical yield. Deracemisation of amino acids, amines and secondary alcohols has been achieved by a variety of methods including a combination of enzymes and stoichiometric chemical reducing agents, multiple transition metal catalysts, multiple enzymes and a combination of enzymes and transition metal catalysts.

## 2. Results and Discussion – Application of GOase in the Deracemisation of Secondary Alcohols

Deracemisation is one of the most promising methods for producing enantiopure compounds. In §1.2.4, methods for the deracemisations of secondary alcohols, amino acids and amines were reviewed.

Previous work conducted in the Turner group showed that a variant ( $M_{3-5}$ ) of GOase was able to catalyse the oxidation of a broad range of secondary alcohols with high enantioselectivities (see §1.1.2).<sup>1</sup> Deracemisation of racemic secondary alcohols could in principle be achieved by carrying out enantioselective oxidation catalysed by GOase  $M_{3-5}$  with concurrent non-selective reduction of the ketone product (Figure 29). The major challenge is to identify a reducing agent that is compatible with the enzyme under aqueous conditions.

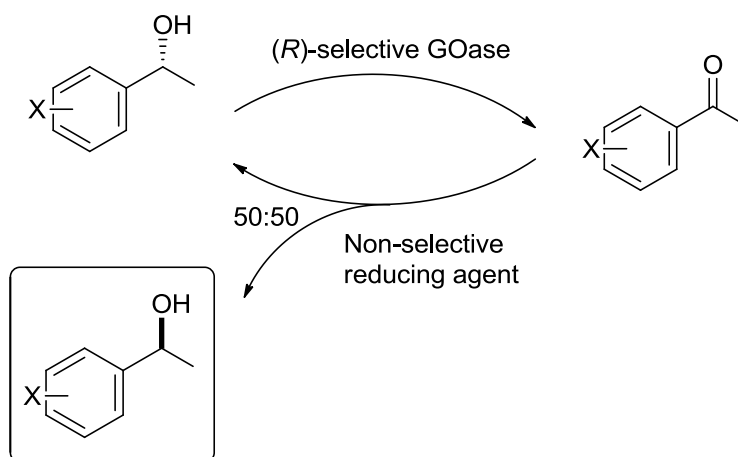


Figure 29. Deracemisation of secondary alcohols.

## 2.1 Production of GOase

### 2.1.1 Expression and purification of GOase

GOase in a purified form is employed in both the projects discussed in §2 and §3. The gene of this protein was expressed in *E.coli* BL21 star cells and the cells were cultivated as described in §6.2.1. The cells were then lysed by sonication to generate a cell free extract (CFE) and the protein was purified on a Hi Trap<sup>TM</sup> Ni affinity column. The principle of the method is based on reversible interaction between the His tag and a chelating complex with Ni<sup>2+</sup> metal ions, resulting in the elution of pure protein. The eluted fractions were then collected, pooled and analysed by SDS-PAGE (sodium dodecylsulphate polyacrylamide gel electrophoresis) as described in §6.2.1.3 (Figure 30).

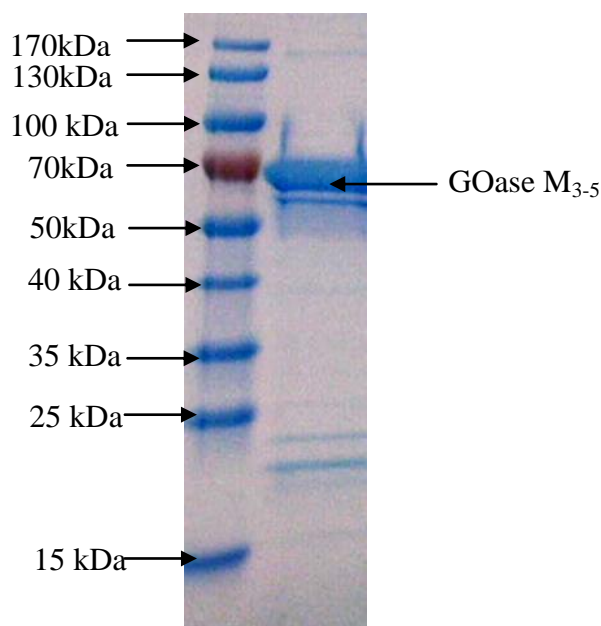


Figure 30. SDS-PAGE image of a pure GOase M<sub>3.5</sub> sample.

Typical yields of 8-10 mg of pure protein per litre of shake flask culture can be obtained from the production of the purified protein. The purified protein was stored at -80 °C in 0.5 mg and 1 mg aliquots in sodium phosphate buffer (NaPi buffer, 100mM), and used directly in the biotransformation reactions.

### 2.1.2 Activity assay of GOase M<sub>3-5</sub>

Kinetic measurements of GOase M<sub>3-5</sub> has been previously published using 3'-fluoro-1-phenylethanol (**64**) as the substrate.<sup>1</sup> The activity of the enzyme was determined by performing the enzymatic oxidation of **64** under the following conditions: 1 g/L GOase M<sub>3-5</sub>, 50 mM substrate, 1 g/L peroxidase and 0.1 g/L catalase, in water with a 0.5 mL total volume at 30 °C and shaking at 250 rpm.

Samples were taken every 10 min during the first hour and again at 90 min. HPLC was employed to analyse the samples and the *ee* was plotted against time. The traces obtained were compared among different batches as shown in Figure 31.

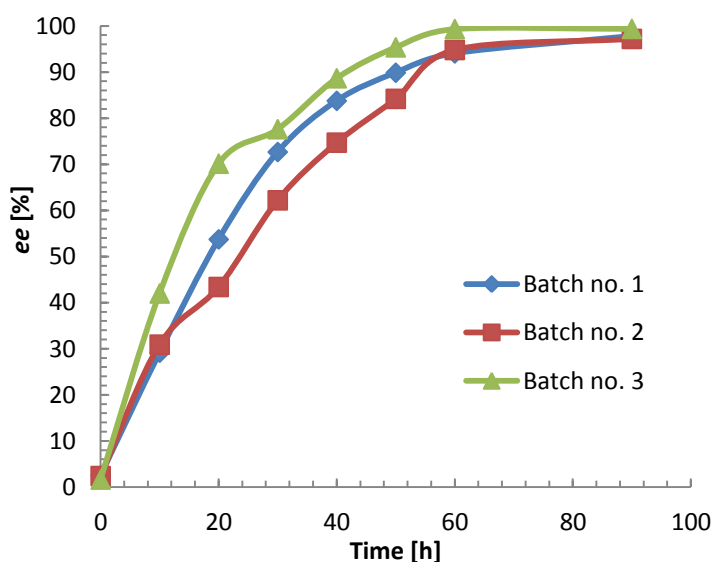


Figure 31. Activity assay for GOase M<sub>3-5</sub>.

As shown in Figure 31, the activity of the enzyme among different batches is comparable. Subsequent biotransformations were then performed by directly defrosting the protein stock from -80 °C.

## 2.2 Deracemisation employing chemical reducing agents

To achieve deracemisation, the reducing agent must be stable and active under aqueous conditions and also be compatible with the enzyme. As a result, the

initial screening was carried out under aqueous conditions with a range of chemical reducing agents against a typical secondary ketone substrate (4'-methoxyacetophenone, **46**). Reactions were monitored by chiral HPLC. The names and structures of the reducing agents are shown in Table 2.

Table 2. Screening of reducing agents for deracemisation.

Reaction scheme: 4'-methoxyacetophenone (**46**) reacts with chemical reducing agents in water at 30 °C to produce a racemic mixture of (R)-45 and (S)-45.

Entry	Reducing Agents	Structures	Activity in water	No.
1	Sodium borohydride	NaBH <sub>4</sub>	Yes	
2	Borane-pyridine complex		No	47
3	Sodium cyanoborohydride	NaCNBH <sub>3</sub>	No	48
4	Borane <i>tert</i> -butylamine complex		Yes	49
5	Amine-borane	NH <sub>3</sub> • BH <sub>3</sub>	Yes	50
6	Lithium triethylborohydride	LiB(C <sub>2</sub> H <sub>5</sub> ) <sub>3</sub> H	Yes	51
7	Sodium trimethoxy borohydride	NaB(OCH <sub>3</sub> ) <sub>3</sub> H	No	52
8	Zinc borohydride, polymer-bound (poly(4-vinylpyridine))		No	53
9	Polymer-bound borane-morpholine		No	54
10	Tributyltin hydride-functionalized silica gel		No	55

Reaction conditions: 50 mM **46**, reducing agents (5 eq., hydride mol excess to the substrate), in water, 30 °C, 250 rpm, total volume: 0.5 - 1 mL.



The reducing agents that showed activity under these conditions were:  $\text{NaBH}_4$ , borane *tert*-butylamine complex (**49**), amine-borane (**50**) and lithium triethylborohydride (**51**).

However, when **51** was dissolved in either water or buffer, a sharp rise in the pH of the solution was observed (pH 10-11), which would not be compatible with the enzyme. Therefore, only  $\text{NaBH}_4$ , **49** and **50** were employed in the further deracemisation studies.

The deracemisation with **50** is shown in Figure 32. The reaction was carried out by employing GOase  $M_{3.5}$  to oxidise (*R*)-**45** to the ketone **46**; followed by the addition of the reducing agent **50** as the second step.

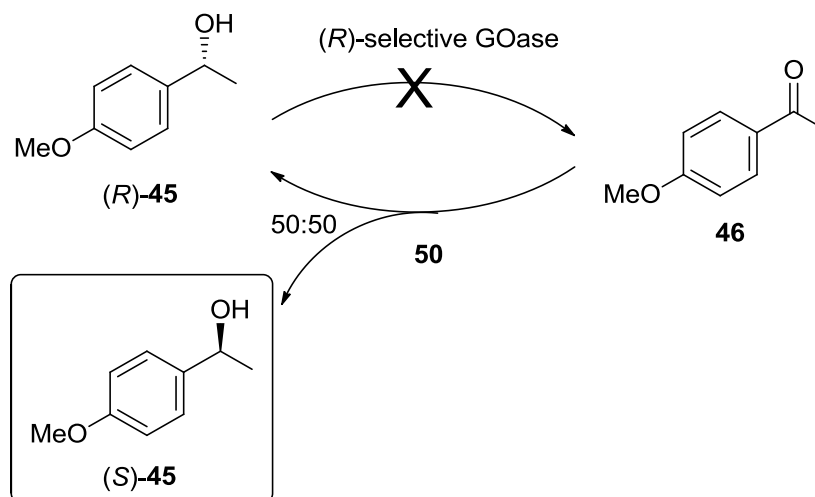


Figure 32. Deracemisation of a secondary alcohol (**45**) with reducing agent **50** and GOase  $M_{3.5}$ .

The oxidation was allowed to proceed for 2 h prior to the addition of an excess of **50**.

Table 3. Deracemisation of **46** with GOase  $M_{3.5}$  and **50**.

Entry	Time [h]	<i>ee</i> [%]	<b>45</b> [%]
<b>1</b>	2	99	45
Addition of 5 eq. <b>50</b>			
<b>2</b>	7	51	96
<b>3</b>	26	49	99

Reaction conditions: 50 mM **46** (0.025 mmol), 14 mg **50** (5 eq.), 1 g/L GOase  $M_{3.5}$ , 1 g/L HRP, 0.1 g/L catalase, in water, 30 °C, 250 rpm, total volume: 0.5 mL.

The reaction was carried out in NaPi buffer (1M, pH 7), and the pH was maintained at 7.5-8.0. Table 3 shows the *ee* and **45** [%] as a function of time. The presence of 45% **45** with 99% *ee* after 2 h indicates that only (S)-**45** and **46** were remaining in the system.

Addition of the reducing agent **50** resulted in a decrease in the *ee* of (S)-**45** to 50% after 5 h and an increase in conversion to 96% suggesting that almost all of the ketone **46** was reduced unselectively.

After a further 24 h there was little change in conversion or *ee*, suggesting that the enzyme had lost its activity. Therefore we concluded that the reducing agent **50** was not compatible with the enzyme under these conditions.

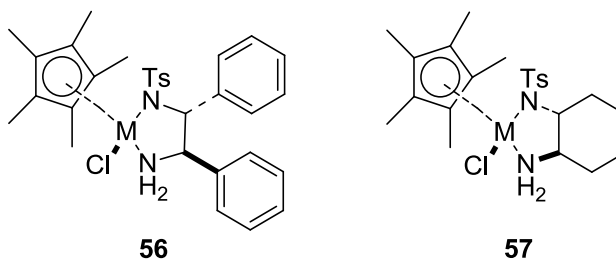
Other attempts using NaBH<sub>4</sub> and **49** met with little success. Therefore, further efforts were invested into identifying an alternative class of reducing agent that might be compatible with GOase M<sub>3-5</sub> activity.

## 2.3 Deracemisation employing transfer hydrogenation (TH) and asymmetric transfer hydrogenation (ATH)

Transfer hydrogenation (TH) and asymmetric transfer hydrogenation (ATH) by transition metal catalysts in water offer several potential advantages compared to conventional chemical reducing agents. Firstly, reduction of the ketone occurs via a catalytic method, thus potentially circumventing the problem associated with stoichiometric reducing agents. Secondly, several of these transition metal catalysts are active in water at neutral pH, room temperature and in the presence of oxygen. Such conditions are likely to be compatible with enzymes compared to the basic conditions generated by the reducing agents in Table 2.

TH and ATH have both attracted increasing attention in the last two decades due to their potential for applications in the synthesis of fine chemicals. Developments in the field of ATH have resulted in a range of

catalysts which show excellent enantioselectivities towards a wide range of substrates in the reduction of ketones.<sup>90</sup>



M-TsDPEN (M = Rh, Ir)

M-TsCYDN (M = Rh, Ir)

Figure 33. Structures for transition metal catalysts developed in the Xiao group.<sup>91-92</sup>

Following work by Noyori, Ikariya, Hashiguchi and co-workers on asymmetric transfer hydrogenation with a TsDPEN-coordinated (TsDPEN = N-(*p*-toluenesulfonyl)-1,2-diphenylethylenediamine) Ru(II) complex (Ru-TsDPEN) precatalyst,<sup>93-94</sup> the group of Professor Jianliang Xiao has also contributed significantly to this area.<sup>90-92,95-98</sup> Several transition metal catalysts were developed in the Xiao group for TH of aldehydes and ATH of prochiral ketones (Figure 33, **56** and **57**).<sup>91,99</sup> A concerted hydrogen transfer mechanism was proposed for ATH of ketones and the full catalytic cycle is shown in Figure 34.

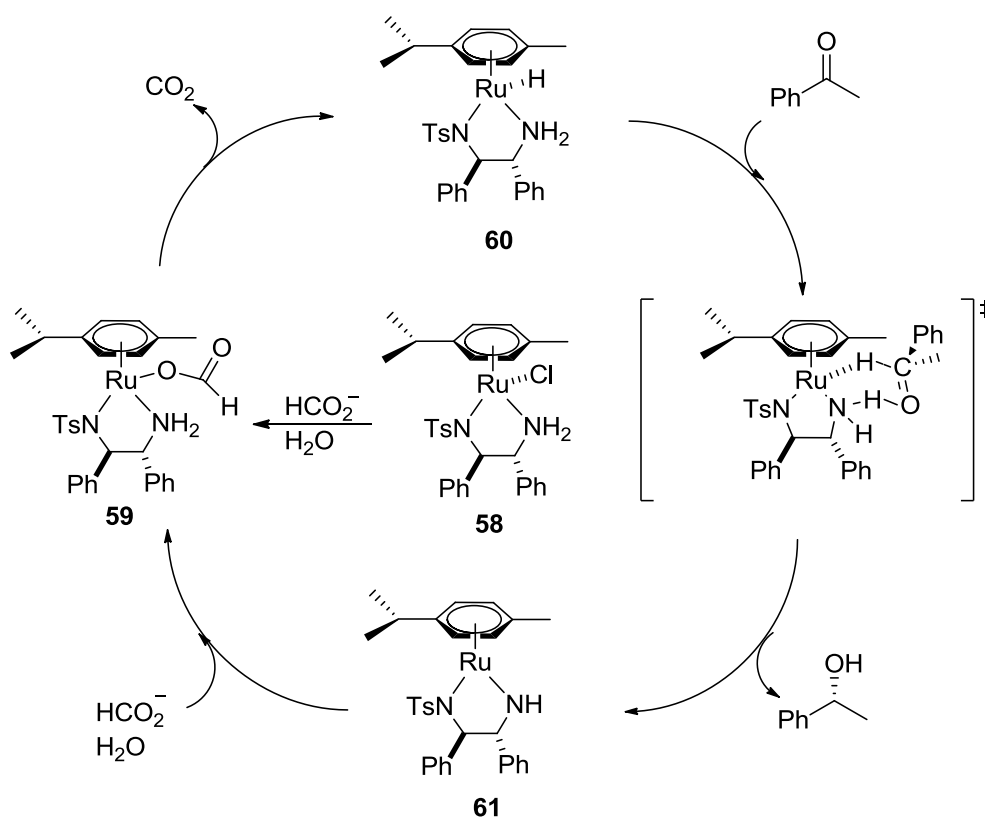


Figure 34. Proposed concerted hydrogen transfer mechanisms for ATH of acetophenone with Ru-TsDPEN in water.<sup>94,100</sup>

Complexes **58**, **60** and **61** were synthesised and isolated by Noyori, Ikariya and co-workers and used in non-aqueous media with **58** being the precatalyst.<sup>101</sup> Reaction rates were measured for the 18e amino hydride **60** and the 16e complex **61** and they were both shown to be active.<sup>100</sup>

As shown in Figure 35, we envisaged a system for deracemisation in which the oxidation step was catalysed by GOase M<sub>3-5</sub> (*R*-selective) and the reduction step catalysed by the transition metal catalysts (non-selective or *S*-selective).

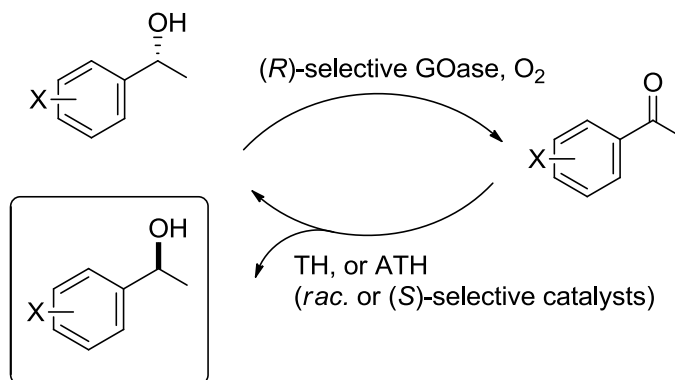


Figure 35. Deracemisation of secondary alcohols employing TH or ATH.

For the transition metal catalysts and GOase  $\text{M}_{3-5}$  to be compatible with each other, it is vital to identify a suitable transition metal catalyst, and more significantly, to identify a system where the performance of the enzyme and the transition metal catalysts are not adversely affected by the presence of each other. Therefore, optimisation was conducted subsequently employing 4'-nitro-1-phenylethanol (**62**) and 3'-fluoro-1-phenylethanol (**64**) as model substrates.

### 2.3.1 Optimisation of the oxidation step

#### 2.3.1.1 Substrate concentration

For the purpose of identifying an optimum substrate concentration, a series of oxidation reactions was performed at varying substrate concentrations in the absence of the reducing agents (Figure 36).

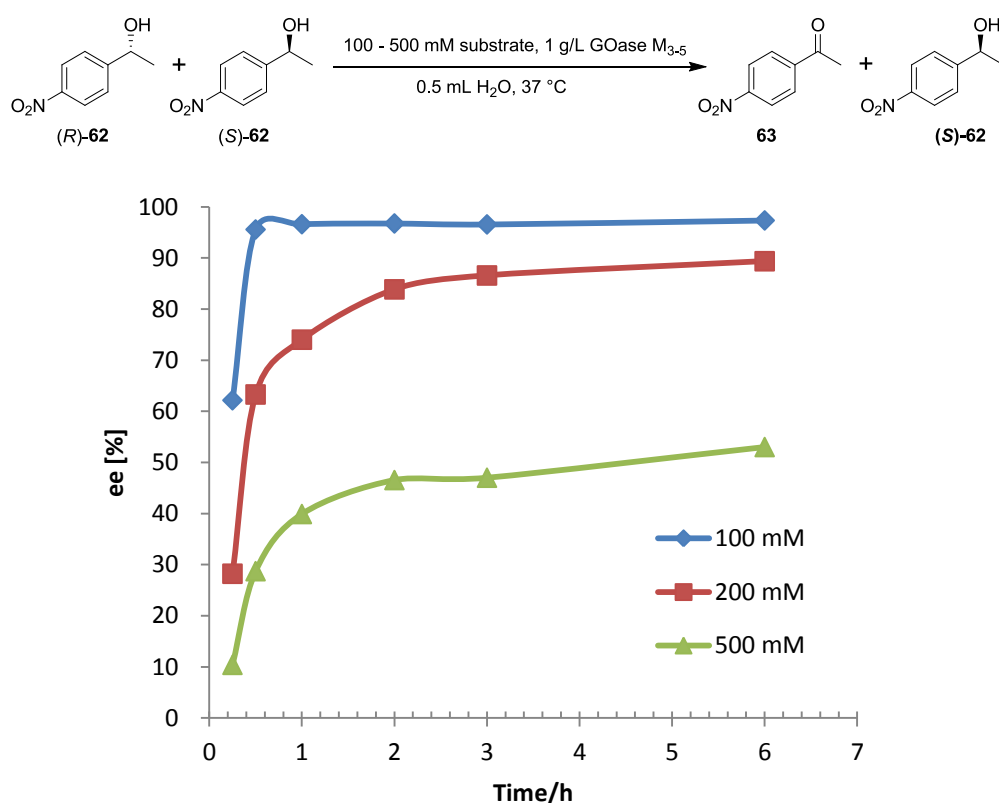


Figure 36. Oxidation of **62** at varying substrate concentrations.

Reaction conditions: 100-500 mM (0.05-0.25 mmol) **62**, 1 g/L GOase M<sub>3-5</sub>, 1 g/L HRP, 0.01 g/L catalase, in water, , 37 °C, 900 rpm, total volume: 0.5 mL.

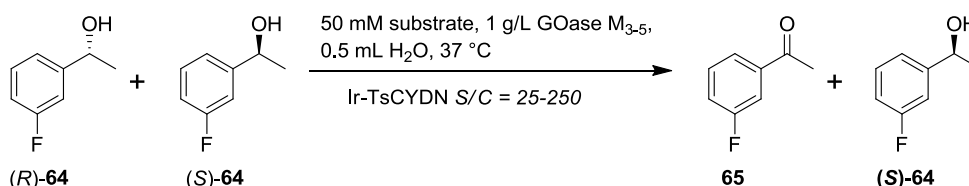
At a substrate concentration above 100 mM, the reaction did not proceed to completion, for example at 200 mM concentration after 6 h the *ee* of the alcohol had only reached 90%. As a result, substrate concentrations less than 100 mM were used in the deracemisations. A reaction temperature of 37 °C was also employed and no loss of activity of the enzyme was observed. Therefore further studies were conducted at 37 °C since this is a good compromise for the enzyme and transition metal catalyst activity.

### 2.3.1.2 Concentration of the transition metal precatalysts

Transition metal catalysts were observed to reduce the activity of GOase M<sub>3-5</sub> to some extent. To investigate the maximum concentration of the metal catalyst that the enzyme could tolerate, a series of oxidation reactions in the presence of

various concentrations of Ir-TsCYDN was performed (Table 4). The metal precatalyst was synthesised by reacting  $[\text{Cp}^*\text{IrCl}_2]_2$  and 1.2 eq. of the ligand TsCYDN in water at 40 °C. The solution containing the catalyst was then used directly for the reactions.

Table 4. Oxidation of **64** by GOase M<sub>3-5</sub> in the presence of Ir-TsCYDN.



Entry	Time [h]	Ir-TsCYDN <sup>[a]</sup> [ $\mu\text{L}$ ]	S/C <sup>[b]</sup>	ee [%]	Enzymatic concentration [g/L]
1	18	10	250	100	1
2	18	20	125	100	1
3	18	40	63	88	1
4	18	60	42	50	1
5	24	40	63	100	2
6	24	50	50	100	2
7	24	80	31	100	2
8	24	100	25	96	2

[a] The quantity is the volume of the precatalyst solution used in the reaction. [b] S/C refers to the substrate to catalyst molar ratio.

Reaction conditions: 50 mM (0.025 mmol) **64**, 10-100  $\mu\text{L}$  Ir-TsCYDN (S/C = 250-31), 1-2 g/L GOase M<sub>3-5</sub>, 1 g/L HRP, 0.1 g/L catalase, in water, 37 °C, 900 rpm, total volume: 0.5 mL.

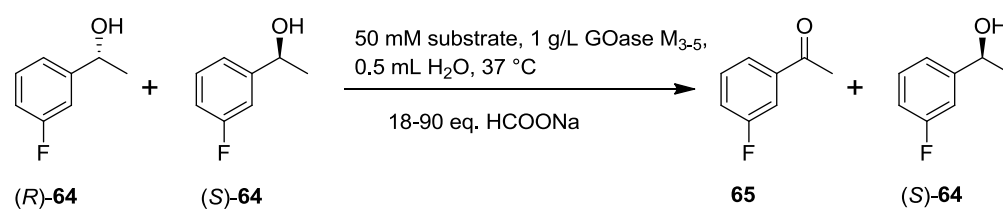
At 1 g/L enzyme concentration, the maximum concentration of Ir-TsCYDN catalyst that can be used in conjunction with GOase M<sub>3-5</sub> without losing enzyme activity is between S/C ratios 125-63 (20 - 40  $\mu\text{L}$ , S/C refers to the substrate to catalyst molar ratio). When a higher concentration of Ir-TsCYDN was used, a dramatic decrease of the *ee* to 50% was observed. These conditions (Ir-TsCYDN in 125-63 S/C ratio) were then applied to a deracemisation reaction but the results were disappointing (conversion to

(*S*)-**64** < 60%). Therefore, the enzyme concentration was increased to 2 g/L so that 80-100  $\mu$ L of Ir-TsCYDN (S/C = 25-31) could be used without loss of activity. As shown in Table 4, only 4% loss of *ee* was observed when 100  $\mu$ L of Ir-TsCYDN (S/C = 31) added. These conditions were subsequently applied to the deracemisation reaction and will be discussed in §2.3.3.

### 2.3.1.3 Concentration of sodium formate (HCOONa)

Other than the precatalyst, another important component for the reduction step is the hydrogen donor sodium formate (HCOONa). It was observed that the addition of HCOONa can reduce the rate of the oxidation step as determined by monitoring the *ee* of the process (Table 5).

Table 5. Oxidation of **64** by GOase M<sub>3-5</sub> in the presence of HCOONa.



Entry	Time [h]	HCOONa [mg]	HCOONa [eq.]	<i>ee</i> [%]
1	18	20	12	100
2	18	60	36	73
3	18	90	54	45
4	18	150	90	29

Reaction conditions: 50 mM (0.025 mmol) **64**, 30-150 mg HCOONa (12-90 eq.), 1 g/L GOase M<sub>3-5</sub>, 1 g/L HRP, 0.1 g/L catalase, in water, 37 °C, 900 rpm, total volume: 0.5 mL.

To determine the maximum concentration of HCOONa compatible with the enzyme, oxidations by GOase M<sub>3-5</sub> were performed in the presence of various concentrations of HCOONa. When 36 eq. of HCOONa was used, the *ee* of the reaction decreased dramatically from 100% to 73%. Further decreases in *ee* was observed with increasing concentrations of HCOONa.



Thus, 12 eq. of HCOONa at a 50 mM substrate concentration (24 eq. at a 25 mM substrate concentration) were used in the deracemisation reactions as the maximum concentration of HCOONa.

### 2.3.2 Optimisation of the reduction step

#### 2.3.2.1 Oxygen (O<sub>2</sub>) bubbling

The presence of O<sub>2</sub>, which is required for the oxidation step, has been shown to decrease the activity of the transition metal catalysts.<sup>91</sup> Heiden *et al.* provided a possible explanation which is that oxygen could serve as a competing hydrogen acceptor and the 18e amino hydride could react with molecular oxygen.<sup>102</sup> Experiments were therefore carried out to establish the effect of O<sub>2</sub> on the reduction step of the deracemisation.

Table 6. Side reaction: O<sub>2</sub> inhibition of the reduction step.

Entry	Time [h]	ee [%]	62 [%]	63 [%]	O <sub>2</sub> bubbling
1	24	68	67	32	Yes
2	24	68	98	2	No

Reaction conditions: 500 mM (0.5 mmol) **63**, 37 °C, 900 rpm, 0.75 mL (*S*)-selective *Rh*-TsDPEN (*S/C* = 100), 340.1 mg HCOONa (10 eq.), total volume: 1 mL.

Table 6 shows that with O<sub>2</sub> bubbling, the percentage of the unreacted **63** is 32%, which is significantly higher compared to the percentage (2%) without O<sub>2</sub> bubbling.

Another two GOase M<sub>3.5</sub> catalysed oxidation reactions were performed with and without O<sub>2</sub> bubbling (data not shown) and it was observed that oxidation without O<sub>2</sub> bubbling only resulted in a 5% loss of *ee*. Hence, O<sub>2</sub> bubbling was not employed in the deracemisations reactions.

### 2.3.2.2 Reversed reaction catalysed by the metal catalyst

Previous research conducted in the Xiao group has established that the Rh-TsDPEN catalyst also catalyses the reverse reaction, namely the oxidation of secondary alcohols.<sup>91</sup> The oxidation of **62** was subsequently performed employing the (*S*)-selective Rh-TsDPEN catalyst and HCOONa (Table 7).

Table 7. Oxidation of **62** catalysed by (*S*)-selective Rh-TsDPEN.

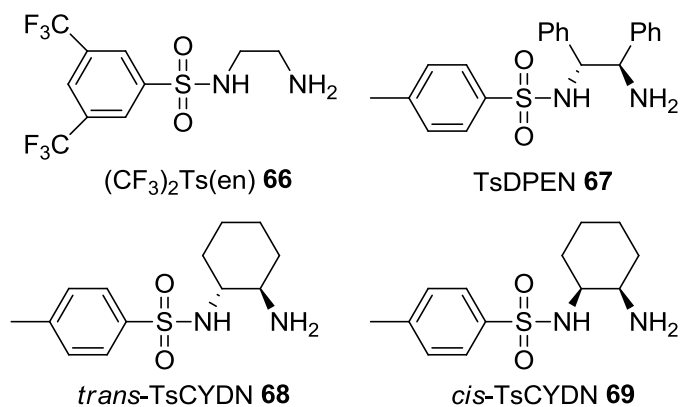
Entry	Time [h]	<i>ee</i> [%]	<b>62</b> [%]	<b>63</b> [%]
1	48	13	98	2

*Reaction conditions: 500 mM (0.5 mmol) 63, 37 °C, 900 rpm, 0.75 mL (S)-selective Rh-TsDPEN (S/C = 100), 340.1 mg HCOONa (10 eq.), total volume: 1 mL.*

Indeed, a small amount (2%) of the ketone was produced after 48 h. Therefore, attention was focused on the first 48 h of the reaction and samples were mostly taken during the first 48 h of the deracemisation reactions.

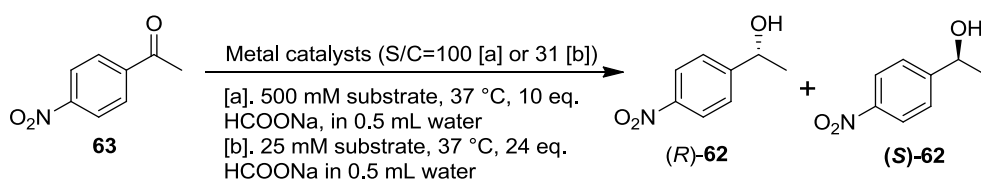
### 2.3.2.3 Transition metal catalysts ligand screening and optimisation of substrate concentration

Four different ligands (**66-69**) were investigated. Metal precatalysts were prepared *in situ* with these ligands and [Cp\**M*Cl<sub>2</sub>]<sub>2</sub> (*M* = Ir, Rh). Reductions of **63** were carried out at a 500 mM concentration, which are the standard conditions reported by Wu *et al.*<sup>91</sup> The structures of the metal ligands are shown in Figure 37.

Figure 37. Transition metal ligands screened against **63**.

The conversion of ketone to alcohol was 99% after 3 h when using Rh-TsCYDN as the catalyst and 73% when using Rh-(CF<sub>3</sub>)Ts(en) (Table 8, entries 1 and 2). Similarly the Ir-TsCYDN catalyst gave a conversion of 99% (Table 8, entries 2 and 3).

Table 8. Optimisation of concentration and ligands for the reducing agents.



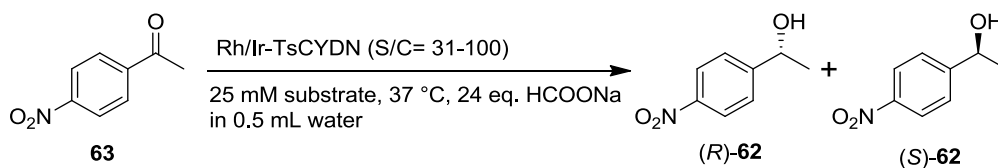
Entry	Time [h]	Transition metal catalysts	<b>62</b> [%]
<b>1</b> <sup>[a]</sup>	3	Rh-(CF <sub>3</sub> ) <sub>2</sub> Ts(en) (ligand <b>66</b> )	73
<b>2</b> <sup>[a]</sup>	3	Rh-TsCYDN (ligand <b>68</b> )	99
<b>3</b> <sup>[a]</sup>	3	Ir-TsCYDN (ligand <b>68</b> )	99
<b>4</b> <sup>[b]</sup>	3	Rh-TsCYDN (ligand <b>68</b> )	98
<b>5</b> <sup>[b]</sup>	3	Ir-TsCYDN (ligand <b>68</b> )	99
<b>6</b> <sup>[b]</sup>	3	Rh-TsDPEN ( <i>rac.</i> ) (ligand <b>67</b> )	72

Reaction conditions: [a], 500 mM (0.5 mmol) **63**, 37 °C, 900 rpm, 0.75 mL transition metal catalysts (S/C = 100), 340.1 mg HCOONa (10 eq.), total volume: 1 mL. [b], 25 mM (0.0125 mmol) **63**, 37 °C, 900 rpm, 80 µL transition metal catalysts, 20 mg HCOONa (24 eq.), total volume: 0.5 mL.

However, a 500 mM substrate concentration could not be applied in the deracemisations due to the limitation of substrate loading of the enzyme as discussed in §2.3.1.1. Moreover, the concentration of metal catalyst and HCOONa at this substrate concentration are higher than the enzyme can tolerate. Therefore, further optimisation of the reduction step was performed with lower concentrations of metal catalyst (Table 8, entries 4-6; Table 9). The metal catalyst Rh-(CF<sub>3</sub>)<sub>2</sub>Ts(en) was not employed in further studies due to the low activity as shown in Table 8, entry 1. The catalysts Ir/Rh-TsCYDN also showed significantly higher activity than (*rac.*) Rh-TsDPEN. Therefore, the catalyst Rh-TsDPEN was not investigated further. Employing a non-chiral metal catalyst, Ir-*cis*-TsCYDN, only gave poor conversions. Thus, unless otherwise specified, all of the Ir-TsCYDN catalysts used thereafter in the deracemisation reactions were *rac.* Ir-*trans*-TsCYDN.

As a result, Rh/Ir-TsCYDN were employed in further studies of the reduction of **63** and the results are shown in Table 9.

Table 9. Optimisation of metal catalyst concentration.



Entry	Time [h]	Transition metal catalysts [μL]		S/C	62 [%]
1	3	Rh-TsCYDN	25 μL	100	77
2	3	Rh-TsCYDN	30 μL	83	81
3	3	Rh-TsCYDN	35 μL	71	84
4	1	Rh-TsCYDN	80 μL	31	79
5	4	Rh-TsCYDN	80 μL	31	99
6	3	Ir-TsCYDN	25 μL	100	87
7	3	Ir-TsCYDN	30 μL	83	89
8	3	Ir-TsCYDN	35 μL	71	93
10	3	Ir-TsCYDN	40 μL	63	99
11	3	Ir-TsCYDN	50 μL	50	99
12	1	Ir-TsCYDN	80 μL	31	97
13	3	Ir-TsCYDN	80 μL	31	99
14	1	Ir- <i>cis</i> -TsCYDN	80 μL	31	65

Reaction conditions: 25 mM (0.0125 mmol) **63**, 37 °C, 900 rpm, 25-80  $\mu$ L Ir-TsCYDN/Rh-TsCYDN (S/C = 31-61), 20 mg HCOONa (24 eq.), total volume: 0.5 mL.

Various concentrations of both Ir-TsCYDN and Rh-TsCYDN were employed in the reduction of **63**. Better conversions were observed employing Ir-TsCYDN than Rh-TsCYDN (Table 9), indicating that Ir-TsCYDN is more active towards **63** than Rh-TsCYDN at low substrate concentrations. Reductions with Ir-TsCYDN were further exploited with S/C ratios between 100-31 (Table 9, entries 6-14). The conversions reached 99% with a S/C ratio lower than 61 (Table 9, entries 10-13).

Based on the results obtained above, 80  $\mu$ L Ir-TsCYDN (S/C = 31) was

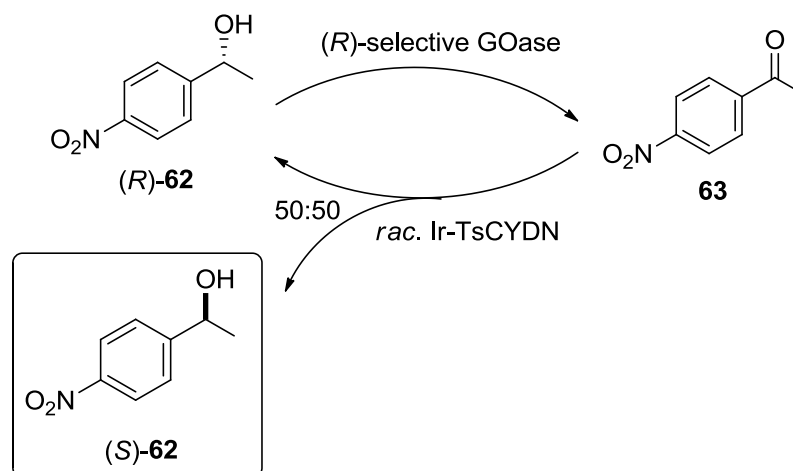
employed in the deracemisation reactions. This represented the optimal concentration of metal catalyst to achieve sufficient reduction of the ketone without impairing the activity of the enzyme.

### **2.3.3 Deracemisation reactions employing optimised reaction conditions**

#### **2.3.3.1 Deracemisation reactions employing *rac.* Ir-TsCYDN metal catalyst**

With the optimised conditions in hand, deracemisations were performed and the results are shown in Table 10.

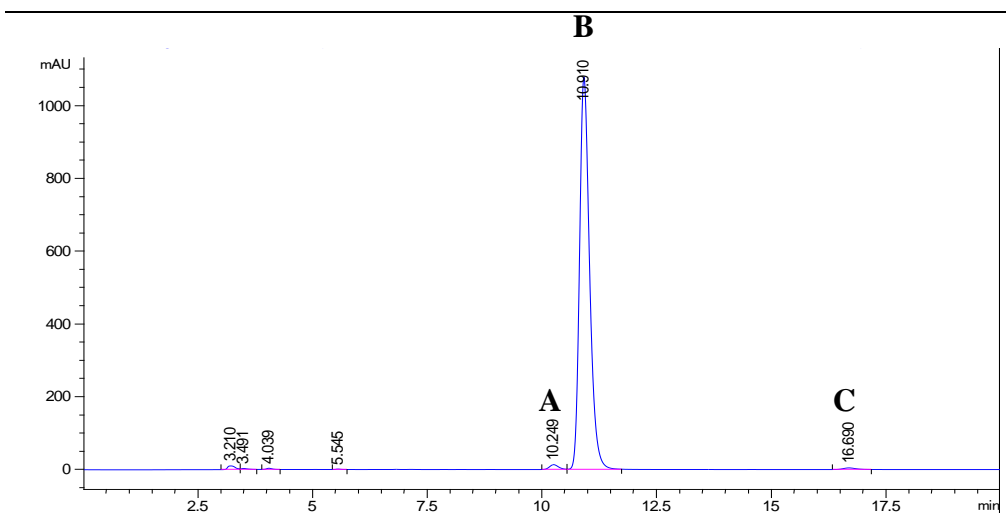
Starting from the ketone **63**, the conversion to **62** reached 99% after 1.5 h. Subsequently, GOase M<sub>3-5</sub> was added, and after 3 h, an increase in *ee* to 94% was observed. Further samplings revealed that both the *ee* and conversion to the alcohol increased to 98% and 99%, respectively (Table 10).

Table 10. Deracemisation of **63** by GOase M<sub>3-5</sub> and (*rac.*) Ir-TsCYDN.

Entry	Time [h]	<i>ee</i> [%]	<b>62</b> [%]
<b>1</b>	1.5	1	99
Addition of GOase M <sub>3-5</sub> (1 mg)			
<b>2</b>	3	94	78
<b>3</b>	6	96	81
<b>4</b>	24	96	92
<b>5</b>	48	98	99

Reaction conditions: 1). Reduction. 25 mM (0.0125 mmol) **63**, 37 °C, 900 rpm, 80  $\mu$ L Ir-TsCYDN (*S/C* = 31), 20 mg HCOONa (24 eq.), total volume: 0.5 mL. 2). Oxidation. 2 g/L GOase M<sub>3-5</sub>, 1 g/L HRP, 0.1 g/L catalase.

The results established that both the metal catalyst and the enzyme were active in the reaction system. After 48 h, very little **63** (< 1%) could be detected and (*R*)-enantiomer of the **62** remaining in the reaction mixture was shown to be 99% *ee* by HPLC (Figure 38).



A = (*R*)-**62**; B = (*S*)-**62**; C = **63**.

Figure 38. HPLC spectrum for the reaction mixture of the deracemisation at 48 h.

Deracemisation reactions were also performed starting with the racemic alcohol. **62** was used as the substrate and oxidation by GOase M<sub>3-5</sub> was performed first as shown in Table 11.

Table 11. Deracemisation starting with the oxidation step.

Entry	Time [h]	<i>ee</i> [%]	<b>62</b> [%]
1	1.5	99	49
Addition of Ir-TsCYDN (S/C = 31) and HCOONa (24 eq.)			
2	1	78	75
3	3	73	81
4	24	71	99
5	48	76	99

*Reaction conditions:* 1). Oxidation. 25 mM (0.025 mmol) **62**, 2 g/L GOase M<sub>3-5</sub>, 1 g/L HRP, 0.1 g/L catalase, 37 °C, 900 rpm. 2). Reduction. 80 μL Ir-TsCYDN (S/C = 31), 20 mg HCOONa (24 eq.), total volume: 0.5 mL.

After 1.5 h, a sample was taken to examine the progress of the oxidation reaction and the *ee* was found to be 99% with a 49% conversion to the alcohol. The transition metal catalysts as well as HCOONa were then added to the reaction mixture and the results are shown in Table 11. It was observed that the conversion to **62** increased to 99% in 24 h, indicating that the metal



catalyst was active in the reaction mixture. However, the *ee* showed no further improvement beyond 77%, suggesting that the enzyme was deactivated after 48 h.

To further optimise the deracemisation reaction, the enzyme concentration was increased to 4 g/L (Table 12). At 72 h, a good *ee* (81 %) with an excellent 99% conversion to the alcohol were obtained.

Table 12. Deracemisation with 4 g/L enzymatic concentration.

Entry	Time [h]	<i>ee</i> [%]	<b>62</b> [%]
<b>1</b>	1.5	99	49
Addition of Ir-TsCYDN (S/C = 31) and HCOONa (24 eq.)			
<b>2</b>	24	73	100
<b>3</b>	40	75	99
<b>4</b>	48	78	99
<b>5</b>	72	81	99

*Reaction conditions: 1). Oxidation. 25 mM (0.025 mmol) **62**, 4 g/L GOase M<sub>3.5</sub>, 1 g/L HRP, 0.1 g/L catalase, 37 °C, 900 rpm. 2). Reduction. 80 µL Ir-TsCYDN (S/C = 31), 20 mg HCOONa (24 eq.), total volume: 0.5 mL.*

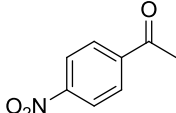
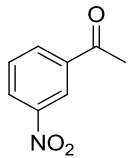
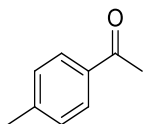
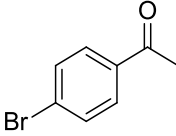
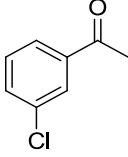
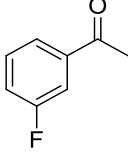
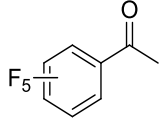
### 2.3.3.2 Expanding the substrate scope of the deracemisation

In summary, deracemisations with the model substrate **62** and **63** showed that excellent *ee* and conversions could be obtained by employing the enzyme GOase M<sub>3.5</sub> and (*rac.*) Ir-TsCYDN in a one-pot system. These results established that the enzyme is compatible with the metal catalyst to some extent. To further exploit the application of this method, a range of substrates was screened under the same reactions as the model substrate.

As shown in Table 13, this deracemisation system was successfully applied for the production of a range of enantiopure chiral secondary alcohols. Aryl ketones which are *meta*-substituted on the phenyl ring are typically difficult substrates for ATH. Selectivities of *ca.* 90% *ee* have been obtained by

ATH for most of these substrates.<sup>92,96,98,103</sup> A notable improvement in *ee* was observed with the *meta*-substituted substrates (Table 13, entries 2, 5 and 6) by deracemisation compared to asymmetric reduction by ATH. In addition, the electron deficient substrate pentafluoroacetophenone (**75**) (Table 13, entry 7) showed a very good *ee* and conversion, demonstrating that the deracemisation process is tolerant of various substrates with different substituents.

Table 13. Deracemisation of a range of secondary alcohols.

Entry	Substrates	Time [h]	<i>ee</i> [%]	Alcohol [%]	Substrate no.
1		48	98	99	<b>63</b>
2		48	99	70	<b>70</b>
3		48	99	81	<b>71</b>
4		48	99	88	<b>72</b>
5		48	91	99	<b>73</b>
6		48	99	90	<b>74</b>
7		48	89	92	<b>75</b>

Reaction conditions: 1). Reduction. 25 mM (0.0125 mmol) **63**, **70-75**, 37 °C, 900 rpm, 80  $\mu$ L *Ir-TsCYDN* (*S/C* = 31), 20 mg *HCOONa* (24 eq.), total volume: 0.5 mL. 2). Oxidation. 2 g/L *GOase M<sub>3-5</sub>*, 1 g/L *HRP*, 0.1 g/L *catalase*.

### 2.3.3.3 Deracemisation reactions employing (*S*)-selective Rh-TsDPEN metal catalyst

The (*S*)-selective Rh-TsDPEN metal catalyst has been applied in the reduction of a wide range of ketone substrates.<sup>91</sup> The *ee* and conversions for these reductions are often high (*ee* > 94% for over 20 examples), although in some cases a lower *ee* was observed with selected substrates. For example, an *ee* of 88% was obtained for the reduction of **63** by the (*S*)-selective Rh-TsDPEN as reported by Wu *et al.*<sup>91</sup> Therefore, deracemisation employing the (*S*)-selective Rh-TsDPEN metal catalyst was performed on this substrate.

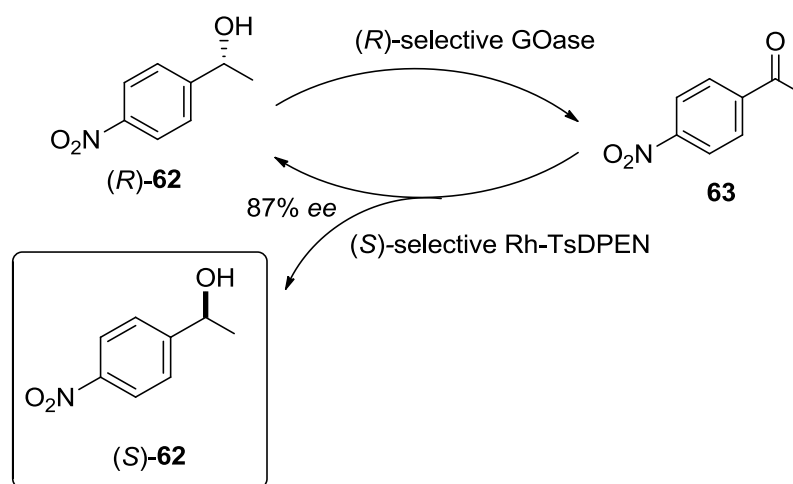


Figure 39. Deracemisation employing (*S*)-selective Rh-TsDPEN catalyst.

Since in this case the metal catalyst also contributes to the final *ee* of the product, the reaction conditions were allowed to be less stringent (lower concentration of enzyme and transition metal catalysts) compared to the reactions employing the racemic transition metal catalysts.

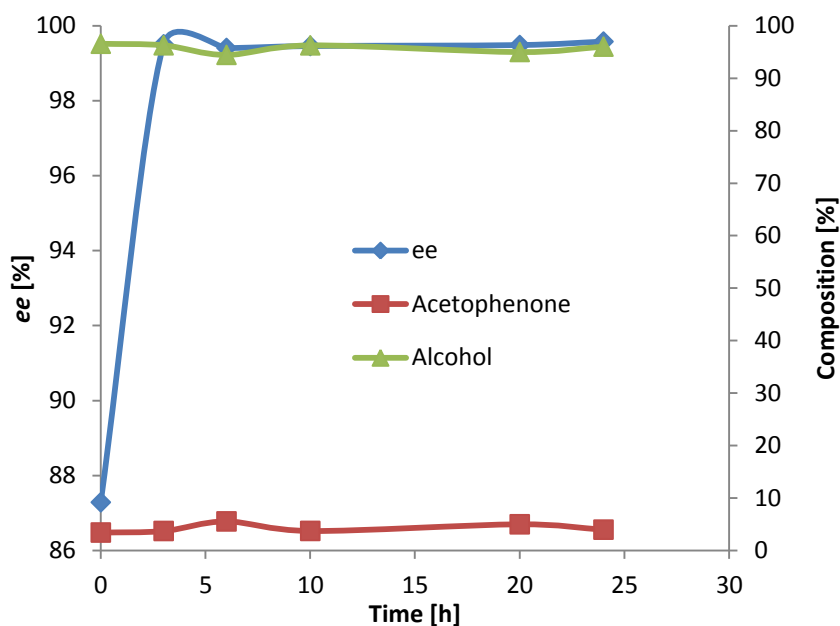


Figure 40. Deracemisation of **63** by GOase M<sub>3.5</sub> and the (*S*)-selective Rh-TsDPEN.

Reaction conditions: 1). Reduction. 50 mM (0.025 mmol) **63**, 30 °C, 250 rpm, 18.4  $\mu$ L Rh-TsDPEN (*S/C* = 250), 5 mg HCOONa (6 eq.), total volume: 0.5 mL. 2). Oxidation. 1 g/L HRP, 0.1 g/L catalase, 1 g/L GOase M<sub>3.5</sub>.

With only 1 g/L GOase M<sub>3.5</sub>, at *S/C* = 250, *ee* and conversions to alcohol reached 99% and 95% after 3 h, respectively (Figure 40). As a result, with the combination of the enzyme GOase M<sub>3.5</sub>, a 12% improvement in *ee* can be obtained compared to the ATH by (*S*)-selective Rh-TsDPEN.

## 2.4 Summary and outlook

Although initial attempts for applying stoichiometric reducing agents in the deracemisations was unsuccessful, notable success was obtained employing the racemic metal catalyst Ir-TsCYDN in the deracemisation of secondary alcohols (Figure 41). By optimising each of the oxidation and reduction system itself and each of the steps in presence of a component from the other step, deracemisation was achieved by employing only one enzyme GOase M<sub>3.5</sub> ((*R*)-selective) and a transition metal catalyst (*rac.* or (*S*)-selective).

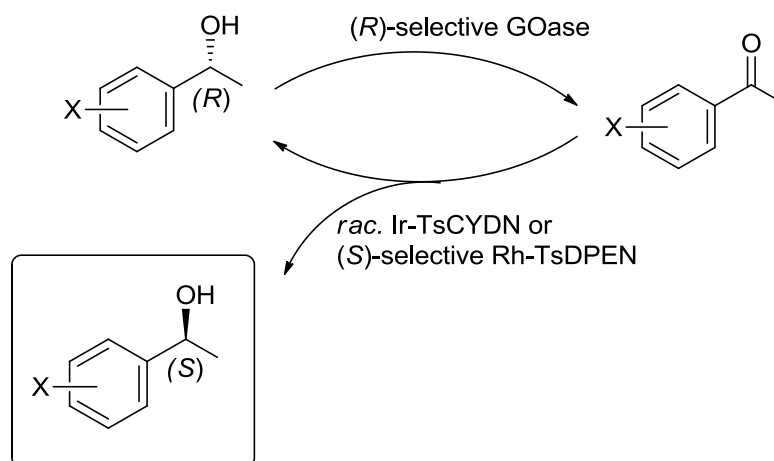


Figure 41. Deracemisation of secondary alcohols.

Outstanding *ee* and conversions were obtained when employing the metal precatalyst Ir-TsCYDN for deracemisation of the model substrate **63**. When the (*S*)-selective Rh-TsDPEN was applied in the deracemisation, both *ee* and conversions were improved compared to ATH by (*S*)-selective Rh-TsDPEN. In addition, this system can be directly applied to a range of secondary ketone substrates and outstanding results were obtained.

In the future, further screenings of secondary alcohols employing GOase  $M_{3-5}$  and the transition metal catalysts (Ir-TsCYDN or Rh-TsDPEN) would be advantageous. More achiral and chiral metal ligands for the transition metal catalysts could also be screened for the optimum activities and selectivities for applications in deracemisation reactions. There is great potential for improvement of this process, and it is envisaged that broad applications of this process can be developed in the future.

### 3. Results and Discussion - Application of GOase in the Production of Single Atropisomers

#### 3.1 Introduction

Atropisomerism (from Greek, *a* = not and *tropos* = turn) is an area of stereochemistry that is receiving increasing attention.<sup>41</sup> Atropisomers are stereoisomers that result from restricted rotation about an axis, where the rotational barrier is high enough for isolation of the conformers. An arbitrary, but useful, definition is when at a given temperature, the conformers can be isolated and have a half-life ( $t_{1/2}$ ) of at least 1000 s (16.7 min).<sup>104</sup>

Named by Kuhni in 1933, atropisomerism was first detected in 6,6'-dinitro-2,2'-diphenic acid (Figure 42, **76**), the enantiomers of which were successfully resolved by Christie and Kenner in 1922.<sup>105</sup> Similar structural elements have since been used in chiral ligands for catalysis and have also been discovered in a range of biologically active compounds.

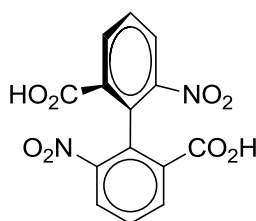


Figure 42. 6,6'-dinitro-2,2'-diphenic acid (**76**).<sup>105</sup>

The synthesis of single atropisomers can be achieved by both chemical and enzymatic methods as discussed below.

##### 3.1.1 Synthesis of single atropisomers by chemical methods

Atropisomers represent significant challenges to synthesise chemically as single atropisomers.<sup>104,106-108</sup> Conventional, non-selective chemical

synthesis<sup>109</sup> cannot meet the surging demand for single atropisomers and research interests have seen a rapid increase in the asymmetric synthesis of atropisomers. Several strategies have been explored for the synthesis of atropisomers, including resolution or desymmetrisation, atroposelective coupling and atroposelective biaryl formation.<sup>110</sup>

For the enantioselective synthesis of atropisomers by thermodynamic resolution, Clayden *et al.* have reported the production of atropisomeric amides,<sup>111-114</sup> diaryl ethers,<sup>115</sup> biaryls<sup>116</sup> and diaryl sulfones<sup>117</sup> via dynamic thermodynamic control. Interactions between dipoles associated with the S-O bond,<sup>118</sup> were demonstrated to show good control over functional group orientation. Substrates based on the 2-arylpyridine structure **77** can be resolved in diastereoisomeric ratios (d.r.) as high as 20:1 by thermodynamic control (Figure 43).<sup>116</sup>

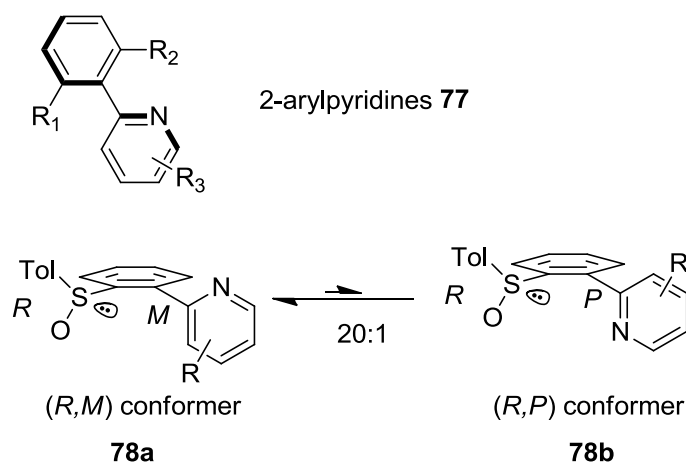


Figure 43. Thermodynamic control of 2-arylpyridines **77**: conformation and conformational preference.<sup>116</sup>

The monophosphine ligand QUINAP (**81**) can be synthesised via the sulfoxide-containing intermediate **80** (Figure 44). The d.r. obtained from thermodynamic control is around 4:1, and the final isolated yield for the sulfoxide intermediate (*R,M*)-**80** is 77%, compared to a 47% yield before equilibration.<sup>119</sup>

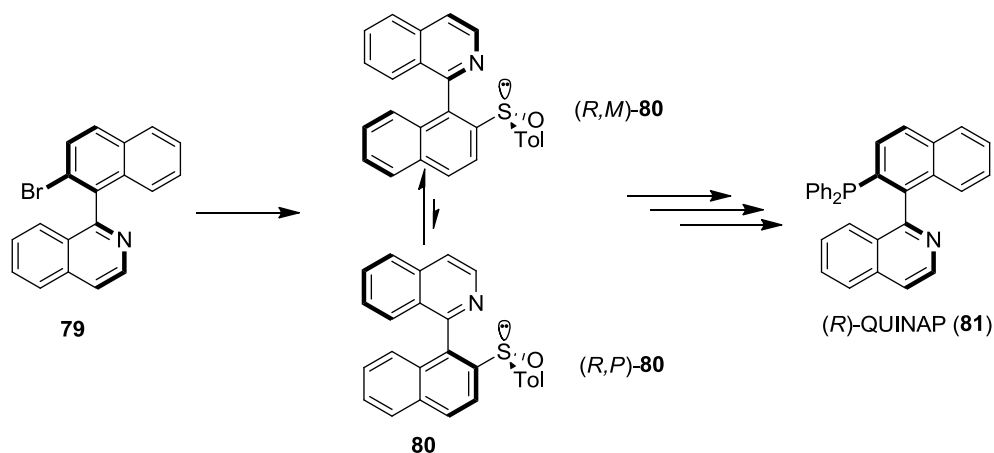


Figure 44. Resolution route to (R)-QUINAP (**81**) via a sulfoxide-containing intermediate.<sup>116</sup>

DKR can be employed for the synthesis of single atropisomers. A range of proatropisomers with low rotation barriers were transformed to single atropisomers via a bromination reaction catalysed by a peptide based organocatalyst.<sup>66</sup> In addition to DKR by adding substituents, it can also be achieved by forming<sup>120</sup> or cleaving a bridge.<sup>121</sup>

For selective coupling, intramolecular coupling has been achieved and the enantioselectivity induced by the use of chiral auxiliaries such as derivatives of binol,<sup>122</sup> diol,<sup>123</sup> amino alcohols<sup>124</sup> or sugars.<sup>125</sup> Intermolecular coupling can also be achieved by Ullmann coupling<sup>126</sup> or asymmetric Suzuki coupling.<sup>127-128</sup>

### 3.1.2 Synthesis of single atropisomers by enzymatic methods

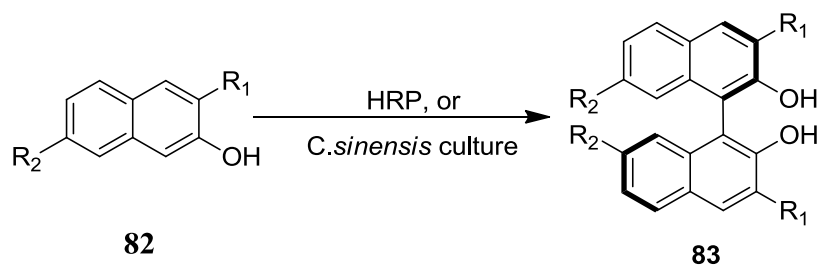
Enzymatic synthesis of single atropisomers is an area that is relatively underdeveloped. Few examples have been reported in the literature to date, most of which employed lipase catalysed resolutions.<sup>129-133</sup>

In 1997, Sridhar *et al.* reported a novel method employing horseradish peroxidase (HRP) as the catalyst for the oxidation of 2-naphthol derivatives (**82**) to 1,1'-binaphthyl-2,2'-diols (**83**).<sup>133</sup> Later, as reported by Takemoto *et al.*, cell cultures from *Camellia sinensis* were found to possess the ability to catalyse oxidative coupling of 2-naphthol derivatives.<sup>134</sup> The results are



presented in Table 14.

Table 14. Enzymatic oxidative couplings of 2-naphthol derivatives.<sup>133-134</sup>

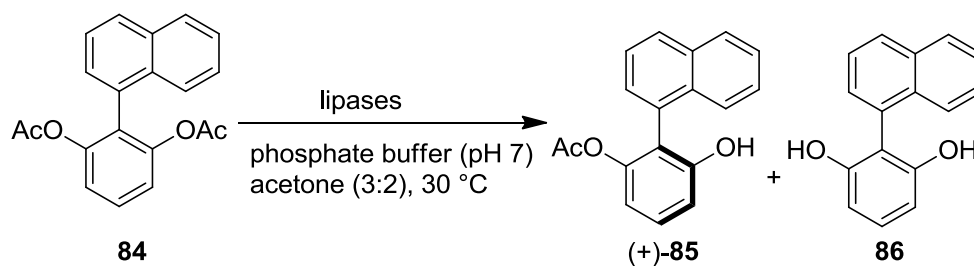


Conditions	R <sub>1</sub>	R <sub>2</sub>	Yield [%]	ee [%]
A	H	H	75	52
A	Br	H	80	64
A	H	CO <sub>2</sub> Me	65	45
A	H	Me	60	38
B	H	H	47	59
B	H	Br	28	36

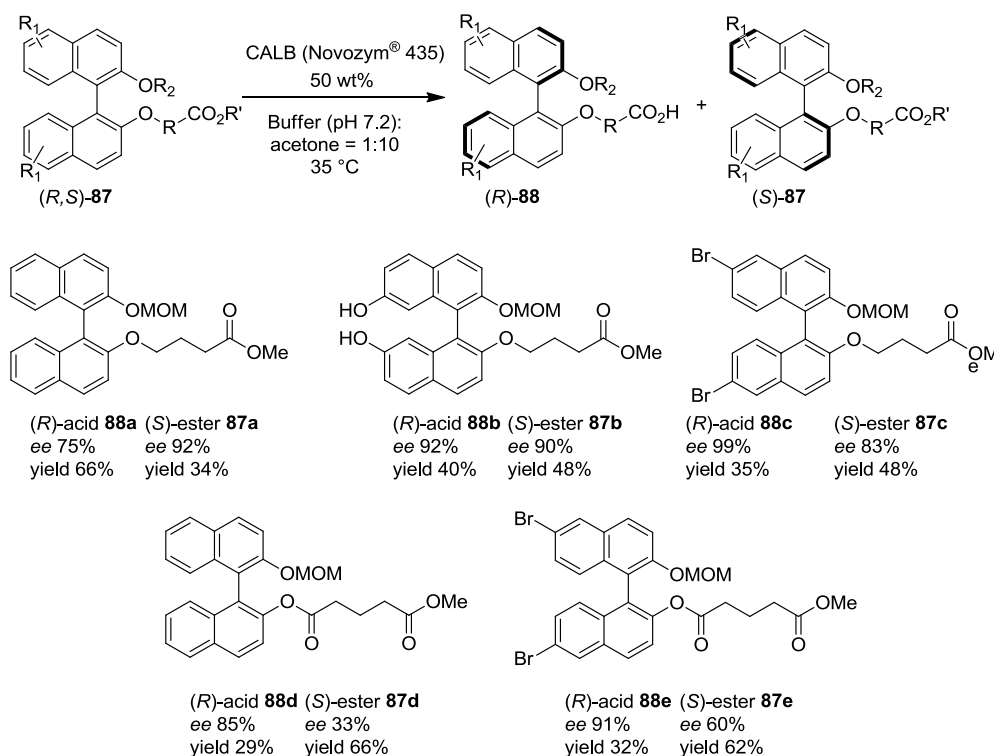
Reaction conditions: A: HRP, H<sub>2</sub>O<sub>2</sub>, phosphate buffer (pH 6.0), MeCN; B: *C.sinensis* cell culture, H<sub>2</sub>O<sub>2</sub>, B5 medium (pH 5.4).

Only moderate to good yields and *ee*'s were obtained from the enzymatic coupling reactions. On the other hand, investigations into enzymatic desymmetrisation and kinetic resolutions of proatropisomeric and atropisomeric substrates showed that this is an area with great potential.

Enzymatic desymmetrisation of proatropisomeric biaryls was reported by Matsumoto *et al.* employing lipase catalysed hydrolysis as shown in Figure 45.<sup>130</sup> A range of commercially available lipases were screened against **84**, including PFL, CRL (*Candida rugosa* lipase), PPL (porcine pancreas lipase), PLE (pig liver esterase), CALB (*Candida antarctica* lipase B), and PCL (*Pseudomonas cepacia* lipase). Among these lipases, the best results were obtained from PCL and CALB. Both of these lipases were employed in preparative scale studies with various substrates. Outstanding *ee* (96% - 99%) and good yields (51% - 86%) were obtained.

Figure 45. Desymmetrisation of **84** by lipase catalysed hydrolysis.<sup>130</sup>

Taniguchi *et al.* reported an impressive CALB catalysed kinetic resolution of binaphthol derivatives (Figure 46).<sup>131</sup> Due to the relatively narrow active site of CALB, it is somewhat difficult for it to accept large substrates. However, they overcame this problem by attaching a linker to the binaphthol ring so that the reactive ester bond can be approached in the active site. Indeed, excellent *ee*'s were obtained for a number of substrates (**87a-e**), despite the great distance between the hydrolysis point and the chiral fragment.

Figure 46. CALB catalysed kinetic resolution of binaphthol derivatives.<sup>131</sup>

In summary, both chemical and enzymatic methods have been employed for the synthesis of single atropisomers. However, enzymatic production of

atropisomers is still a relatively unexplored area and there is great potential to be exploited.

### 3.1.3 Applications of atropisomers

Atropisomers have found numerous applications as chiral ligands for resolution and asymmetric synthesis<sup>135</sup> and as building blocks for pharmaceuticals.<sup>136-137</sup>

The development of the atropisomeric diphosphine ligand BINAP (Figure 47, **89**),<sup>135</sup> earned Noyori a share of the Nobel Prize for chemistry in 2001. Atropisomers have been employed with great success as chiral ligands for metal complexes, due to their ability to adapt various ‘bite angles’ to suit the metal and manner of coordination. Other examples of atropisomers include QUINAP (Figure 47, **81**), a heteroaromatic atropisomer used in palladium catalysed asymmetric allylic alkylations and rhodium catalysed hydroborations,<sup>138</sup> BINOL (**83**) and MeOMOP (**90**) (Figure 47).

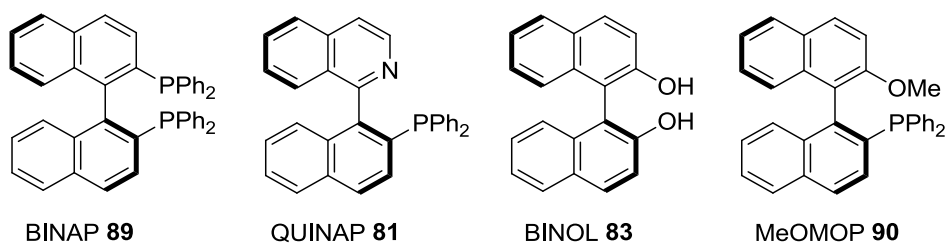


Figure 47. Atropisomeric ligands.

Atropisomers are also important building blocks for a number of natural products. One of the most important examples is Vancomycin, a widely used antibiotic first discovered by Eli Lilly in 1956.<sup>136</sup> In addition, the anti-HIV drug Michellamine is another well known example of a natural product containing atropisomeric subunits.<sup>137</sup>

In summary, the synthesis of atropisomers in high optical purities is an expanding yet challenging area, especially using enzymatic methods. GOase M<sub>3-5</sub> is potentially capable of catalysing the production of atropisomers based

on previous results, in which it showed excellent enantioselectivities towards oxidation of alcohols.<sup>139</sup> In the following sections (§3.2 and §3.3), the utilisation of GOase M<sub>3-5</sub> in the enantioselective enzymatic production of atropisomers will be discussed.

### 3.2 Asymmetric synthesis of diaryl ethers

It has been shown that GOase M<sub>3-5</sub> catalyses the oxidation of a broad range of chiral primary and secondary alcohols.<sup>1</sup> It was therefore of interest to examine its activity towards proatropisomeric and atropisomeric substrates bearing enantiotopic hydroxyl groups. Several proatropisomeric and atropisomeric compounds were obtained from the group of Professor Jonathan Clayden as shown in Figure 48. These compounds are the proatropisomeric methyl *tert*-butyl diol (**91a**) and dialdehyde (**91c**), and the atropisomeric methyl *tert*-butyl monoaldehyde (**91b**). Their rotation barriers were published previously.<sup>140</sup>

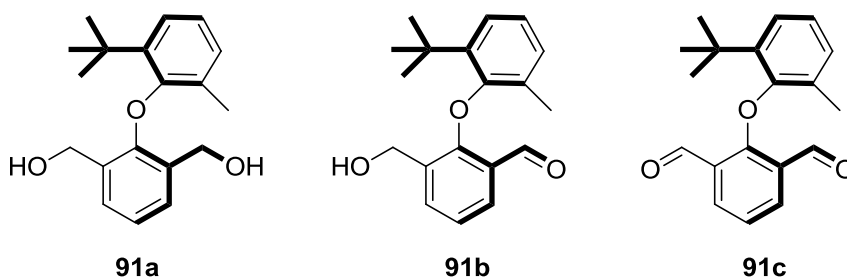


Figure 48. Methyl *tert*-butyl diaryl ethers (**91a-c**) obtained from the Clayden group.

GOase M<sub>3-5</sub> was applied in both desymmetrisation and kinetic resolution reactions. In the desymmetrisation reaction (Figure 49A), the symmetrical diol **91a** reacted with GOase M<sub>3-5</sub> variant to yield the atropisomeric monoaldehyde **91b**. In principle a secondary oxidation reaction may also occur yielding two potential products: the atropisomeric monoaldehyde **91b** and the symmetrical dialdehyde **91c**.

In the kinetic resolution reaction (Figure 49B), the atropisomeric

monoaldehyde **91b** was found to react with GOase M<sub>3-5</sub> to produce the symmetrical dialdehyde **91c**. Both these reactions were investigated in detail and the results are discussed in the following sections.

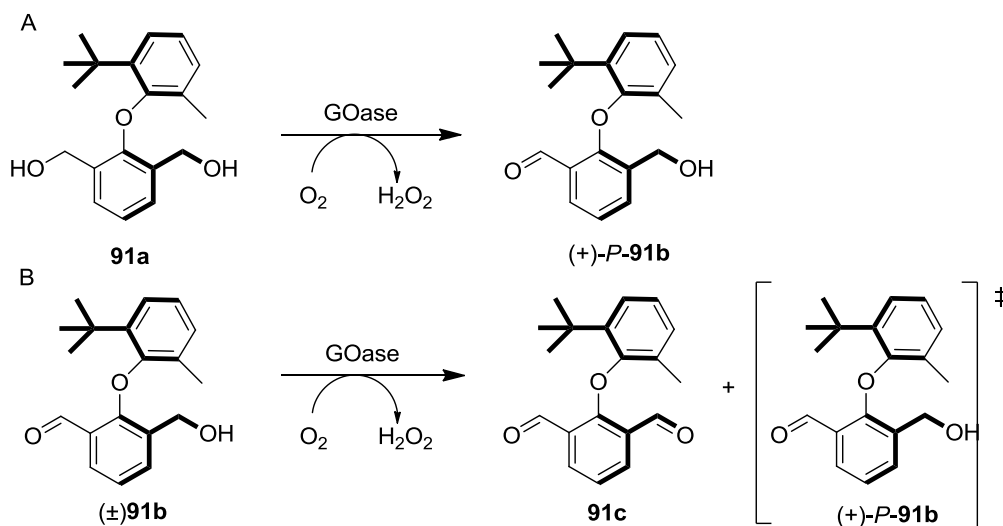
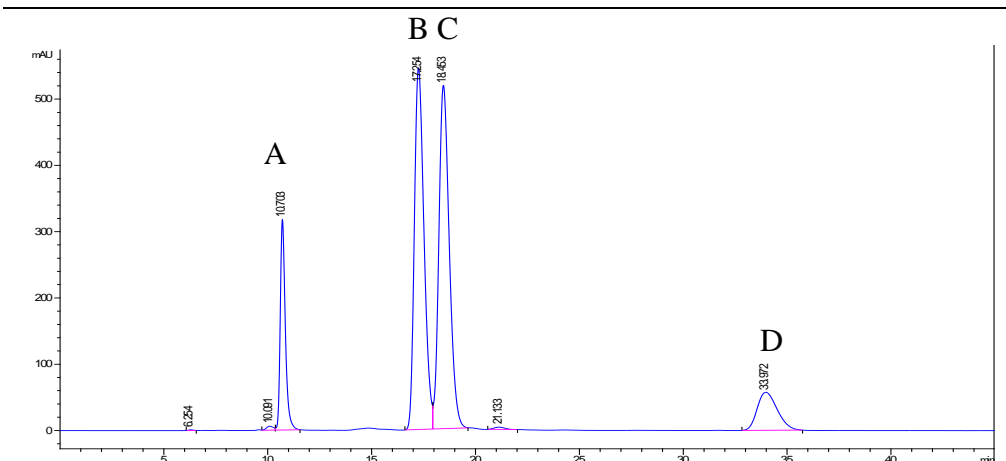


Figure 49. Desymmetrisation (A) and kinetic resolution (B) of proatropisomeric and atropisomeric diaryl ethers by GOase M<sub>3-5</sub>.  $\pm$  Less reactive enantiomer.

### 3.2.1 HPLC method development

To monitor the selectivity and the conversion of the reaction, an analytical method was required. HPLC was chosen as an effective method for the analysis. HPLC method development was therefore conducted using normal phase HPLC equipped with chiral columns for the separation of enantiomers. Several HPLC solvents were screened including isohexane, heptane, ethanol and propan-2-ol (IPA). A number of chiral HPLC columns were also screened, such as Chiralcel<sup>®</sup> ADH, OJH, ODH and ASH. Good separations were obtained using an ASH column with a mobile phase composition of 93% isohexane and 7% IPA at 1 mL/min flow rate. HPLC traces for a mixture of the dialdehyde **91c**, monoaldehyde **(P,M)-91b** and the diol **91a** are shown in Figure 50.



**A** = dialdehyde **91c**; **B** = monoaldehyde (*M*)-**91b**; **C** = monoaldehyde (*P*)-**91b**; **D** = diol **91a**

Figure 50. HPLC traces for a mixture of **91a-c**.

Almost baseline separation for the enantiomers of monoaldehyde **91b** was observed. The HPLC traces for all three compounds in the mixture were also well resolved. Therefore, this method was employed for monitoring all the following biotransformations using methyl *tert*-butyl diaryl ethers as substrates.

### 3.2.2 Optimisation of reaction conditions

The diaryl ether compounds are insoluble in pure water; therefore, it is important to identify a suitable co-solvent for the biotransformations without causing loss of activity of the enzyme. Hence, a suitable model substrate 4'-methoxy-1-phenylethanol (**45**), which undergoes highly enantioselective oxidation with GOase M<sub>3-5</sub>, was chosen for assaying the tolerance of the enzyme for various organic solvents. The compatibility profile of GOase M<sub>3-5</sub> in 30% of various organic solvents is shown in Figure 51. The *ee* was monitored against time for first 3 h of the reactions.

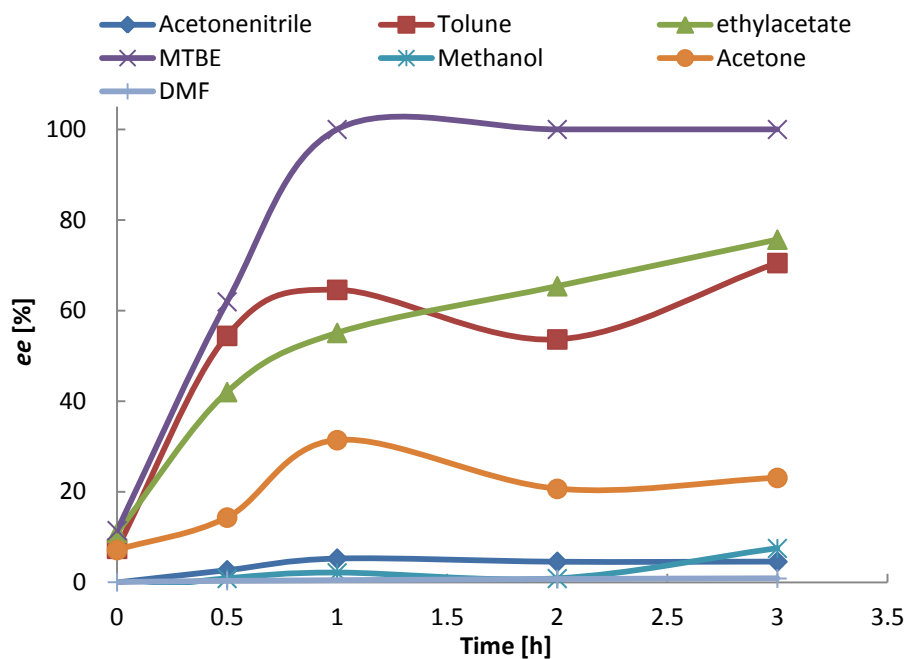


Figure 51. Compatibility profile of GOase M<sub>3.5</sub> in 30% various organic solvents.  
 Reaction conditions: 50 mM **45**, 30% (v/v) various organic solvents, 1 g/L HRP, 0.1 g/L catalase, 1 g/L GOase M<sub>3.5</sub>, in water, 30 °C, 250 rpm, total volume: 0.5 mL.

Methyl *tert*-butyl ether (MTBE) was found to be the most compatible organic co-solvents amongst the solvents tested, with almost no reduction of *ee* observed from the reaction.

However, although GOase showed outstanding tolerance for MTBE, the reproducibility of the reactions in MTBE/water mixture was found to be poor. As can be seen from Figure 52, the data sets 1-3 are reactions performed under the same reaction conditions, however, at the same time point 3 h, 2%, 26%, and 43% *ee* were obtained, respectively.

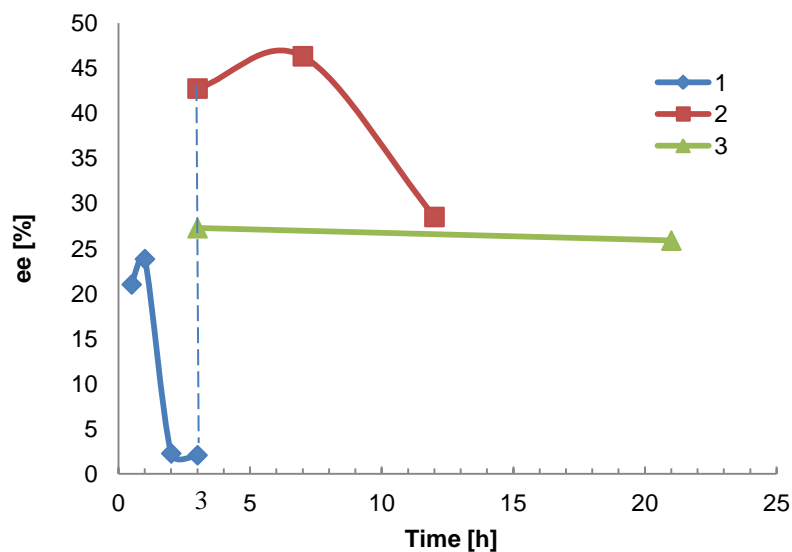


Figure 52. Reproducibility of kinetic resolution of **91b** in MTBE (30%).

*Reaction conditions: 10 mM **91b**, 30% (v/v) MTBE, 1 g/L HRP, 0.1 g/L catalase, 70% NaPi buffer (100 mM), 2 g/L GOase M<sub>3-5</sub>, 30 °C, 250 rpm, total volume: 0.5 mL.*

Since MTBE is volatile at room temperature, it could undergo evaporation during the oxygen bubbling process and the course of the reaction. In addition, the immiscibility between MTBE and water creates a biphasic system where the substrate stays in the organic phase and the enzyme in the aqueous phase. As a result, the reaction may only occur at the surface of the biphasic system and a slight change of mixing could result in a significant variation in the results.

Previous work conducted by Dr. Franck Escalettes (Figure 53, unpublished results) showed that DMSO is also a very good co-solvent for the biotransformations. With another model substrate 3'-fluoro-1-phenylethanol (**64**), which also undergoes enantioselective oxidation with GOase M<sub>3-5</sub>, almost no loss of selectivity was observed with up to 40% DMSO as co-solvent.



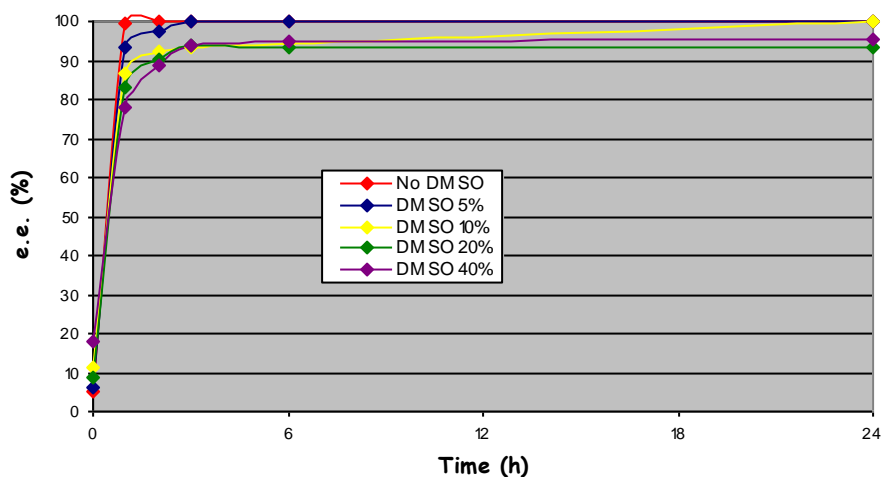


Figure 53. Compatibility assay in presence with DMSO by Dr. Franck Escalettes.

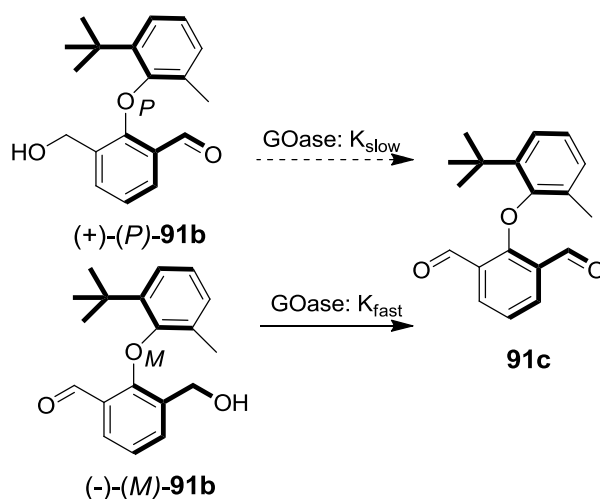
Reaction conditions: 50 mM **64**, 1 g/L HRP, 0.1 g/L catalase, 0 to 40% (v/v) DMSO, in water, 1 g/L GOase M<sub>3-5</sub>, 30 °C, 250 rpm, total volume: 0.5 mL.

Therefore, further studies were carried out using DMSO as the co-solvent.

### 3.2.3 Enzymatic production of methyl *tert*-butyl diaryl ethers

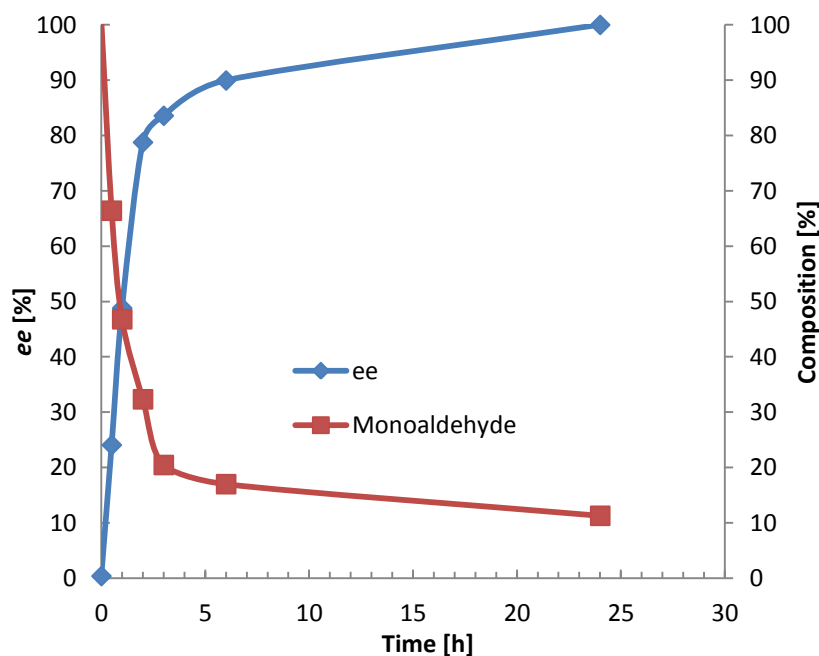
#### 3.2.3.1 Kinetic resolution of monoaldehyde **91b**

Kinetic resolution was conducted employing monoaldehyde **91b** as the substrate with DMSO as the co-solvent. In this reaction, GOase M<sub>3-5</sub> was employed to selectively oxidise the monoaldehyde **91b** to the dialdehyde **91c** (Figure 54).

Figure 54. Kinetic resolution of monoaldehyde **91b**.

For the HPLC sampling method, a portion of the reaction mixture was taken and extracted by MTBE. The organic layer was evaporated under reduced pressure then ethanol was added to dissolve the sample and the solution was used directly for HPLC analysis.

With an effective analytical technique in hand, the kinetic resolution was performed with the substrate **91b**.

Figure 55. Kinetic resolution of monoaldehyde **91b** by GOase.

Reaction conditions: 10 mM **91b**, 30% (v/v) DMSO, 1 g/L HRP, 0.1 g/L catalase, in NaPi buffer (100 mM), 2 g/L GOase  $M_{3.5}$ , total volume: 0.5 mL, 30 °C, 250 rpm.

An 89% conversion to **91c** was observed after 24 h. The remaining atropisomer was of *P* configuration (absolute configuration determination see §3.2.4) with an *ee* value of 99%. The kinetic resolution under these conditions has a selectivity (*E*) value of approximately 4. Theoretically the maximum yield for kinetic resolution is 50% if the resolution is highly selective. In this case the reaction rates for the two enantiomers are relatively similar, resulting in a lower *ee* with a yield higher than 50%. This conversion also indicates that 39% of the conversion results from the oxidation of the undesired atropisomer ((*P*)-**91b**), which means 78% of (*P*)-**91b** was oxidised to the dialdehyde **91c**.

It was noted that the maximum *ee* was significantly improved from 45% using MTBE as the co-solvent, to 99% using DMSO as the co-solvent. This result could be attributed to better miscibility and lower volatility of DMSO compared to MTBE.

### 3.2.3.2 Desymmetrisation of diol **91a**

After the establishment of the kinetic resolution process, it was important to investigate the desymmetrisation reaction.

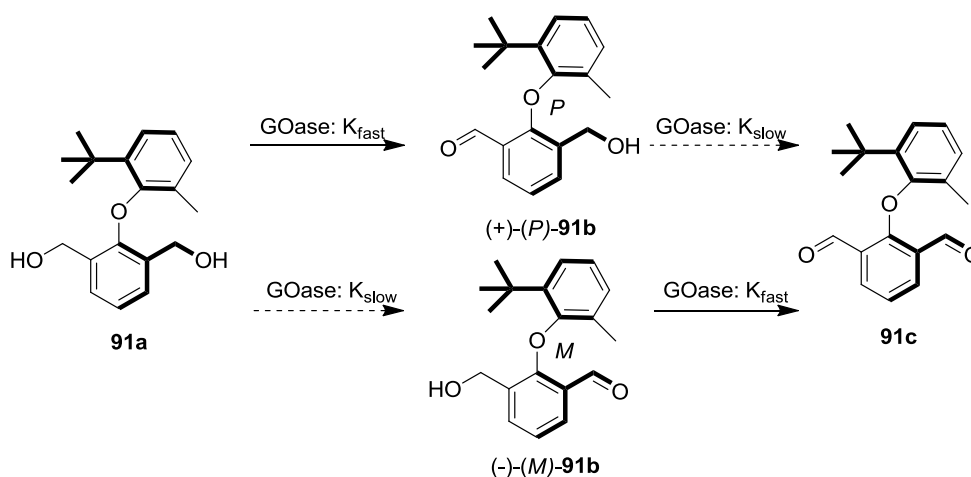


Figure 56. Desymmetrisation of diol **91a** by GOase.

As shown in Figure 56, we envisaged the possibility for a two step process combining first the desymmetrisation of diol **91a**, followed by kinetic

resolution of the monoaldehyde **91b** formed. The secondary oxidation process should lead to an improvement in the *ee* of **91b** although would be accompanied by a reduction in the conversion to the desired product monoaldehyde **91b**.

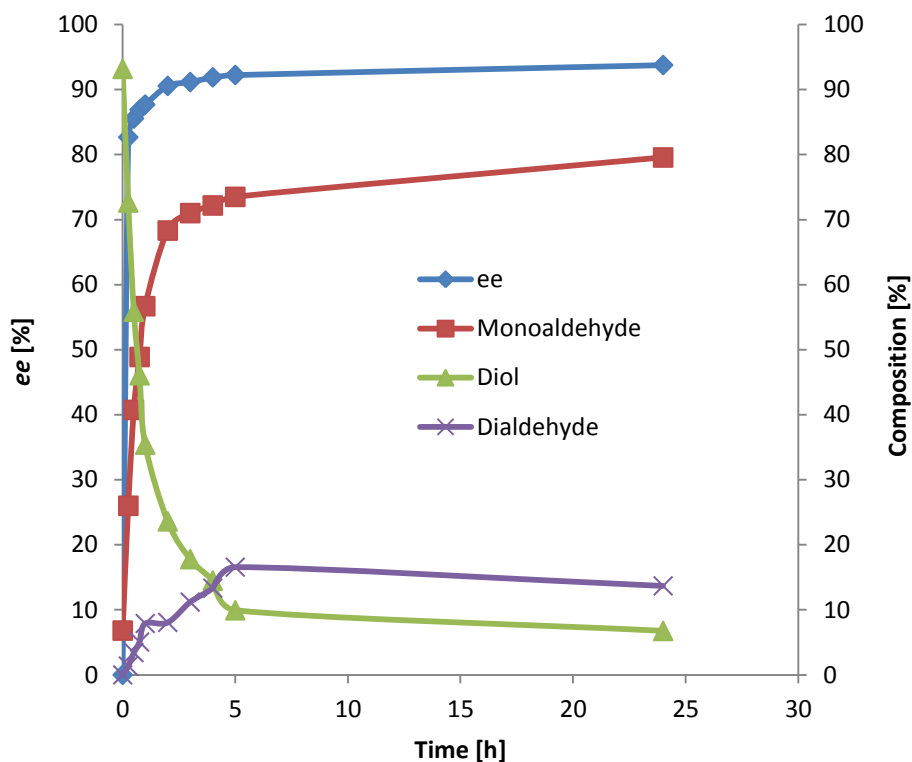


Figure 57. Desymmetrisation of diol **91a** by GOase M<sub>3-5</sub>.

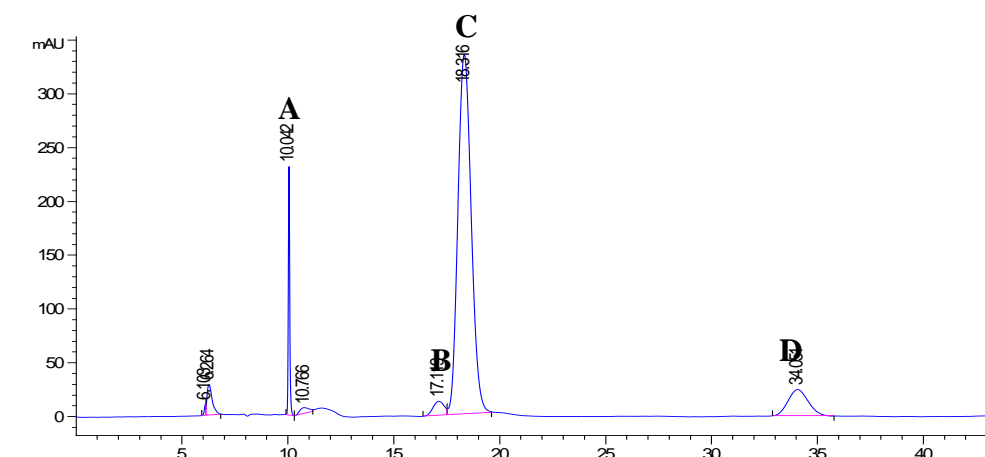
Reaction conditions: 10 mM **91a**, 30% (v/v) DMSO, 1 g/L HRP, 0.1 g/L catalase, in NaPi buffer (100 mM), 2 g/L GOase M<sub>3-5</sub>, total volume: 0.5 mL, 30 °C, 250 rpm.

Consequently, the reaction was performed by incubating the substrate diol **91a** with GOase M<sub>3-5</sub> and the results are shown in Figure 57. Rapid oxidation was observed, leading to an 80% conversion to the monoaldehyde **91b** in 24 h. (*P*)-**91b** with approximately 88% *ee* (see §3.2.4 for assignment of the absolute configuration) was rapidly formed after 1 h by the primary oxidation, followed by a slower increase in *ee* to a maximum value of 94%.

Proof for the secondary oxidation process was obtained from the observed slow production of the dialdehyde **91c** during the reaction (14% after 24 h). This data suggests that the minor enantiomer (*M*)-**91b** was

preferentially oxidised to the dialdehyde **91c**. Thus, the final enantiomeric purity of (*P*)-**91b** results from a combination of enantioselective desymmetrisation and kinetic resolution. The fact that the conversion to the monoaldehyde **91b** did not decrease further could be attributed to the fact that GOase had lost activity to some extent after incubation for 24 h at 30 °C. The secondary oxidation could also be suppressed to some extent by the presence of the diol, which may cause a more sluggish oxidation of **91b** compared to the kinetic resolution.

Figure 58 shows one example of an HPLC spectrum for the reaction mixture at 24 h. The peaks are well separated and the *ee* is 93% after 24 h of reaction.



A = dialdehyde **91c**; B = monoaldehyde (*M*)-**91b**; C = monoaldehyde (*P*)-**91b**; D = diol **91a**.

[Chiralcel® ASH, isohehexane:IPA = 93:7 at 254 nm, flow rate: 1 mL/min.]

Figure 58. Reaction mixture at 24 h for the desymmetrisation of diol **91a** by GOase M<sub>3-5</sub>.

### 3.2.3.3 Enzymatic oxidation employing the mutant GOase F11

Dr. Julie Rannes from the Turner group had previously generated a mutant F11 of GOase which had shown interesting activity towards primary and secondary alcohols. The mutant was identified by screening a double saturation mutagenesis library at position Tyr405/Gln406 of the M<sub>3</sub> variant towards GlcNAc as substrate. The library was designed using the principle of

CASTing by Reetz.<sup>32</sup> This variant carries the mutation Tyr405Phe and Gln406Glu in addition to the mutations in the M<sub>3</sub> variant (mutations in the M<sub>3</sub> variant see §1.1.2, Table 1). The F11 variant possesses activity towards a broad range of sugars such as Glc, mannose (Man), N-acetylglucosamine (GlcNAc), Gal (**1**), talose (Tal) and also 1-phenyl-1,2-ethanediol (PED). Therefore, it seemed interesting to study its activity towards the diaryl ethers. Expression and purification of F11 were carried out and the desymmetrisation and kinetic resolution reactions of **91a** and **91b** were performed using purified GOase F11, respectively (Figure 59).

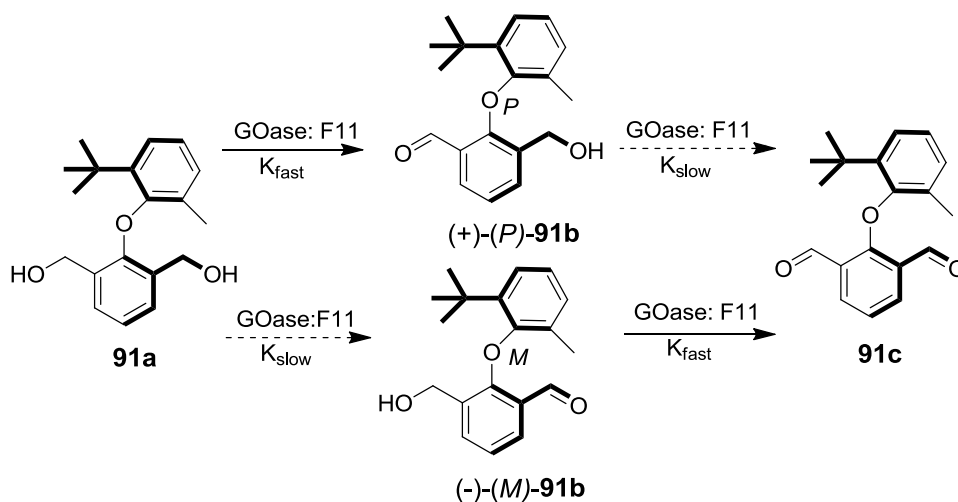


Figure 59. Enzymatic oxidation of **91a** by GOase F11.

Results for the desymmetrisation are shown in Figure 60. 50% *ee* was obtained after 3 h from the oxidation of diol **91a** by F11 whereas 93% *ee* was obtained from the oxidation by GOase M<sub>3-5</sub>.

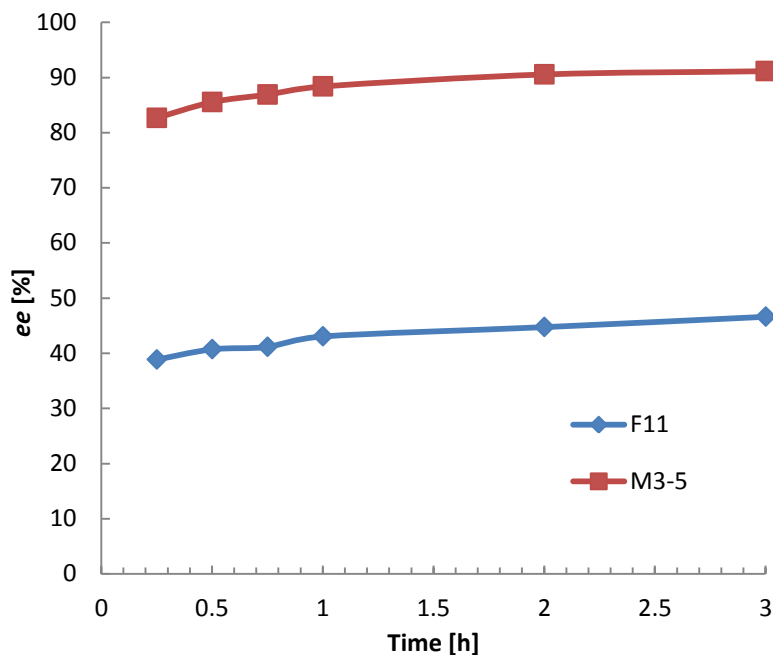


Figure 60. Desymmetrisation of **91a** by GOase F11.

Reaction conditions: 10 mM **91a**, 30% (v/v) DMSO, 1 g/L HRP, 0.1 g/L catalase, in NaPi buffer (100 mM), 2 g/L GOase F11, total volume: 0.5 mL, 30 °C, 250 rpm.

Kinetic resolution of **91b** by F11 was also performed (Figure 61). As expected, a lower *ee* (10%) was obtained, compared to a 99% *ee* by M<sub>3-5</sub>. Hence, oxidation by the mutant GOase F11 was not pursued further.

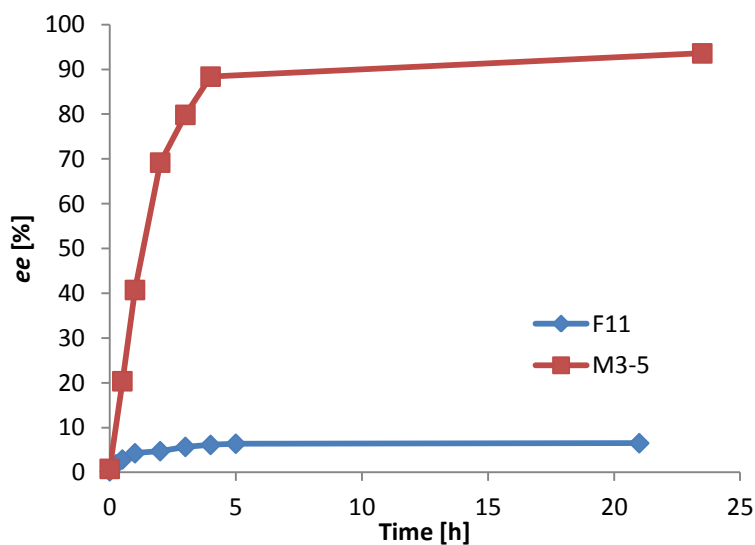


Figure 61. Kinetic resolution of **91b** by GOase F11.

Reaction conditions: 10 mM **91b**, 30% (v/v) DMSO, 1 g/L HRP, 0.1 g/L catalase, in NaPi buffer (100 mM), 2 g/L GOase F11, 30 °C, 250 rpm, total volume: 0.5 mL.

### 3.2.4 Absolute configuration assignment of the atropisomers

The absolute configuration was established by comparison of experimental and modeled circular dichroism (CD) spectra (performed by Mr. Michael Tait from the Clayden group) of the starting material remaining after kinetic resolution, (+)-(*P*)-**91b**. The solid line represents the trace observed for the major atropisomer product of **91b**; and the dashed line represents the calculated spectrum for the lowest-energy conformer of (*P*)-**91b**. The alignment for the positive maximum peak at *ca.* 230 nm and *ca.* 350 nm, the negative maximum peak at *ca.* 310 nm, and a shoulder at 280 nm shows that the modeled and experimental data matches closely (Figure 62). The match confirms that the slower-reacting enantiomers of **91b**, and hence also the product of the desymmetrisation of **91a**, has the *P* configuration.

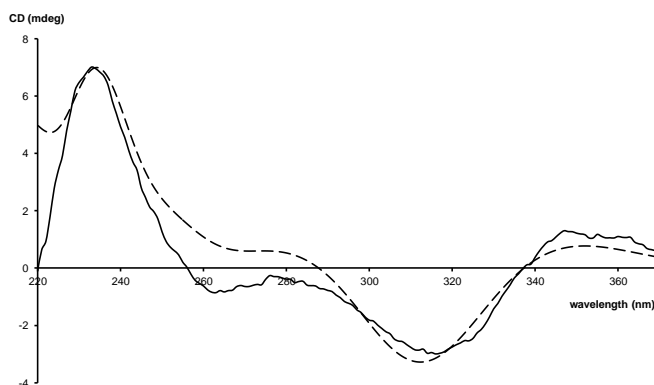


Figure 62. CD spectra of **91b** performed by Mr. Michael Tait: (solid line) observed for the less reactive enantiomer of **91b**; (dashed line) modeled for the lowest energy conformer of (*P*)-**91b**.

Modeling of the two enantiomers of **91b** into the binding site of GOase M<sub>3-5</sub>, performed by Dr. Simon Willies, was in agreement with the assignment of the absolute configuration based on CD. The docking model shows that the active site is very shallow, allowing a wide range of substrates access. It appears that the selectivity for these substrates originates from the surface features surrounding the active site. On one side of the active site is a small "cliff" and on the other is a "plateau". This arrangement ensures that any



bulky group must be situated towards the plateau, or protrude above the cliff. Figure 63 shows that the bulky *tert*-butyl group of the substrate is forced to occupy a position in which it is pointing away from the cliff and towards the surface of the protein. In such a binding mode, the hydroxymethyl group of (*M*)-**91b** is placed close to the copper-containing reactive centre. This model therefore predicts that (*M*)-**91b** is the faster reacting enantiomer product in the kinetic resolution process. This is in agreement with the conclusion from the CD data.

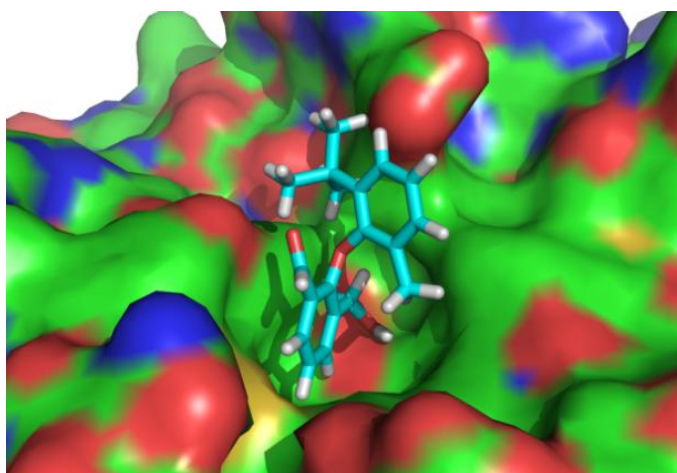


Figure 63. Modeling of the faster-reacting enantiomer (*M*)-**91b**, performed by Dr. Simon Willies, into the active site of GOase M<sub>3-5</sub>.

### 3.2.5 Complementary approaches for the production of single atropisomers

Two complementary approaches were employed for the production of optically pure atropisomers. Ketoreductases (KREDs) are a family of enzymes that reduce ketones to alcohols in high enantioselectivities. They have been shown to possess the ability to accept sterically hindered benzylic ketones as substrates.<sup>141</sup> Thus it was interesting to investigate the activity of these enzymes towards the desymmetrisation of the dialdehyde substrate **91c**.

Another enzymatic approach was employed based upon the acetylation of diol **91a** by immobilised CALB (Novozym<sup>®</sup> 435).

### 3.2.5.1 Reduction of dialdehyde **91c**

Asymmetric reduction of the symmetrical dialdehyde **91c** was examined using a panel of 17 different KREDs obtained from Codexis. KREDs have been widely applied to the asymmetric reduction of ketones, particularly benzylic ones, but to our knowledge had not previously been used for the desymmetrisation of proatropisomeric substrates. Conversions and *ee* values were determined after 24 h and in some cases high enantioselectivities (Table 15, entries 4, 8 and 17) were observed although often with moderate conversions.

Table 15. Reduction of **91c** by KREDs.

Entry	Enzyme <sup>[a]</sup>	<b>91b</b> <sup>[b]</sup> [%]	<i>ee</i> [%]	Configuration <sup>[c]</sup>
1	KRED101 ( <i>R</i> )	53	24	<i>P</i>
2	KRED103	6	22	<i>P</i>
3	KRED104	3	75	<i>M</i>
4	KRED105	2	99	<i>M</i>
5	KRED106	3	11	<i>P</i>
6	KRED108 ( <i>S</i> )	39	78	<i>M</i>
7	KRED109	3	54	<i>M</i>
8	KRED110	1	99	<i>M</i>
9	KRED114	95	40	<i>M</i>
10	KRED115 ( <i>R</i> )	33	9	<i>M</i>
11	KRED116	23	79	<i>M</i>
12	KRED117	7	79	<i>M</i>
13	KRED118 ( <i>S</i> )	91	77	<i>P</i>
14	KRED119 ( <i>S</i> )	99	71	<i>P</i>
15	KRED120 ( <i>S</i> )	22	87	<i>M</i>
16	KRED121 ( <i>R</i> )	84	61	<i>M</i>
17	KRED124 ( <i>R</i> )	3	99	<i>M</i>

[a] The typical selectivity of the KREDs in the reduction of nonsymmetrical diaryl ketones is shown in parentheses (when known).<sup>141</sup> [b] Conversions after 24 h. [c] Major enantiomers produced by reduction.

*Reaction conditions: 5 g/L 91c, 10% (v/v) DMSO, 5 g/L KREDs, 1 g/L Glucose dehydrogenase (CDX-901), 1 g/L NADP<sup>+</sup>, 3.8 g/L Glucose (1.25 mol excess to the substrate), in KPi buffer (100 mM, pH 7.0), 30 °C, 250 rpm, total volume: 1 mL.*

Some notable successes were achieved with KRED118 (entry 13, 91% conversion, 77% *ee*, (*P*)-enantiomer) and KRED121 (entry 16, 84% conversion, 61% *ee*, (*M*)-enantiomer). As can be seen from Table 15, this trend for reduction of bulky benzylic alcohols was not followed for the reduction of dialdehyde **91c**. For example, (*P*)-**91b** was obtained from both an (*R*)-selective KRED101 and an (*S*)-selective KRED118. Similarly, (*M*)-**91b**

was obtained from both (*R*)-KRED121 and (*S*)-KRED108 selective enzymes. These results suggest a different binding mode for the dialdehyde **91c** at the active site of the KREDs compared to that adapted by benzylic ketones.

### 3.2.5.2 Acetylation of diol **91a** by CALB (Novozym<sup>®</sup> 435)

Acetylation by CALB (Novozym<sup>®</sup> 435) was performed by incubating the substrate diol **91a** with Novozym<sup>®</sup> 435 and vinyl acetate (Table 16). Slow acylation of **91a** was observed yielding approximately 50% conversion to the monoacetate after 24 h and moderate enantioselectivity (60% *ee*) was observed.

Table 16. Acetylation of diol **91a** by Novozym<sup>®</sup> 435.

Entry	Time [h]	<i>ee</i> [%]	Conversion [%]
<b>1</b>	1	52	<5
<b>2</b>	2	53	<5
<b>3</b>	3	55	<5
<b>4</b>	24	60	50

*Reaction conditions: 33 mM 91a (10 mg), 280 mM vinyl acetate (9 eq.), 33 g/L Novozym<sup>®</sup> 435, in THF, 45 °C, 900 rpm, total volume: 1 mL.*

### 3.2.6 Enzymatic production of methyl isopropyl diaryl ethers

The HPLC peaks for the methyl isopropyl diaryl atropisomers **92a-c** were well separated using the column ASH and a mobile phase consisting of 95% isohexane and 5% IPA (Figure 64).

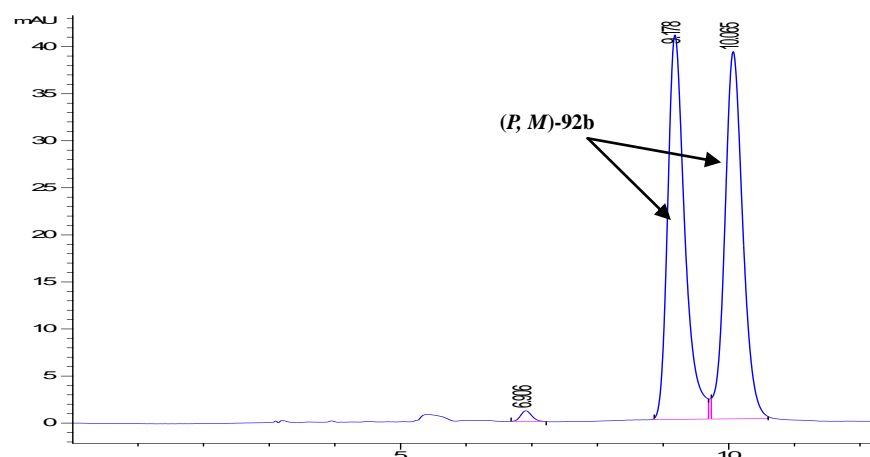


Figure 64. HPLC traces for the methyl isopropyl monoaldehyde **92b**.

Subsequently, GOase M<sub>3-5</sub> was incubated with the methyl isopropyl diol **92a** and the monoaldehyde **92b** to examine the enzymatic activity (Figure 65).

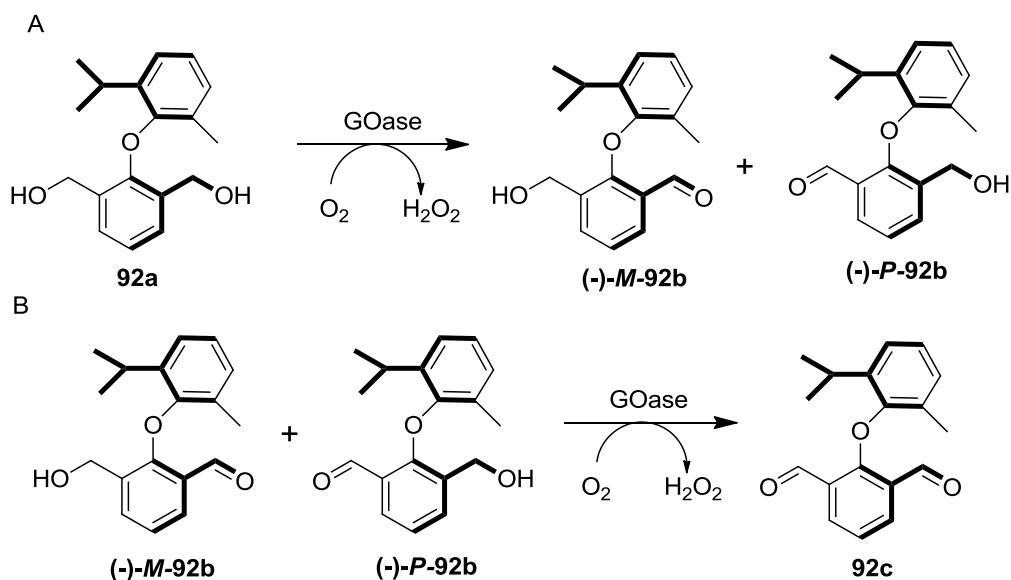


Figure 65. Desymmetrisation (A) and kinetic resolution (B) of proatropisomeric and atropisomeric diaryl ethers by GOase M<sub>3-5</sub>.

For both the kinetic resolution and the desymmetrisation, although the starting material underwent fast oxidation catalysed by GOase M<sub>3-5</sub>, no enantioselectivity was observed for the enzymatic oxidation (data not shown).

It is proposed that this result could be due to either racemisation of the product **92b** or low enantioselectivity by GOase M<sub>3-5</sub> towards the substrate **92a**.

Further screenings of KREDs were subsequently carried out (Table 17). It was observed that although some of the conversions were high (80-90%), almost no *ee* was obtained.

Table 17. Reduction of dialdehyde **92c** by KREDs.

Entry	6 h	<i>ee</i> [%]	<b>92b</b> [%]	24 h	<i>ee</i> [%]	<b>92b</b> [%]
1	KRED101	0	8	KRED101	1	79
2	KRED121	0	72	KRED121	0	88
3	KRED108	2	99	KRED108	0	93
4	KRED118	4	94	KRED118	1	90
5	KRED120	1	94	KRED120	2	86
6	KRED114	1	85	KRED114	1	71
7	KRED119	1	81	KRED119	0	92

*Reaction conditions: 5 g/L 92c, 10% (v/v) DMSO, 5 g/L KREDs, 1 g/L Glucose dehydrogenase (CDX-901), 1 g/L NADP<sup>+</sup>, 3.8 g/L Glucose (1.25 mol excess to the substrate), in KPi buffer (100 mM, pH 7.0), 30 °C, 250 rpm, total volume: 1 mL.*

The fact that no enantioselectivity was observed for both the oxidation of **92a** and reduction of **92c** shows that it is most likely the racemisation of the product monoaldehyde **92b** that leads to the unsatisfactory results.

### 3.2.7 Summary

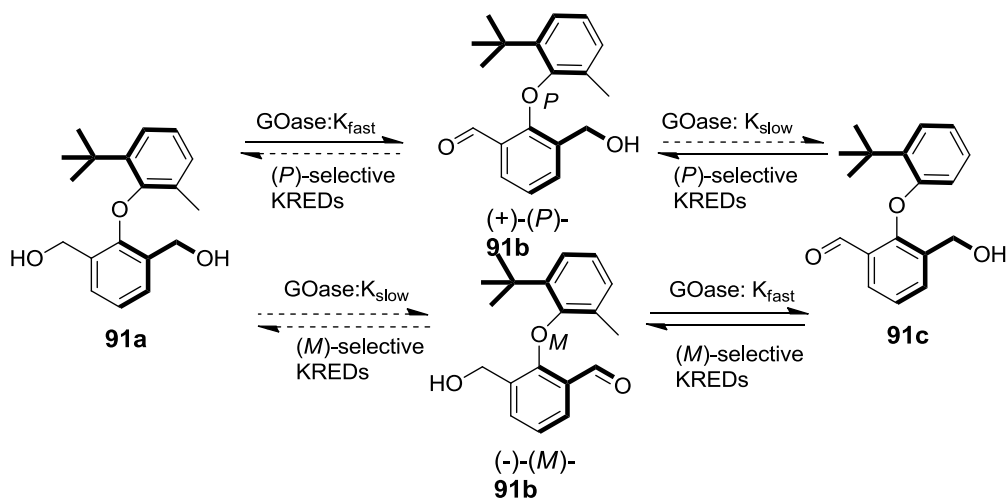


Figure 66 Enantioselective transformations of atropisomeric and proatropisomeric diary ethers.

In summary, as shown in Figure 66, the enantioselective synthesis of atropisomers by desymmetrisation of appropriate proatropisomeric substrates containing a pair of enantiotopic functional groups can be achieved using variants of GOase and a panel of KREDs. Several reaction aspects were investigated for the enzymatic oxidation reactions including the organic co-solvent, concentration of enzymes and the reaction medium. Finally, optimum conditions were identified and applied to both the kinetic resolution of **91b** and the desymmetrisation of **91a**.

Although attempts using mutant GOase F11 and the enzyme Novozym<sup>®</sup> 435 for the synthesis of the enantioenriched atropisomers showed only low to moderate enzymatic activity and selectivity, notable success was achieved using both the variant GOase M<sub>3-5</sub> and KREDs. These results have shown great potential for applications of GOase in the production of atropisomers and hence this approach was explored further in the following studies.

### 3.3 Asymmetric synthesis of biaryls

Atropisomeric biaryls are the most important family of atropisomers.<sup>106</sup> As discussed in §3.1.3, their major applications are as the ligands for transition metal catalysis and building blocks for natural products.<sup>106</sup>

Having developed efficient methods employing GOase M<sub>3-5</sub> and KREDs for the production of optically pure atropisomeric diaryl ethers as described in §3.2, it is interesting to extend the concept to other related substrates.

A series of biaryls with varied functionalities was obtained from the Clayden group. They include the proatropisomeric diols **93a-96a** and dialdehydes **93c-96c**, and the atropisomeric monoaldehydes **93b-96b** in a racemic form (Figure 67).

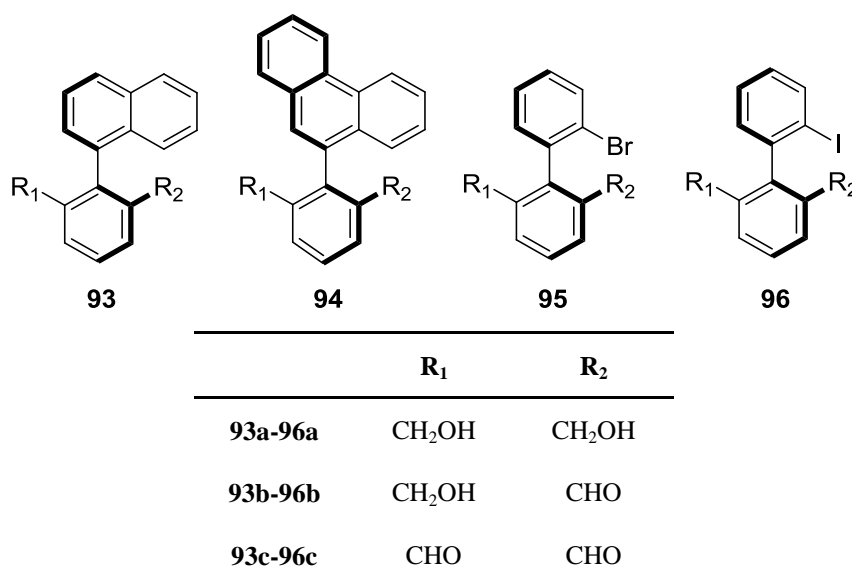


Figure 67. Biaryl substrates obtained from the Clayden group.

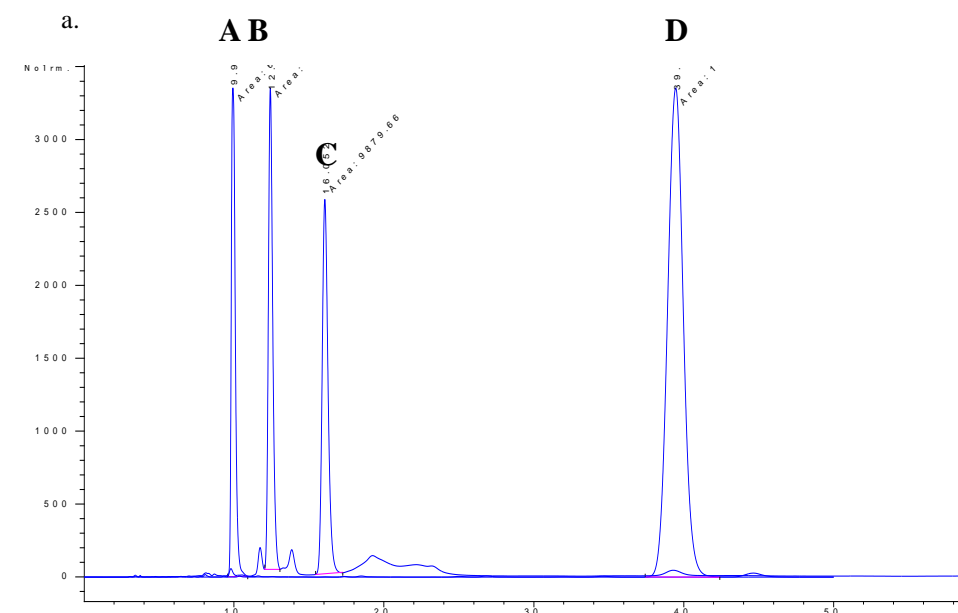
#### 3.3.1 HPLC method development

Chiral normal phase HPLC was employed again for monitoring the kinetics of the reactions. Using the same principles for HPLC method development as discussed in §3.2.1, HPLC solvents (isohexane, heptane, ethanol and IPA) and columns (Chiralcel<sup>®</sup> ADH, OJH, ODH and ASH) were screened against this

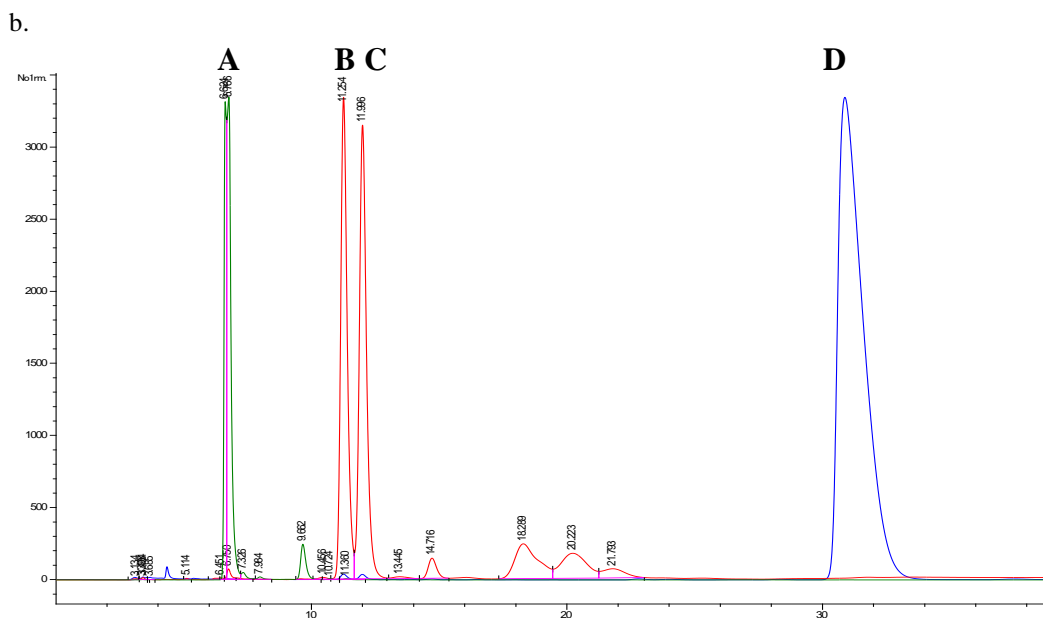


new class of compounds (**93-96**).

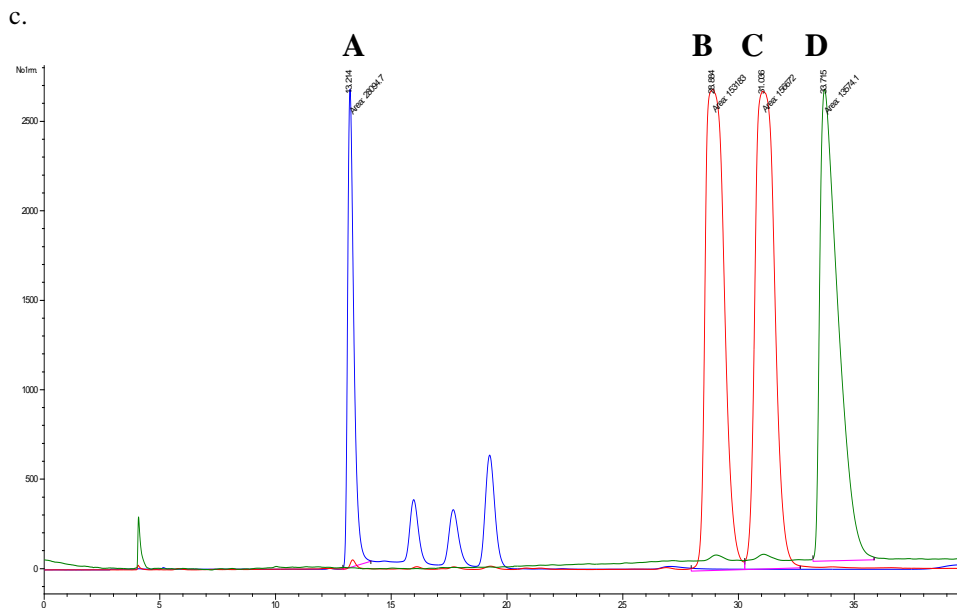
Good separations were obtained and an example for HPLC traces for each of the compounds is shown in Figure 68.



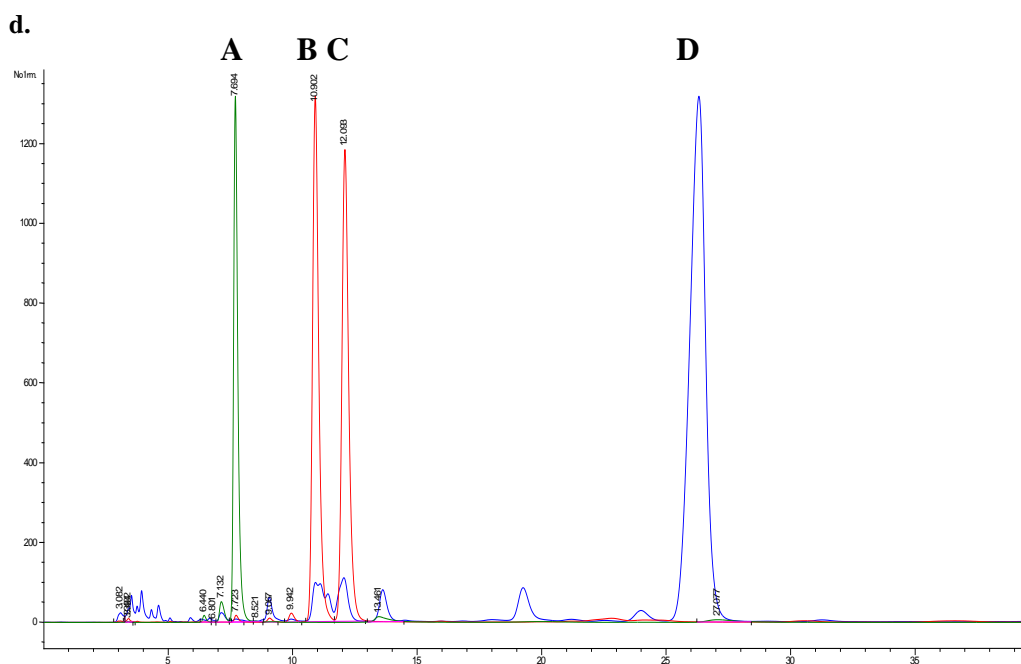
**A** = dialdehyde **93c**; **B** = (*M*)-monoaldehyde **93b**; **C** = (*P*)-monoaldehyde **93b**; **D** = diol **93a**.  
[Chiralcel<sup>®</sup> ADH: isohexane: IPA = 88:12 at 254 nm, flow rate: 1 mL/min]



**A** = dialdehyde **94c**; **B** = (*M*)-monoaldehyde **94b**; **C** = (*P*)-monoaldehyde **94b**; **D** = diol **94a**.  
[Chiralcel<sup>®</sup> ADH: isohexane: IPA = 85:15 at 254 nm, flow rate: 1 mL/min]



**A** = dialdehyde **95c**; **B** = (*P*)-monoaldehyde **95b**; **C** = (*M*)-monoaldehyde **95b**; **D** = diol **95a**.  
 [Chiralcel<sup>®</sup> ADH: n-heptane: ethanol = 95:5 at 210 nm, flow rate: 0.8 mL/min]



**A** = dialdehyde **96c**; **B** = (*P*)-monoaldehyde **96b**; **C** = (*M*)-monoaldehyde **96b**; **D** = diol **96a**.  
 [Chiralcel<sup>®</sup> ADH: isohexane: IPA = 88:12 at 254 nm, flow rate: 1 mL/min]

Figure 68. HPLC standards for: a. **93a-c**; b. **94a-c**; c. **95a-c**; d. **96a-c**.

### 3.3.2 Enzymatic production of naphthyl-substituted biaryls

As shown in Figure 69, same principles for the production of atropisomeric

biaryls were adapted from §3.2.3. Again GOase M<sub>3-5</sub> was employed in the oxidation of the symmetrical diol **93a** to produce the monoaldehyde **93b**, with the possibility of a secondary oxidation. Best KREDs were also chosen based on their performances (*ee* and conversions) in the reduction of the diaryl ether dialdehyde **91c** (see §3.2.5.1), and were screened against the biaryl dialdehyde **93c**.

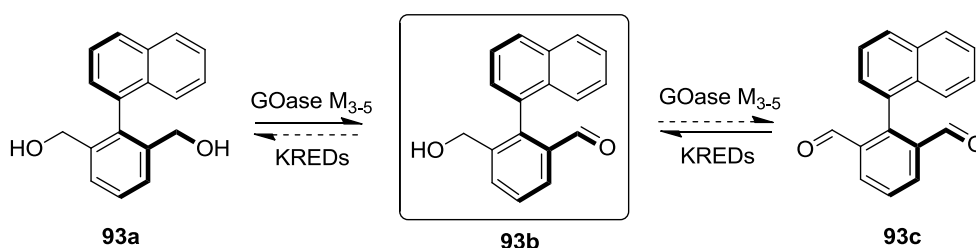


Figure 69. Enzymatic production of atropisomeric naphthyl biaryls.

### 3.3.2.1 Desymmetrisation of diol **93a**

Initial reaction conditions were adapted from the desymmetrisation of diaryl ethers as described in §3.2.3.2. Oxidation by GOase M<sub>3-5</sub> was performed initially at a 2 g/L enzymatic concentration; however, the results were unsatisfactory (*ee* = 57% after 48 h). Therefore, the oxidation reaction was performed with a concentration of GOase M<sub>3-5</sub> of 4 g/L and the results are shown in Table 18.

Table 18. Enzymatic oxidation of diol **93a** by GOase M<sub>3-5</sub> (30 °C).

Entry	Time [h]	<i>ee</i> [%]	<b>93a</b> [%]	<b>93b</b> [%]	<b>93c</b> [%]
1	0.5	84	40	<b>57</b>	3
2	1	90	11	<b>77</b>	12
3	3	<b>99</b>	<b>0</b>	<b>50</b>	<b>50</b>
4	24	99	0	<b>2</b>	98

Reaction conditions: 10 mM diol **93a**, 4 g/L GOase M<sub>3-5</sub>, 30% (v/v) DMSO, 1 g/L HRP, 0.1 g/L catalase, in 100 mM NaPi buffer, 30 °C and 250 rpm, total volume: 0.5 mL.

Rapid formation of the product (*M*)-**93b** in 99% *ee* was observed, with a 50% conversion to (*M*)-**93b** at 3 h (Table 18). As expected, a secondary oxidation was also observed. When allowing the reaction to take place for 24 h, 98% dialdehyde **93c** was produced and the conversion to monoaldehyde **93b** decreased to only 2%.

It was shown that the secondary oxidation simultaneously removed both the desired major atropisomer, (*M*)-**93b**, as well as the undesired minor atropisomer, (*P*)-**93b**. Although to some extent it helped improve *ee* of the monoaldehyde product **93b**, it also severely decreased the conversion. As a result, the secondary oxidation of the desired atropisomer ((*M*)- **93b**) would need to be suppressed.

To suppress the secondary oxidation, the reaction was performed at a lower temperature (20 °C). The results are shown in Table 19.

Table 19. Enzymatic oxidation of diol **93a** by GOase M<sub>3-5</sub> (20 °C).

Entry	Time [h]	<i>ee</i> [%]	<b>93a</b> [%]	<b>93b</b> [%]	<b>93c</b> [%]
1	0.5	86	36	61	3
2	1	87	27	69	4
3	2	90	13	80	7
4	5	96	2	81	17
5	24	99	0	7	93

*Reaction conditions: 10 mM diol 93a, 4 g/L GOase M<sub>3-5</sub>, 30% (v/v) DMSO, 1 g/L HRP, 0.1 g/L catalase, in 100 mM NaPi buffer; 20 °C, 250 rpm, total volume: 0.5 mL.*

Table 19 shows the results for the oxidation of diol **93a** at 20 °C. At 1 h, both *ee* and conversion to monoaldehyde **93b** were lower than the reaction at 30 °C, indicating that the reaction proceeded at a lower rate. After 5 h a higher conversion (81%) was obtained with 96% *ee*. This result shows that a lower reaction temperature is effective in suppressing the secondary oxidation reaction.

### 3.3.2.2 Reduction of dialdehyde **93c**

Next, a panel of KREDs were screened for reduction of the symmetrical dialdehyde **93c**. Results for the screenings are shown in Table 20.

Table 20. Ketoreduction of dialdehyde **93c** by KREDs.

Entry	Enzyme <sup>[a]</sup>	<i>ee</i> [%]	<b>93c</b> <sup>[b]</sup> [%]	Configuration <sup>[c]</sup>
1	KRED 108 ( <i>S</i> )	86	54	<i>P</i>
2	KRED 114 ( <i>S</i> )	88	50	<i>P</i>
3	KRED 118 ( <i>S</i> )	84	86	<i>P</i>
4	KRED 119 ( <i>S</i> )	89	67	<i>P</i>
5	KRED 121 ( <i>S</i> )	29	91	<i>P</i>
6	KRED 124 ( <i>R</i> )	6	41	<i>P</i>

[a] The typical selectivity of the KREDs in the reduction of nonsymmetrical diaryl ketones is shown in parentheses (when known).<sup>141</sup> [b] Conversions after 24 h. [c] Major enantiomers produced by reduction.

*Reaction conditions: 5 g/L 93c, 10% (v/v) DMSO, 5 g/L KREDs, 1 g/L Glucose dehydrogenase (CDX-901), 1 g/L NADP<sup>+</sup>, 3.8 g/L Glucose (1.25 mol excess to the substrate), in KPi buffer (100 mM, pH 7.0), 30 °C, 250 rpm, total volume: 1 mL.*

Good *ee* and conversions were obtained with KRED 108 (Table 20, entry 1), KRED 118 (entry 3), KRED 119 (entry 4). These are also the KREDs that gave the best results towards the diaryl ethers (see §3.2.5.1), indicating that these KREDs are possibly the best ones to accept bulky substrates. It was noted that (*P*)-**93b** was produced from all of the reductions, providing an approach for gaining access to the alternative atropisomer to that produced by GOase M<sub>3-5</sub>.

### 3.3.2.3 Absolute configuration assignment of **93b** (by Mr. Michael Tait and Dr. Simon Willies)

For the purpose of assigning the absolute configuration, the product from the reduction of dialdehyde **93b** by KRED 119 (*ee* = 89%) was analysed by CD

spectrometry by Mr. Michael Tait.

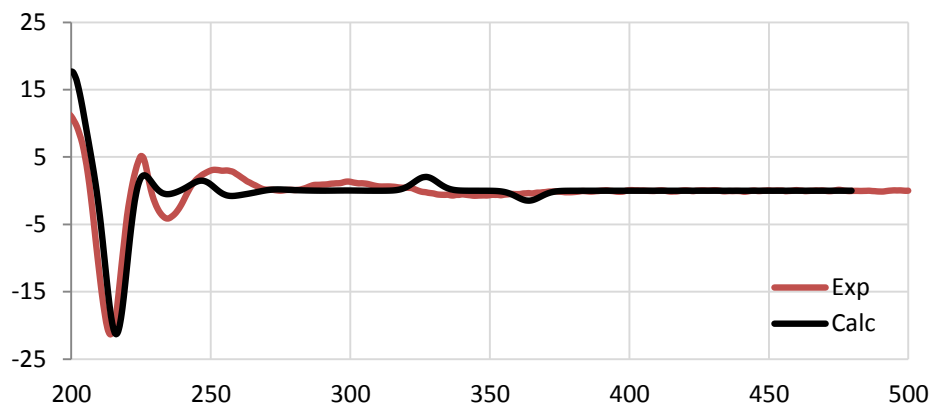
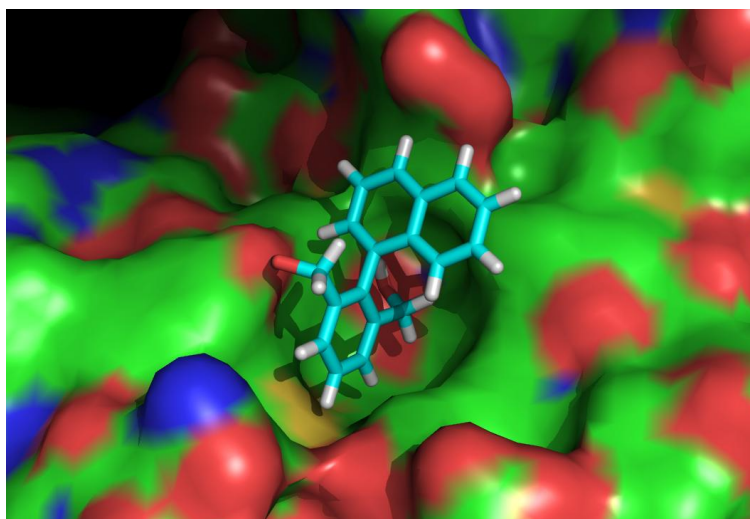


Figure 70. CD spectra obtained by Mr. Michael Tait of monoaldehyde **93b**: (red line) observed for the major atropisomer of monoaldehyde **93b**; (black line) modeled for the lowest energy conformer of (*P*)-**93b**.

Figure 70 shows the data for CD experiments and calculations. The red line represents the trace observed for the major atropisomer of **93b**; and the black line represents the calculated spectrum for the lowest-energy conformer of (*P*)-**93b**. The alignment for the negative maximum peak at *ca.* 220 nm and the positive maximum peak at *ca.* 230 nm shows that the modeled and experimental data matches closely. As a result, KRED 119 can be confirmed to be *P* selective towards **93c** and (*M*)-**93b** to be the major atropisomer produced by desymmetrisation of diol **93a**. This result establishes that the selectivity of GOase M<sub>3-5</sub> is opposite towards the biaryl substrates compared to the diaryl ether substrates (see §3.2.4).

A



B

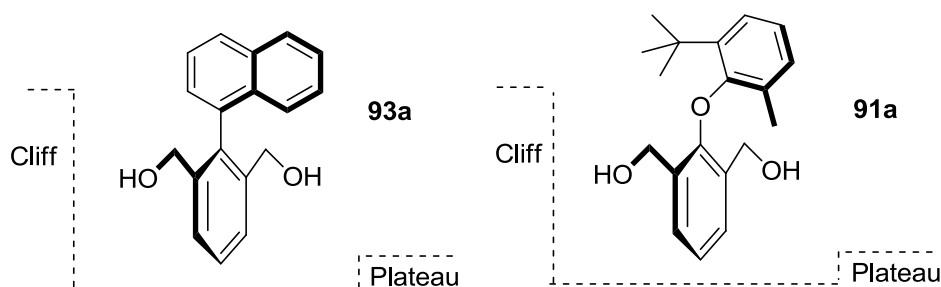


Figure 71. A. Docking model by Dr. Simon C. Willies of **93a** in the active site of GOase M<sub>3-5</sub>; B. Schematic representation for dockings of biaryls and diaryl ethers in the active site of GOase M<sub>3-5</sub>.

To gain further insights into the binding mode, naphthyl diol **93a** was docked into the active site of GOase M<sub>3-5</sub> (performed by Dr. Simon C. Willies from the Turner group). Figure 71A shows the model of the preferential position of the proatropisomeric diol **93a** in the active site. Upon oxidation this substrate would be converted into (*M*)-**93b**. As discussed in §3.2.4, a small cliff and a plateau can be observed at the active site of GOase M<sub>3-5</sub>. A schematic representation of the dockings of diaryl ethers and biaryls can be seen in Figure 71B. Due to the additional oxygen linker in diaryl ethers, the upper ring was pointed away by a certain angle from the bottom ring. Therefore, the *tert*-butyl group in diaryl ethers can sit above the cliff whereas in biaryls the bulky naphthyl group can only sit above the plateau. Therefore, the

enantioselectivity shown with these biaryl substrates is the opposite to that was previously observed with the diaryl ether substrates. This is consistent with the results obtained from the desymmetrisation and CD data.

In summary, atropisomeric naphthyl monoaldehyde **93b** was obtained with *ee* over 90% by the enzymatic desymmetrisation of the diol **93a**. Reduction of the symmetrical dialdehyde **93c** also provides a complementary method for the production of the atropisomeric naphthyl biaryls, especially for the production of (*P*)-**93b** which is not obtainable by the oxidation by GOase M<sub>3-5</sub>. These results demonstrated that the previous method for desymmetrisation of the diaryl ether substrates can be applied to biaryl substrates. Both the diaryl ethers and biaryls have been established to be excellent substrates for the enzyme GOase M<sub>3-5</sub>.

### 3.3.3 Enzymatic production of phenanthryl-substituted biaryls

With the success from the desymmetrisation of the naphthyl series of substrates in hand, a more hindered substrate **94a** was investigated (Figure 72). Previous experiments showed that solubility of the naphthyl substrate **93a** was significantly lower than that of the diaryl ethers. Thus the phenanthryl substrates were expected to have a lower solubility than the naphthyl substrates. Indeed, the extraction method (50-100  $\mu$ L sample extracted by 500  $\mu$ L MTBE) used for all the previous substrates failed for the phenanthryl substrates.

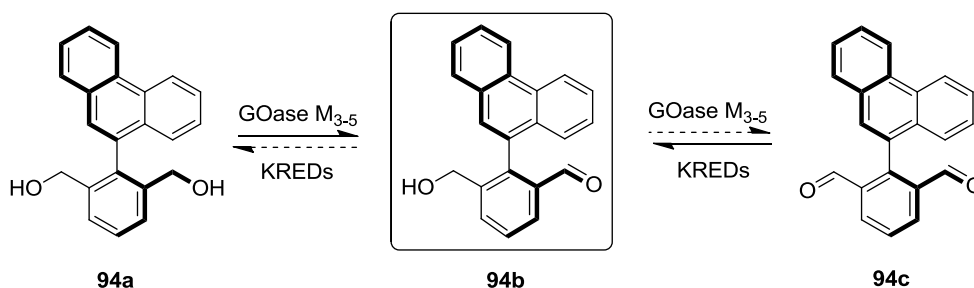


Figure 72. Enzymatic production of atropisomeric phenanthryl biaryls.



Therefore, a new extraction method was developed (100  $\mu$ L sample extracted by 500  $\mu$ L chloroform 3 times, dried under reduced pressure and then 200  $\mu$ L MTBE was added). This new method proved to be efficient.

### 3.3.3.1 Desymmetrisation of diol **94a**

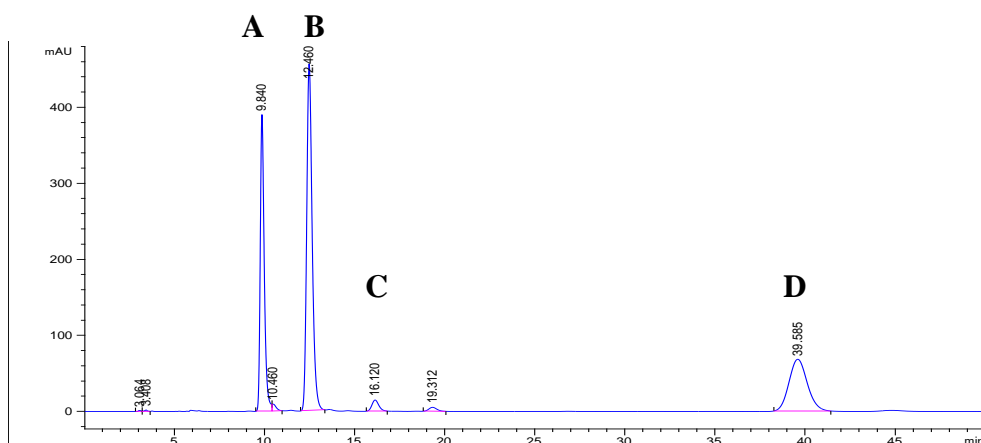
Enzymatic oxidations of the symmetrical diol **94a** by GOase M<sub>3-5</sub> were performed and the results are shown in Table 21.

Table 21. Enzymatic oxidation of diol **94a** by GOase M<sub>3-5</sub>.

Entry	Time [h]	<i>ee</i> [%]	<b>94a</b> [%]	<b>94b</b> [%]	<b>94c</b> [%]
<b>1</b>	0.5	77	62	37	1
<b>2</b>	1	83	48	47	4
<b>3</b>	<b>3</b>	<b>92</b>	<b>14</b>	<b>66</b>	<b>19</b>
<b>4</b>	24	89	15	37	48

Reaction conditions: 10 mM diol **94a**, 4 g/L GOase M<sub>3-5</sub>, 30% (v/v) DMSO, 1 g/L HRP, 0.1 g/L catalase, in 100 mM NaPi buffer, 30 °C, 250 rpm, total volume: 0.5 mL.

It was observed that effective enzymatic oxidation of diol **94a** led to the production of (*M*)-**94b** with 92% *ee* and 66% conversion in 3 h. As an example, the HPLC spectrum of the reaction mixture at 3 h is shown in Figure 73.



A = dialdehyde **94c**; B = monoaldehyde (*M*)-**94b**; C = monoaldehyde (*P*)-**94b**; D = diol **94a**.

Figure 73. HPLC spectrum for the desymmetrisation of diol **94a** by GOase M<sub>3-5</sub> at 3 h (*ee* of **94b** = 92%).

### 3.3.3.2 Reduction of dialdehyde **94c**

KREDs were screened against the symmetrical substrate dialdehyde **94c** (Table 22). The six best KREDs were chosen based on their activities and selectivities towards the diaryl ethers (see §3.2.5.1).

Table 22. Ketoreduction of dialdehyde **94c** by KREDs.

Entry	Enzyme <sup>[a]</sup>	<i>ee</i> [%]	<b>94b</b> <sup>[b]</sup> [%]	Configuration <sup>[c]</sup>
1	KRED 108 (S)	16	40	<i>P</i>
2	KRED 112 (R)	62	27	<i>M</i>
3	KRED 114 (S)	86	39	<i>M</i>
4	KRED 119 (S)	48	35	<i>M</i>
5	KRED 123	95	20	<i>M</i>
6	KRED 124 (R)	30	31	<i>M</i>

[a] The typical selectivity of the KREDs in the reduction of nonsymmetrical diaryl ketones is shown in parentheses (when known).<sup>141</sup> [b] Conversions after 24 h. [c] Major enantiomers produced by reduction.

*Reaction conditions: 5 g/L 94c, 10% (v/v) DMSO, 5 g/L KREDs, 1 g/L Glucose dehydrogenase (CDX-901), 1 g/L NADP<sup>+</sup>, 3.8 g/L Glucose (1.25 mol excess to the substrate), in KPi buffer (100 mM, pH 7.0), 30 °C, 250 rpm, total volume: 1 mL.*

Good to excellent *ee* were obtained with KRED 114 (Table 22, entry 3) and KRED 123 (Table 22, entry 5) though with only moderate conversions to **94b**. Little correlation of the selectivities of KREDs between the naphthyl substrate **93c** and the phenanthryl substrates **94c** was observed. This result suggests that minor alteration in the substrate structure can cause a major change in the selectivity by KREDs. In addition, (*P*)-**94b** was produced from reduction by KRED 108, providing a good approach for gaining access to the alternative atropisomer to that produced by GOase M<sub>3-5</sub>.

### 3.3.3.3 Absolute configuration assignment of **94b** (by Mr. Michael Tait and Dr. Simon Willies)

Again for the purpose of confirming the absolute configuration, the product from the oxidation of diol **94a** by GOase at 3 h (*ee* = 92%) was analysed by CD by Mr. Michael Tait.

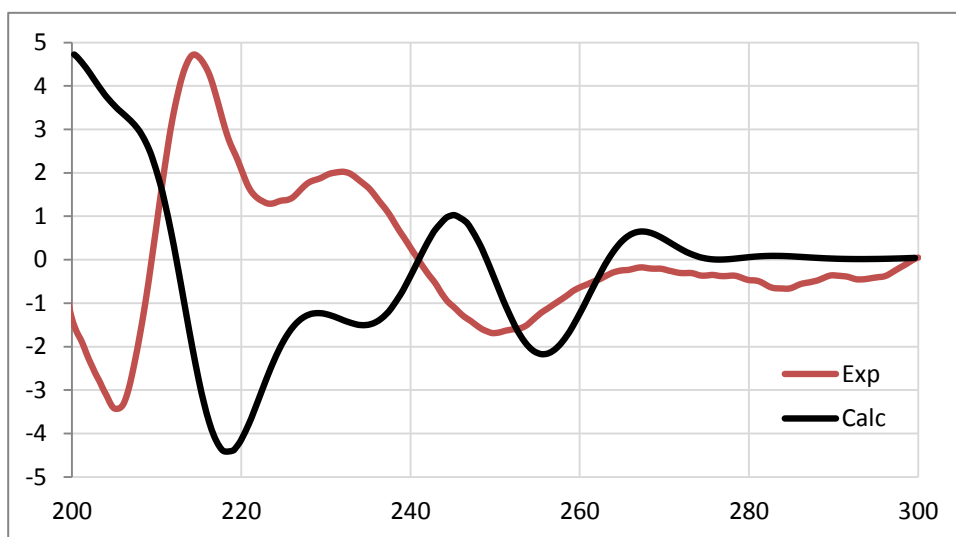


Figure 74. CD spectrum (by Mr. Michael Tait) of monoaldehyde **94b**: (red line) observed for the major atropisomer product of monoaldehyde **94b**; (black line) modeled for the lowest energy conformer of (*P*)-**94b**.

Figure 74 shows the data for CD experiments and calculations. The red line represents the trace observed for the major atropisomer product of **94b**; and the black line represents the calculated line for the lowest-energy conformer of (*P*)-**94b**. The opposite alignment for the positive maximum peak of the experimental data at *ca.* 220 nm and the negative maximum peak of the experimental data at *ca.* 205 nm shows that the modeled and experimental data matches closely. As a result, GOase M<sub>3-5</sub> can be confirmed to be *M* selective towards **94a**. Therefore, the selectivity of GOase M<sub>3-5</sub> towards the diol **94a** is consistent with the naphthyl diol **93a**.

To investigate further how the ligand binds in the active site of GOase, docking models were constructed by Dr. Simon C. Willies (Figure 75).

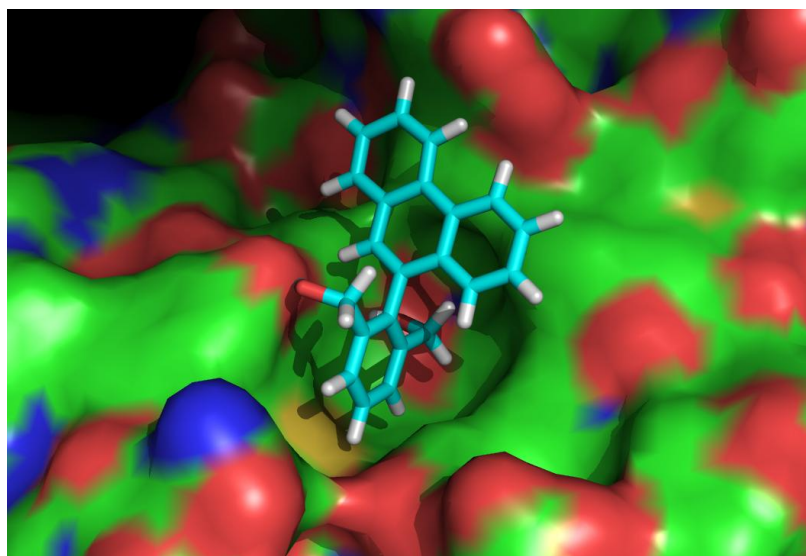


Figure 75. The docking model for phenanthryl substituted diol **94a** in the active site of GOase M<sub>3-5</sub>

Figure 75 shows the model of the preferential position of the proatropisomeric diol **94a** in the active site of GOase M<sub>3-5</sub>. Upon oxidation this would be converted to the monoaldehyde (*M*)-**94b**. This is consistent with the results obtained from the desymmetrisation and CD data.

### 3.3.4 Enzymatic production of halogen-substituted biaryls

Two halogen-substituted biaryls were also obtained from the Clayden group. These substrates are the bromo-substituted (**95a-c**) and iodo-substituted (**96a-c**) biaryls (Figure 76). It was observed that these substrates were soluble in MTBE and that they could be extracted directly by this solvent.

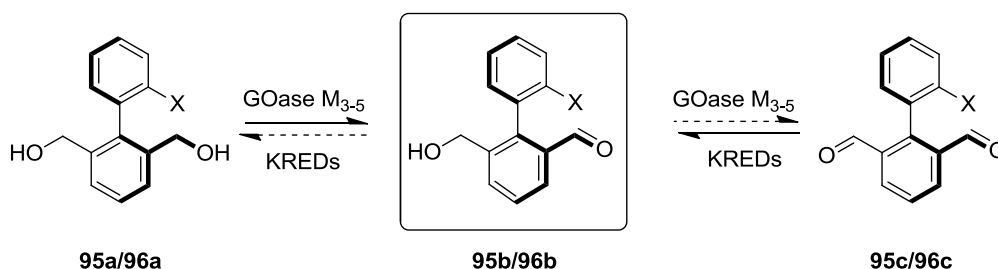


Figure 76. Enzymatic production of atropisomeric halogen-substituted biaryls. Where **95a-c**: X = Br; **96a-c**: X = I.

### 3.3.4.1 Desymmetrisation of diols **95a/96a** by GOase M<sub>3-5</sub> and reduction of dialdehydes **95c/96c** by KREDs

Same conditions were applied as described in §3.3.2.1 and §3.3.2.2. Both enzymatic oxidation by GOase M<sub>3-5</sub> and reduction by KREDs were performed and results are shown in Table 23.

The selectivity with GOase M<sub>3-5</sub> was observed to be lower than that of the naphthyl and phenanthryl substituted biaryls (Table 23, entries 1 and 8). However, as a good complementary method, a number of KREDs show outstanding *ee* towards the production of **95b/96b**. Both KRED 120 for bromo-substituted biaryls (entry 6, *ee* = 88%, conversion = 50%,) and KRED 121 for iodo-substituted biaryl (entry 14, *ee* = 92%, conversion = 49%) are good examples for the production of **95b/96b** in high optical purity.

Table 23. Enzymatic production of monoaldehydes **95b/96b**.

Entry	Substrate	Enzyme <sup>[a]</sup>	<i>ee</i> [%]	<b>95b/96b</b> <sup>[b]</sup> [%]	Configuration <sup>[c]</sup>
<b>1</b>	<b>95a</b>	<b>GOase M<sub>3,5</sub></b>	<b>48</b>	<b>14</b> <sup>[c]</sup>	<i>M</i>
<b>2</b>	<b>95c</b>	KRED 108 ( <i>S</i> )	83	59	<i>P</i>
<b>3</b>	<b>95c</b>	KRED 114 ( <i>S</i> )	86	43	<i>M</i>
<b>4</b>	<b>95c</b>	KRED 118 ( <i>S</i> )	20	39	<i>P</i>
<b>5</b>	<b>95c</b>	KRED 119 ( <i>S</i> )	2	66	<i>M</i>
<b>6</b>	<b>95c</b>	KRED 120 ( <i>S</i> )	88	50	<i>P</i>
<b>7</b>	<b>95c</b>	KRED 121 ( <i>R</i> )	87	69	<i>P</i>
<b>8</b>	<b>96a</b>	<b>GOase M<sub>3,5</sub></b>	<b>21</b>	<b>37</b>	<i>M</i>
<b>9</b>	<b>96c</b>	KRED 108 ( <i>S</i> )	84	27	<i>P</i>
<b>10</b>	<b>96c</b>	KRED 114 ( <i>S</i> )	65	34	<i>M</i>
<b>11</b>	<b>96c</b>	KRED 118 ( <i>S</i> )	11	38	<i>M</i>
<b>12</b>	<b>96c</b>	KRED 119 ( <i>S</i> )	6	30	<i>M</i>
<b>13</b>	<b>96c</b>	KRED 120 ( <i>S</i> )	78	83	<i>P</i>
<b>14</b>	<b>96c</b>	KRED 121 ( <i>R</i> )	92	49	<i>P</i>

[a] The typical selectivity of the KREDs in the reduction of nonsymmetrical diaryl ketones is shown in parentheses (when known).<sup>141</sup> [b] Conversions after 24 h. [c] Major enantiomers produced by reduction.

*Reaction conditions for the oxidation: 10 mM diol 95a/96a, 4 g/L GOase M<sub>3,5</sub>, 30% (v/v) DMSO, 1 g/L HRP, 0.1 g/L catalase, in 100 mM NaPi buffer, total volume: 0.5 mL, 30 °C, 250 rpm. Reaction conditions for the reduction by KREDs: 5 g/L 95c/96c 10% (v/v) DMSO, 5 g/L KREDs, 1 g/L Glucose dehydrogenase (CDX-901), 1 g/L NADP<sup>+</sup>, 3.8 g/L Glucose (1.25 mol excess to the substrate), in KPi buffer (100 mM, pH 7.0), 30 °C, 250 rpm, total volume: 1 mL.*

Although most of the KREDs showed consistency in the selectivity, there is one exception which is KRED 118. It is (*P*)-selective for bromo dialdehyde **95c** and (*M*)-selective for iodo dialdehyde **96c** (entries 4 and 11). It shows that even minor alteration such as from bromo group to iodo group can cause the reverse of selectivity for KREDs.

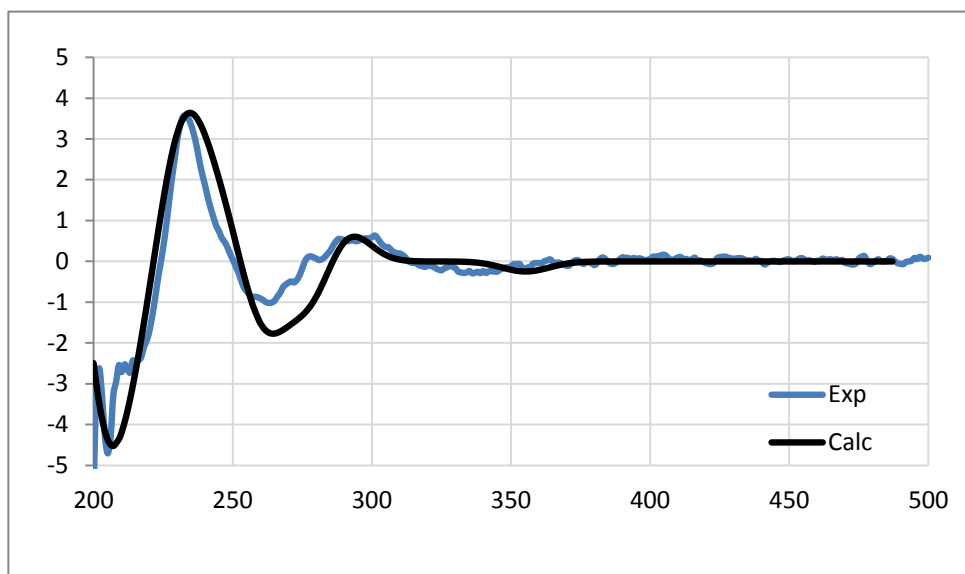
### 3.3.4.2 Absolute configuration assignment of **95b** and **96b** (by Mr. Michael Tait and Dr. Simon Willies)

The products from the reduction of the **95c** by KRED 108 ( $ee = 80\%$ ) and the reduction of **96c** by KRED 121 ( $ee = 92\%$ ) were analysed by CD by Mr. Michael Tait.

As shown in Figure 77, the modeled spectra for (*P*)-**95b**/*(P)*-**96b** and experimental data for the major atropisomer product of **95b/96b** show close matches; thus, KRED 108 and KRED 121 were determined to be *P* selective towards diols **95a** and **96a**, respectively.

As a result, it can be confirmed that GOase M<sub>3-5</sub> is *M*-selective towards both diol **95a** and **96a**. This is consistent with the results obtained from the naphthyl and phenanthryl substituted substrates.

a.



b.

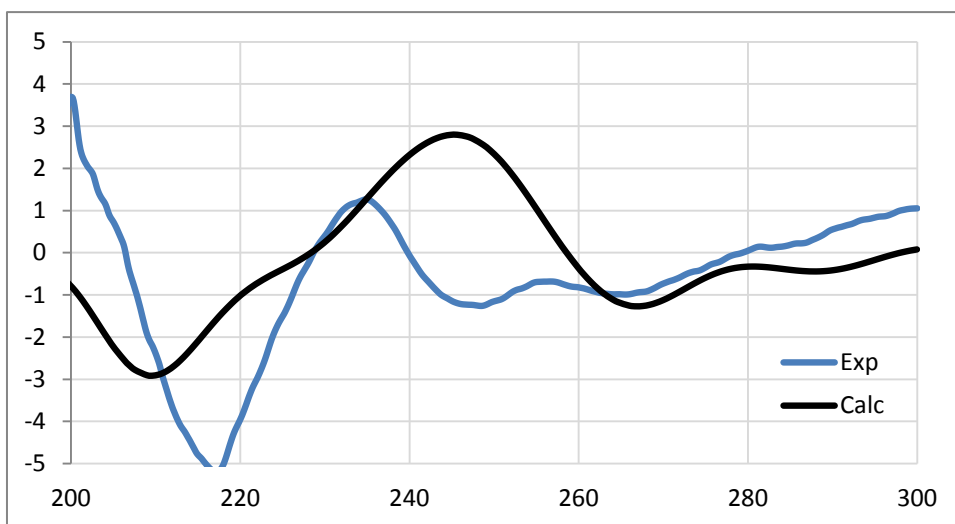


Figure 77. CD spectrum (by Mr. Michael Tait) of a. (*P*)-**95b** and b. (*P*)-**96b**: (blue line) observed for the major atropisomer product of **95b/96b**; (black line) modeled for the lowest-energy conformer of (*P*)-**95b/96b**.

Both **95a** and **96a** were docked into the active site of GOase M<sub>3.5</sub> subsequently. Since the models show similar characteristics for the two substrates, only the model of **95a** is shown.



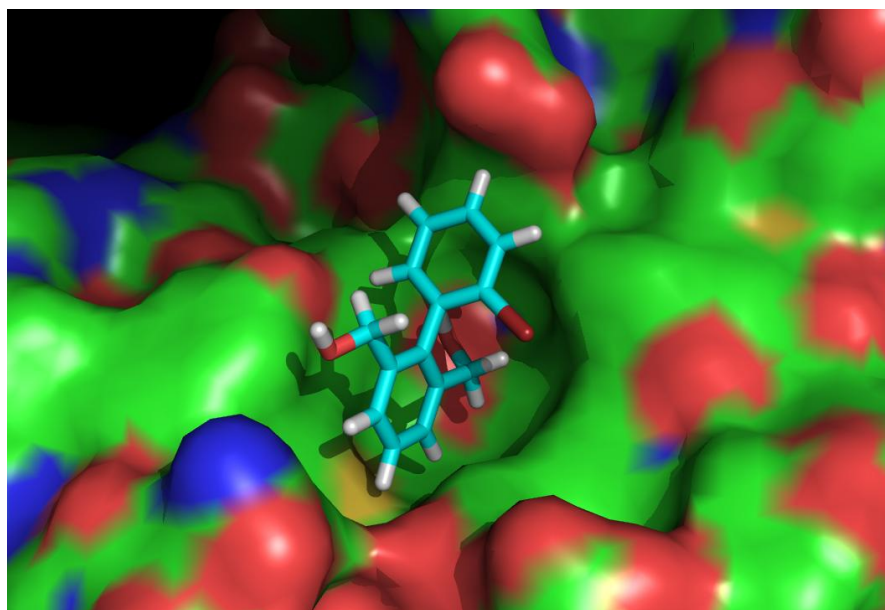


Figure 78. The docking model for **95a** in the active site of GOase M<sub>3-5</sub>.

Figure 78 shows the model of **95a** in the active site of GOase M<sub>3-5</sub>. The pro-(*M*) hydroxyl group is placed preferentially close to the copper centre. Therefore, oxidation at this position would lead to the monoaldehyde (*M*)-**95b**. This is consistent with the conclusions drawn from the desymmetrisation and CD results.

### 3.3.5 Summary and outlook

In summary, as shown in Figure 79, single atropisomers of a number of biaryls with various functionalities can be obtained by enzymatic desymmetrisations. Both the desymmetrisations of diols by GOase M<sub>3-5</sub> and the desymmetrisations of dialdehydes by KREDs led to the production of the monoaldehyde of the biaryls in high *ee*. *M* atropisomer was obtained from the oxidation of all the diols by GOase M<sub>3-5</sub> and both *M* and *P* atropisomers are accessible by the reduction by KREDs.

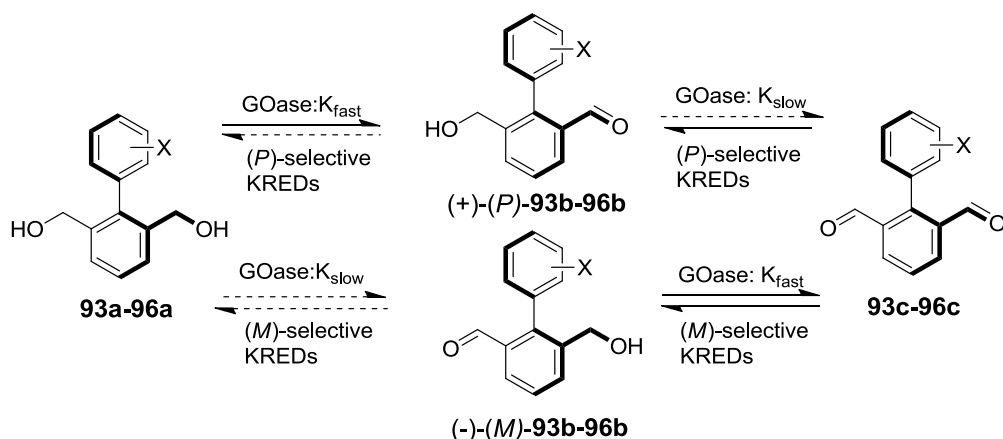
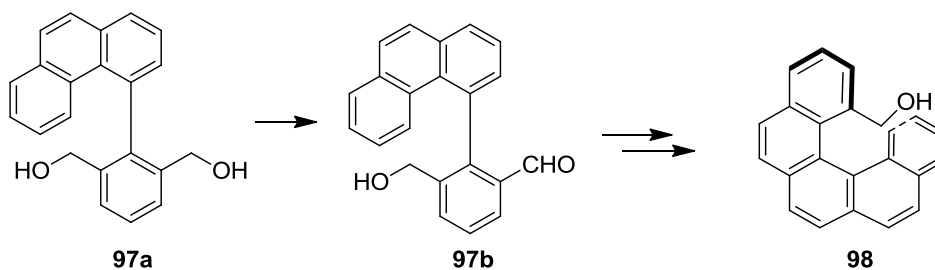


Figure 79. Enzymatic enantioselective production of biaryls.

The results show that the variant GOase M<sub>3.5</sub> possesses very attractive and unconventional selectivity towards the production of single atropisomers. In addition, reduction by KREDs obtained from Codexis Ltd. is also a good complementary approach in the production of single atropisomers.

In the future, by screening a broad range of proatropisomeric and atropisomeric substrates, the application of this variant in the production of single atropisomers can be exploited further. As a single example, GOase M<sub>3.5</sub> can potentially be applied in the desymmetrisation of an isomer of **94a** (Figure 80, **97a**). The product **97b** has potential applications for the synthesis of helicenes (**98**), which have applications in a broad range of areas and are challenging to synthesise chemically in high optical purity.<sup>142-144</sup>

Figure 80. Potential application of GOase for the production of helicenes (**98**).

Furthermore, by subjecting this variant to further rounds of directed evolution, mutants with higher activity and broader substrate range can be

obtained. These mutants can then serve as biocatalysts in broader and larger scale applications for the synthesis of single atropisomers.

## 4. Results and Discussion - Application of CALB (Novozym<sup>®</sup> 435) in the Production of Erucamide

### 4.1 Introduction

Interest in the primary amides of fatty acids (two typical fatty acids, oleic acid (**99a**) and erucic acid (**100a**), are shown in Figure 81) has increased significantly ever since Cravatt *et al.* isolated oleamide and erucamide (Figure 81, **99b** and **100b**) from the cerebrospinal fluid of cat, rat and human.<sup>145</sup> Research studies concerning primary amides have proceeded rapidly since then, and a number of clinical applications have been investigated, including regulation of the sleep/wake cycle<sup>145</sup> and stimulation of the growth of blood vessels.<sup>146</sup> Primary amides of fatty acids are also widely applied in the polymer industry. They are produced in large quantities each year (oleamide: 77,000+ tons/year).<sup>147</sup> The major application for amides of fatty acids is in the extrusion process of polymers, such as lubricants and anti-slip agents.<sup>148</sup>

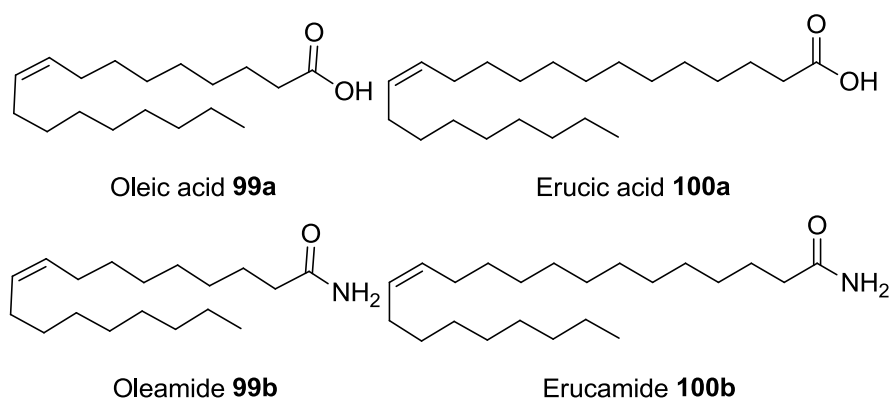


Figure 81. Structures for two typical fatty acids and their amides.

#### 4.1.1 The enzyme *Candida antarctica* Lipase B (CALB)

Lipases (EC 3.1.1.3) are the most important and widely applied enzymes from

the hydrolase group.<sup>149</sup> They possess excellent chemo-, regio- and stereoselectivity and often do not require co-factors.<sup>150</sup> A considerable number of lipases has been applied in industry for the production of fine chemicals, pharmaceuticals and agrochemicals.<sup>151-154</sup>

CALB is one of the most widely applied lipases in organic synthesis.<sup>155-156</sup> This lipase has superior promiscuity, catalysing a variety of reactions including kinetic resolution of racemic alcohols, acids, esters or amines,<sup>157</sup> and desymmetrisation of *meso* or prochiral compounds.<sup>36</sup> In addition, non-conventional processes including aldol reactions and Michael additions can also be catalysed by CALB.<sup>158-159</sup>

CALB consists of 317 aa, with a molecular mass of 33 kDa (Figure 82). CALB was firstly obtained from the *Candida antarctica* yeast, which is also the origin of CALA, a non-specific and more thermostable lipase. The structure of CALB was resolved in 1994.<sup>160-161</sup> It has an  $\alpha/\beta$ -hydrolase-like fold, which typically exists in lipases, esterases, amidases, epoxide hydrolases, dehydrogenases and hydroxynitrile lyases.<sup>162</sup> The catalytic triad Asp187-His224-Ser105 is situated below a large hydrophobic pocket and above a medium-sized pocket. CALB has shown excellent enantiopreference towards secondary alcohols and other nucleophiles such as primary amines, which can be attributed to its restricted active site. CALB has also been subjected to genetic engineering to improve selectivity<sup>163-164</sup> and create novel synthetic applications.<sup>165</sup>

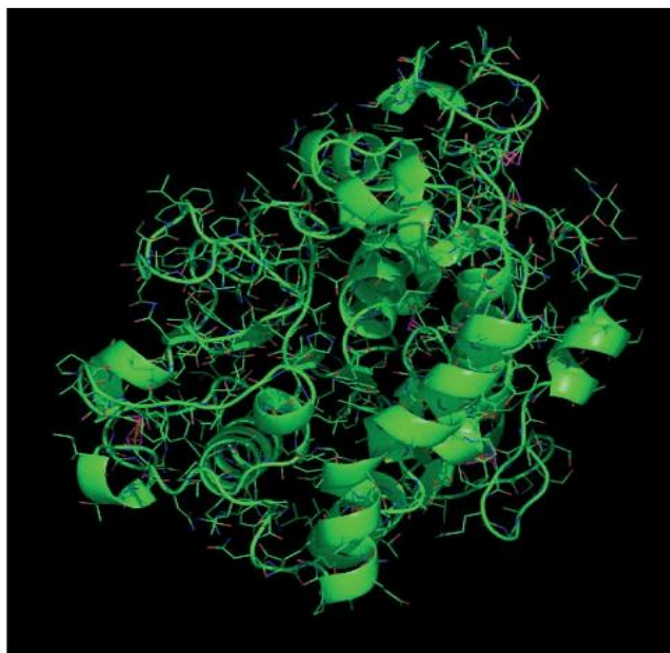


Figure 82. Structure of *Candida antarctica* lipase B.<sup>155</sup>

Different trade names have been used for CALB and one of the most widely applied is Novozym<sup>®</sup> 435 (trade name of a commercially available, recombinant, immobilised product).

CALB has been applied in a number of studies for the direct amidation of fatty acids to produce fatty amides, using either gaseous or solid form of ammonia source.<sup>147-148,166-168</sup> However, most of these studies were conducted in organic solvents.<sup>147-148,166</sup> So far, no study has been reported for the enzymatic solvent-free production of **100b**. Due to the industrial demand for the production of **100b** based upon an environmentally friendly, low energy process, studies were conducted for the solvent-free enzymatic production of **100b**.

#### 4.1.2 Lipase catalysed amidation of fatty acids in organic solvents

For the direct amidation of free carboxylic acids with ammonia, harsh chemical conditions (200 °C, 7 bar, anhydrous ammonia) have been described. However,

Litjens *et al.* demonstrated that butyramide and **99b** can be synthesised by direct lipase-catalysed reaction with saturated ammonia (NH<sub>3</sub>) solution (in methyl isobutyl ketone, MIBK) in an organic solvent at 25 °C and atmospheric pressure (Figure 83).<sup>148,166</sup>

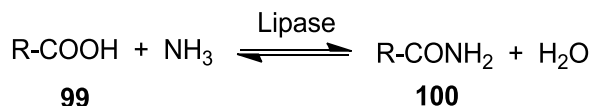


Figure 83. Direct amidation of a fatty acid with ammonia.<sup>148</sup>

Litjens *et al.*<sup>166</sup> reported yields at equilibrium (after 17 days) for the amide of 80–90% when using ammonium bicarbonate and 90–100% when using ammonium carbamate as the ammonia source. They have also demonstrated that the combined effect of a higher ammonia concentration and a lower water concentration gives rise to better conversions. Ammonium carbamate was also shown to be advantageous; this is because one eq. of ammonia, water and carbon dioxide are produced when ammonium bicarbonate is dissolved in water, whereas ammonium carbamate provides two eq. of ammonia and one eq. of carbon dioxide. Subsequently, most studies on this subject have employed ammonium carbamate as the choice of ammonia source.<sup>147,168-169</sup>

Slotema *et al.* have developed an economically pertinent process for the lipase catalysed synthesis of amides.<sup>147</sup> A continuous plug-flow reactor system for the direct amidation of **99a** to **99b** has been employed and CALB catalysed the continuous conversion of 85% of **99a** to **99b**. The choice of the solvent was found to be important for the reaction performance; it should be miscible with water, ammonia and **99a**. It should also allow fast reaction kinetics and high conversion at thermodynamic equilibrium without destroying the enzyme support. As a result, 2-methyl 2-butanol (2M2B) was chosen as a good compromise.

### 4.1.3 Solvent-free lipase catalysed amidation of fatty acids

Organic solvents have a lot of advantages in lipase-catalysed synthesis including shifting the equilibrium of hydrolytic reactions and improving the solubility. However, their application in industrial processes is less desirable for a variety of reasons. For example, organic solvents are volatile organic compounds (VOCs), resulting in low-level ozone and smog.<sup>168</sup> Expensive post-treatments, including solvent evaporation and recycling, are also required. In addition, the reactants are diluted by the organic solvent, so that larger and more costly reactors and auxiliary equipment are needed. Thus, a solvent-free process would be advantageous from both an environmental and economical perspective.

Tufvensson *et al.* have reported an environmentally benign, and volume efficient process for the enzymatic production of alkanolamides.<sup>168</sup> CALB was used to catalyse the condensation of lauric acid ( $C_{12}H_{24}O_2$ ) with monoethanolamine. A temperature of 90 °C was required to keep the system in a liquid state, at which the enzyme was both very active and stable, with half of the activity remaining after 2 weeks. A yield of 75% was obtained using one molar eq. of the reactants, and the yield was improved to 95% upon water removal.

Prasad *et al.* have described a solvent-free, lipase catalysed, enantioselective amidation of aliphatic carboxylic acid with various amines.<sup>167</sup> The reaction was performed at 90 °C and the equilibrium shifted towards amide synthesis by the removal of water under reduced pressure. 80-91% yields of the amides were obtained.

In summary, studies have been conducted for the synthesis of primary amides and showed that ammonia carbamate can serve as an outstanding ammonia source. Nevertheless, few examples of solvent-free processes have been reported. In this study, further investigation into the production of **100b**



using ammonia carbamate under solvent-free conditions was carried out and is now described.

## 4.2 Lipase catalysed amidation of fatty acids in organic solvents

Initial studies to investigate the activity of Novozym<sup>®</sup> 435 in the amidation of erucic acid (**100a**), involved reacting the latter with ammonium carbamate in the organic solvent 2M2B (Figure 84). These conditions were adapted from the work reported by Slotema *et al.*,<sup>147</sup> in which they presented studies comparing various ammonia sources and organic solvents, and showed that ammonium carbamate and 2M2B were the best choice of ammonia source and solvent, respectively.

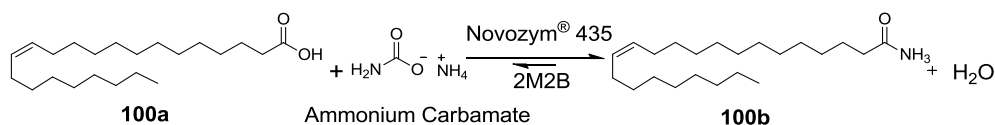


Figure 84. Enzymatic amidation of **100a** catalysed by Novozym<sup>®</sup> 435 using ammonium carbamate in 2M2B.

Figure 85 shows the conversions to **100b** in the solvent 2M2B over 5 days. It can be seen that the reaction reached equilibrium after 30 h and the maximum conversion (46%) was obtained. This result is comparable to that obtained by Slotema *et al.*<sup>147</sup>

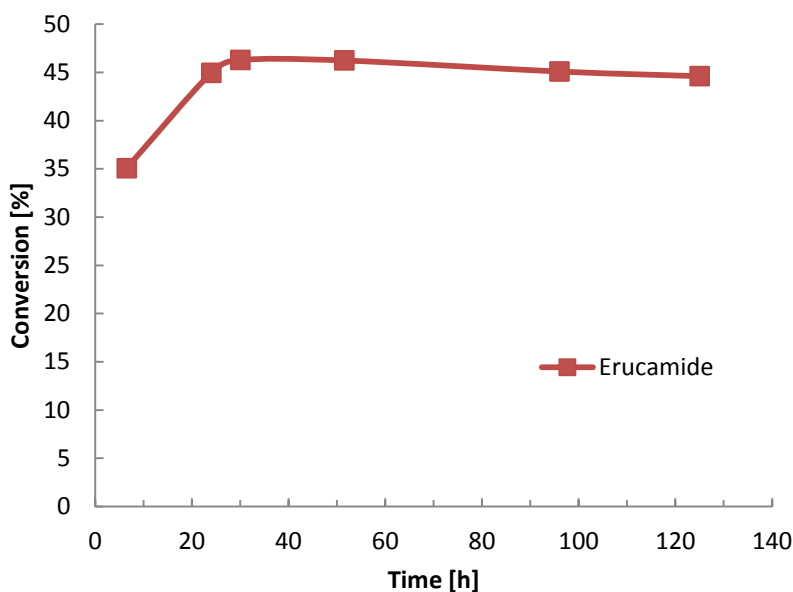


Figure 85. Conversions to **100b** for the reaction in 2M2B.

Reaction conditions: 100 mM **100a**, 1 eq. ammonia, 5 mL 2M2B, 30 wt%  
Novozym<sup>®</sup> 435, 60 °C.

These results also established the feasibility of performing Novozym<sup>®</sup> 435 catalysed amidation of **100a**. Therefore, further investigations of the amidation reactions under solvent-free conditions were conducted.

### 4.3 Solvent-free lipase catalysed amidation of fatty acids

In this section attempts for production of **100b** without the utilisation of organic solvents are discussed.

Ammonium carbamate slowly decomposes to 2 eq. of ammonia and 1 eq. of CO<sub>2</sub>, and the ammonia released can serve as the ammonia source for the reaction. The water produced from the reaction could drive the reaction equilibrium into the undesired direction and hence it is necessary to remove water during the reaction by evacuation. However, this process is also likely to remove ammonia as well as water.

The melting point for **100a** is 33-34 °C, and the melting point for **100b** is 83-84 °C. As a result, 90 °C was chosen as the reaction temperature according

to the melting points and published studies<sup>167-168</sup> on the benefit of maintaining the reaction mixture in a liquid state.

#### 4.3.1 Optimisation of evacuation

A reaction was performed with the application of a vacuum during the reaction to remove water produced from the reaction and to shift the equilibrium towards the formation of **100b**.

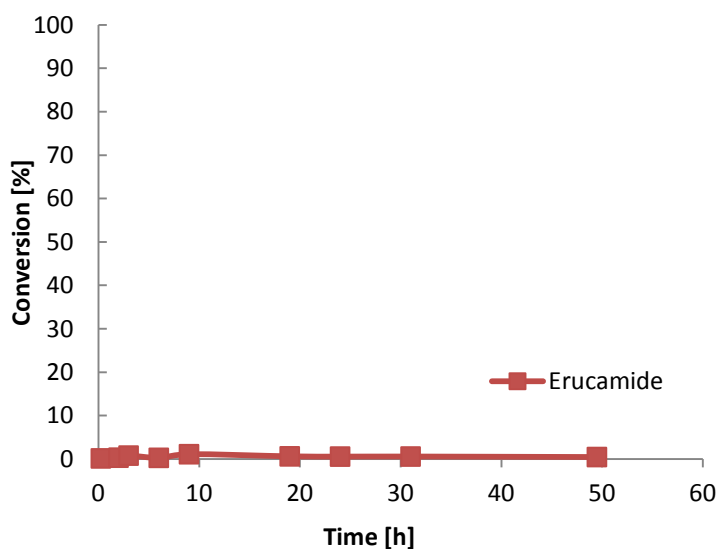


Figure 86. Conversions to **100b** for the solvent-free reaction under evacuation.  
Reaction conditions: 3 mmol **100a**, 1 eq. ammonia, 3 wt% Novozym<sup>®</sup> 435, 90 °C.

Almost no conversion was observed (Figure 86), a result attributed to the simultaneous removal of ammonia by evacuation. Therefore, it was deemed not possible to apply vacuum continuously throughout the reaction. However, if vacuum were to be applied in cycles, this problem could be circumvented. Therefore, cyclical evacuations were applied to the amidation of **100a** (Figure 87).

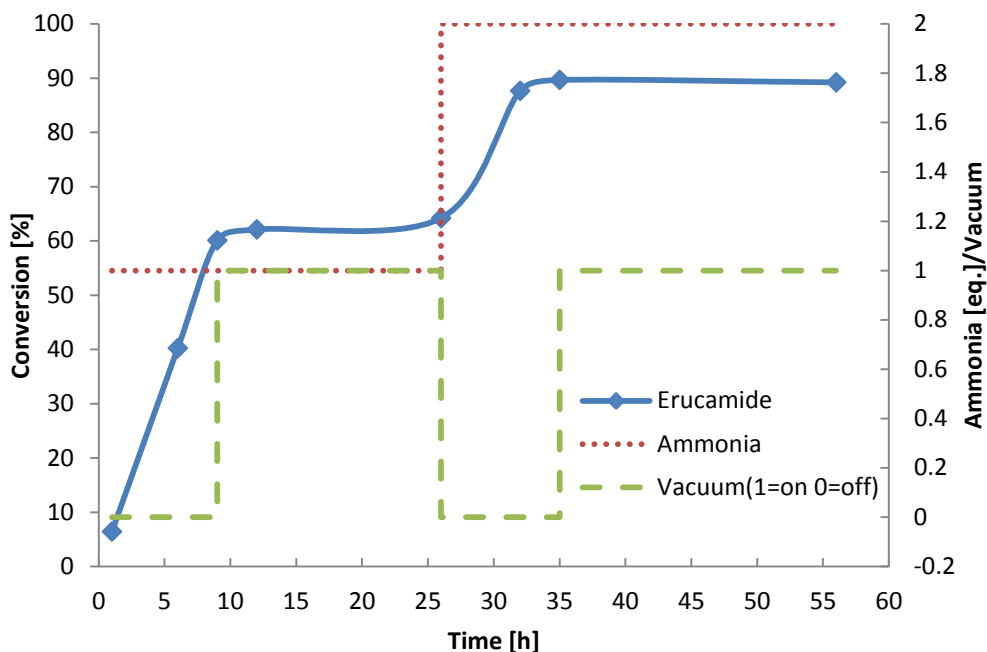


Figure 87. Conversions to **100b** with cyclical evacuation.

Reaction conditions: 10 mmol **100a**, 1 eq. ammonia, 3 wt% Novozym® 435, 90 °C.

Two cycles were performed to drive the reaction further in the desired direction. Previous results with only 1 eq. ammonia showed that the reaction reaches equilibrium after around 9 h. Therefore, during the first cycle, upon addition of 1 eq. ammonia the reaction was allowed to proceed for 10 h before vacuum was applied overnight. At the beginning of the second cycle, the vacuum was turned off and the first cycle was repeated.

Around 60% yield of **100b** was obtained after the first cycle. The improvement in yields further established that ammonia was indeed simultaneously removed when the vacuum was applied throughout the reaction. An improved yield (89%) of **100b** was obtained after 2 cycles in 55 h with 2 eq. ammonia added. A control reaction was conducted under the same reaction conditions but in the absence of Novozym® 435, leading to a yield of **100b** of only 12%. This observation establishes that Novozym® 435 serves as a good catalyst for the amidation reaction.

To examine the effect of evacuation, two reactions were performed in parallel under the same conditions, with and without evacuation. Reactions

were also scaled up to 120 mmol fatty acid substrate for the purpose of examining larger scale reaction for industrial applications (Figure 88).

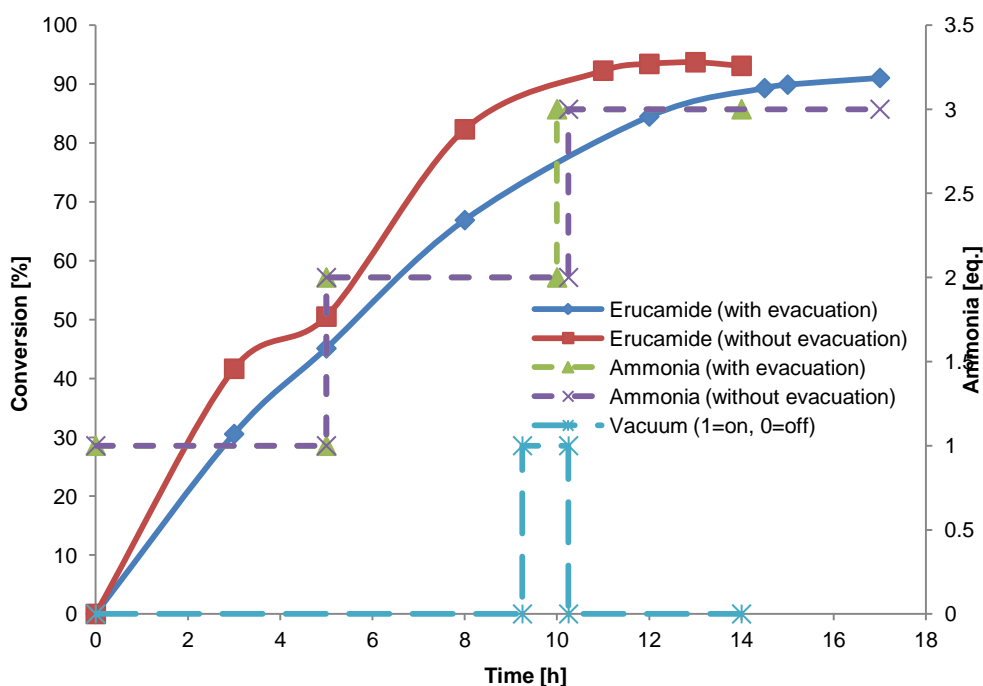


Figure 88. Examination of the effect of evacuation.

Reaction conditions: 120 mmol **100a**, 1 eq. ammonia, 1.5 wt% Novozym<sup>®</sup> 435, 90 °C.

It can be seen that the final conversions after 16 h were comparable for these two reactions. Therefore, no evacuation was applied in further studies.

#### 4.3.2 Optimisation of the enzymatic concentration

To examine the optimum enzymatic concentration for the amidation of **100a**, a series of reactions was performed over a range of 0.75%-3% w/w enzyme concentration.

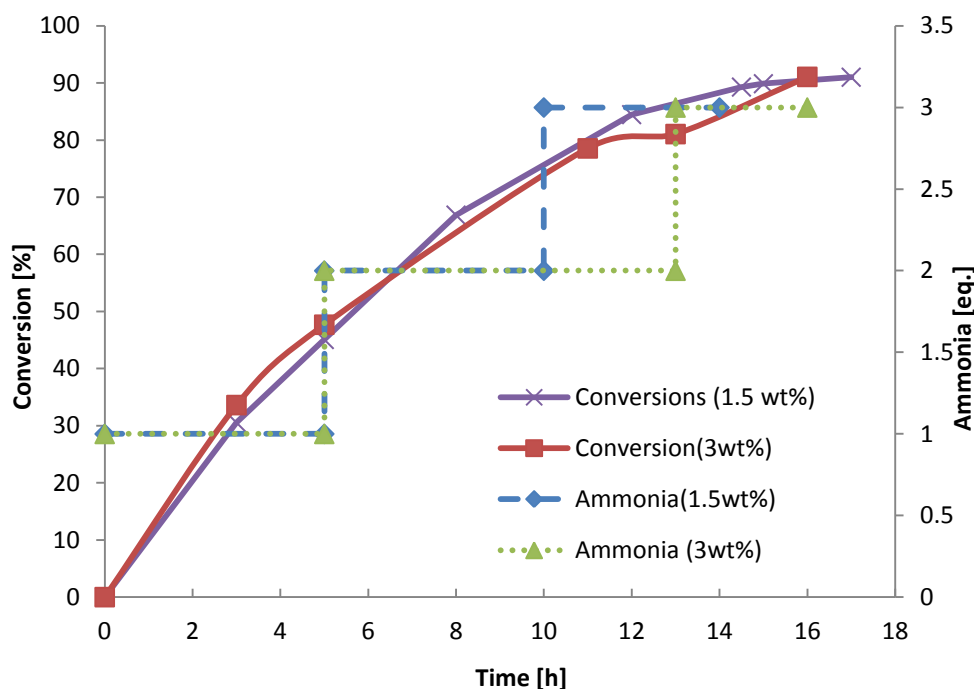


Figure 89. Optimisation of enzymatic concentration.

Reaction conditions: 120 mmol **100a**, 3 eq. ammonia, 1.5-3 wt% Novozym<sup>®</sup> 435, 90 °C.

0.75 wt%, 1.5 wt% and 3 wt% of Novozym<sup>®</sup> 435 were added and the results for the reactions with 1.5 wt% and 3 wt% Novozym<sup>®</sup> 435 are shown in Figure 89. The data for the reaction with 0.75% have not been included due to low conversions obtained (data not shown). Since the conversions for the reactions with 1.5 wt% and 3 wt% were comparable, 1.5 wt% of Novozym<sup>®</sup> 435 was used in the following reactions.

### 4.3.3 Enzyme recycling

Immobilised enzymes have been shown to display enhanced stability compared to their non-immobilised counterpart.<sup>170-172</sup> The biocatalyst Novozym<sup>®</sup> 435 employed in this project is comprised of *Candida antarctica* lipase B immobilised on a macroporous acrylic resin. Novozym<sup>®</sup> 435 has shown excellent thermostability in continuous processes at 60 °C and below. However, no study has been reported concerning Novozym<sup>®</sup> 435 stability at 90 °C under solvent-free conditions. In the following experiment, two

amidation reactions were performed in parallel, one employing fresh Novozym<sup>®</sup> 435 and the other using Novozym<sup>®</sup> 435 recovered from a previous amidation reaction (Figure 90).

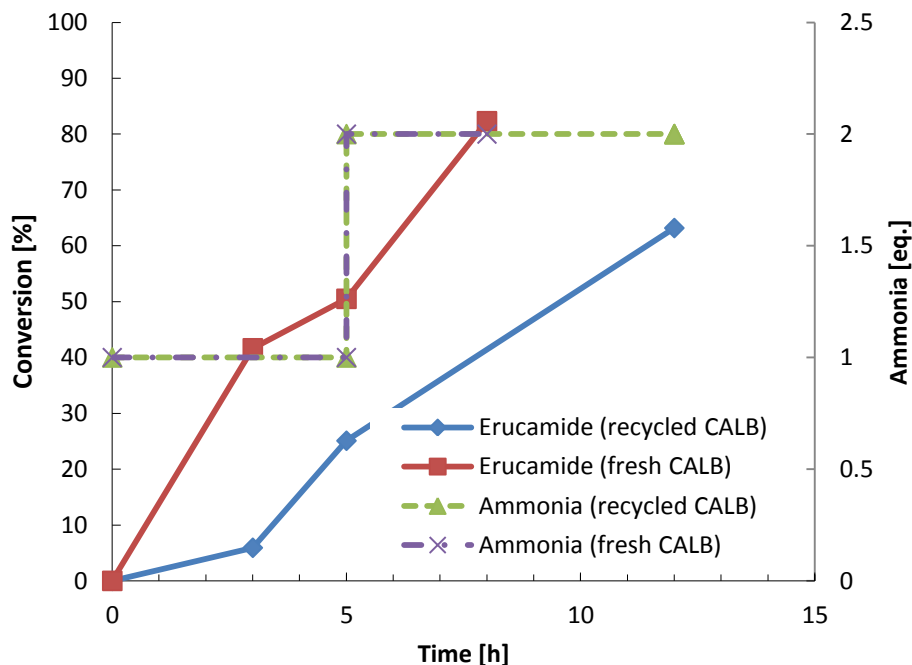


Figure 90. Amidation of **100a** by both fresh and recycled Novozym<sup>®</sup> 435.  
 Reaction conditions: 13 mmol **100a**, 2 eq. ammonia, 1.5 wt% fresh and recycled  
 Novozym<sup>®</sup> 435, 90 °C.

The initial rate of the reaction catalysed by recycled Novozym<sup>®</sup> 435 was approximately half of the rate of reaction of fresh Novozym<sup>®</sup> 435. This result indicates that Novozym<sup>®</sup> 435 is less stable at 90 °C than at 60 °C which is the optimum operational temperature for Novozym<sup>®</sup> 435. However, part of the activity of the recycled Novozym<sup>®</sup> 435 could also be lost during the separation process; therefore, the conversions to **100b** could be further optimised with better recycling techniques. For example, packed-bed reactors or flow reactors<sup>147</sup> are widely employed in industry when immobilised enzymes are used in biotransformations. Both of these reactors are potentially good choices for improvement of recycling efficiency.

### 4.3.4 Enzyme support

One major limitation concerning the application of Novozym<sup>®</sup> 435 in industrial processes is the high cost. In contrast, the free CALB liquid is 10 times cheaper than its immobilised version. The liquid CALB (Lipozyme<sup>®</sup> CALB L) consists of the enzyme CALB dissolved in *ca.* 50% water, 25% glycerol, 25% sorbitol, and small amounts of sodium and potassium salts. Lipozyme<sup>®</sup> CALB L was employed in amidation reactions as a comparison to Novozym<sup>®</sup> 435 (Figure 91).

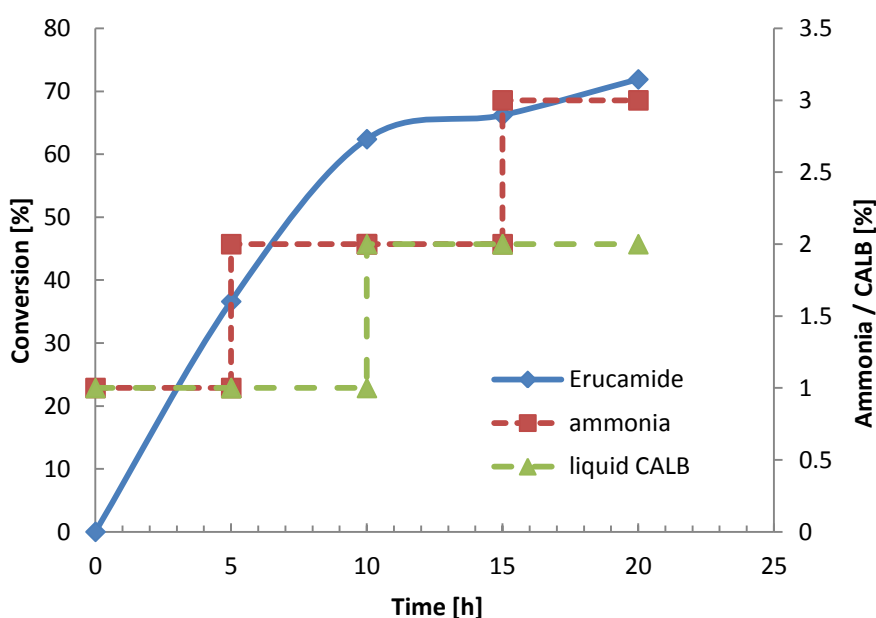


Figure 91. Adding Lipozyme<sup>®</sup> CALB L and ammonia in a stepwise manner.  
 Reaction conditions: 60 mmol **100a**, 2 eq. ammonia, 12 wt% Lipozyme<sup>®</sup> CALB L (2 eq. to Novozym<sup>®</sup> 435, calculated according to the units of both forms of CALB), 90 °C.

Upon addition of Lipozyme<sup>®</sup> CALB L and ammonia simultaneously, low conversions to **100b** were obtained (data not shown). Thus Lipozyme<sup>®</sup> CALB L and ammonia were added in a stepwise manner for improvement of conversions.

When ammonia and Lipozyme<sup>®</sup> CALB L were added stepwise, a maximum of 72% conversion was observed, a value that is lower than the



conversions obtained by Novozym<sup>®</sup> 435. Three causes could potentially contribute to this result: 1) evaporation of water from Lipozyme<sup>®</sup> CALB L at 90 °C; 2) Denaturing of Lipozyme<sup>®</sup> CALB L at 90 °C; 3) Esterification reaction between glycerol from Lipozyme<sup>®</sup> CALB L and the fatty acid.

#### 4.3.5 Optimisation of the ammonia concentration

The concentration of ammonia in the amidation reaction is likely to be a major factor affecting the yield of **100b**. However, although a large excess would be beneficial in terms of driving the reaction to completion it would be unattractive for economical reasons and hence limit industrial applications. Therefore, optimisation of ammonia quantity is of significant importance to the process. A number of reactions were performed employing various concentrations of ammonia to search for the optimum condition. Firstly, a reaction with only 1 eq. ammonia was conducted (Figure 92).

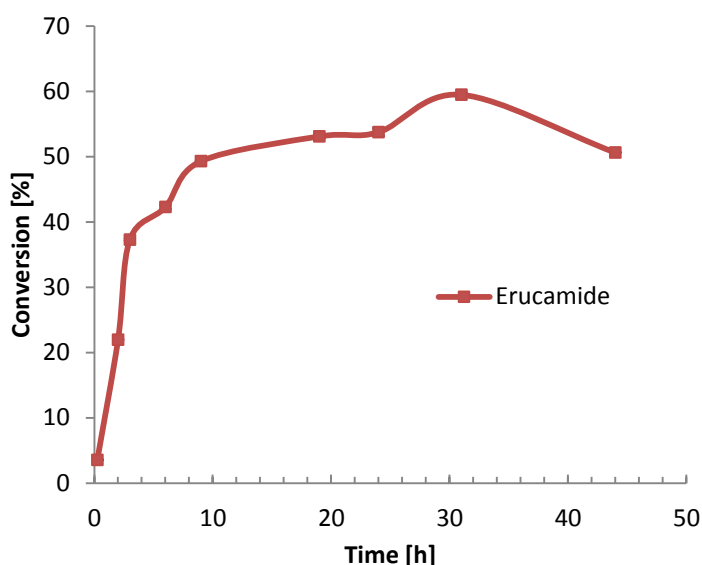


Figure 92. Conversions to **100b** with 1 eq. of ammonia.

*Reaction conditions: 3 mmol **100a**, 1 eq. ammonia, 3 wt% Novozym<sup>®</sup> 435, 90 °C.*

Approximately 60% conversion was obtained with only 1 eq. of ammonia added. This indicates that the reaction reaches equilibrium at 60% conversion

when 1 eq. of ammonia added, and more ammonia is needed for higher conversions. Therefore, 3 eq. and 4 eq. ammonia were added to the reaction in 3 and 4 portions, respectively. This is to examine how the maximum yield can be reached with minimum amount of ammonia (Figure 93).

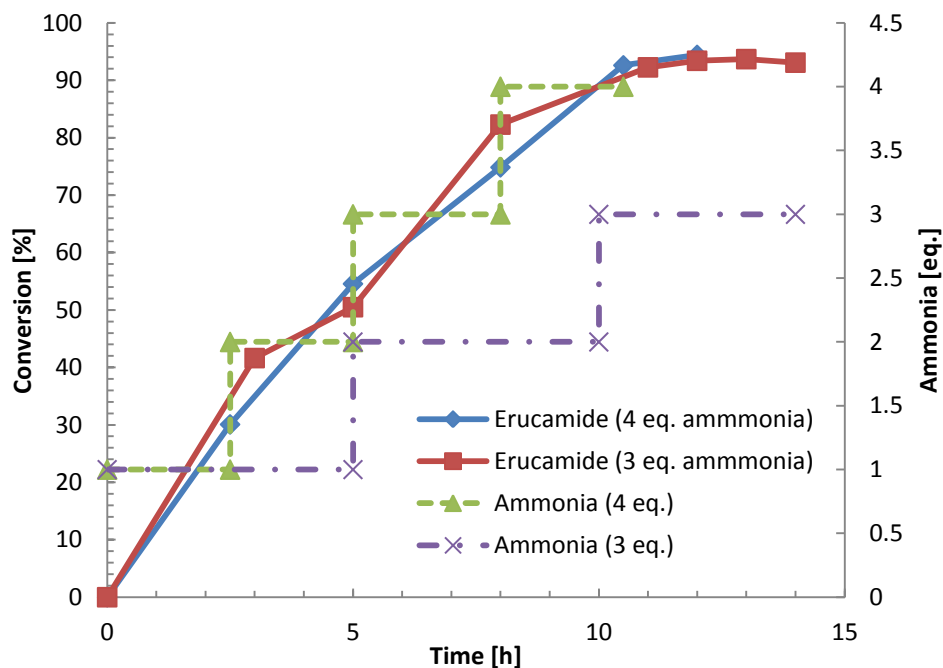


Figure 93. Optimisation of ammonia concentration.

Reaction conditions: 120 mmol **100a**, 3 or 4 eq. ammonia, 1.5 wt% Novozym® 435, 90 °C.

It can be seen that addition of more than 1 eq. of ammonia is necessary to drive the reaction equilibrium towards the production of **100b**. Similar conversions to **100b** (90%) were obtained employing 3 and 4 eq. of ammonia. The maximum conversion of 94% was obtained in 10 h when 4 eq. of ammonia was added, and it took 14 h for the reaction to reach maximum yield when 3 eq. of ammonia was added.

## 4.4 Summary and outlook

In summary, biocatalytic production of **100b** was achieved via a solvent-free process with conversions in excess of 94% in 10 h under milder reaction conditions than the current industrial chemical process (200 °C, 7 bar,

anhydrous ammonia). Ammonium carbamate was employed as the ammonia source and Novozym<sup>®</sup> 435 used as the biocatalyst. A number of reaction parameters that could affect the reaction conversions were optimised to obtain the optimum yield.

Full evaluation of the process for industrial applications is currently ongoing in the industry. Isolation and full characterisation of the product will be carried out. More advantageous processes for industrial applications could also be developed in the future. The reactions could be attempted at lower temperatures where the product is allowed to precipitate and be separated. Screening a wide range of enzymes that are more tolerant to high temperatures and stable for recycling would also be advantageous.

## 5. Conclusions and Future Outlook

This research has developed several advantageous processes in the area of biocatalysis. From enantiopure secondary alcohols, single atropisomers of diaryl ethers and biaryls, to amides of fatty acids, successful biocatalytic processes were accomplished employing two enzymes: GOase and CALB.

Deracemisation of secondary alcohols shows for the first time that the GOase catalysed oxidation can be combined with reduction catalysed by transition metal catalysts. Enantiopure secondary alcohols were produced in high yields under reaction conditions that were carefully adjusted to improve the compatibility of the enzyme and the transition metal catalysts.

Future work in this area should focus on further screening of a broad range of substrates to demonstrate broader applicability of the deracemisation process. Further screening of transition metal catalysts, optimisation of the reaction conditions and scale-up of the current process would also be advantageous.

Desymmetrisation of proatropisomeric compounds including diaryl ethers and biaryls can also be catalysed by GOase. High optical purity of the product atropisomers were obtained in good yields.

Production of single atropisomers employing biocatalysis is a relatively less explored area. This project could serve as a starting point for future investigation. Directed evolution can be an advantageous tool for obtaining more variants possessing higher activity and enantioselectivity and broader substrate specificity towards the production of single atropisomers.

CALB catalysed production of fatty amides under solvent-free conditions were also achieved. Compared to the current industrial chemical process, this biocatalytic process is more advantageous, demonstrated by a *ca.* 100 °C decrease in the reaction temperature and a solid ammonia source that causes less handling issues compared to the gaseous ammonia source currently

employed.

Future work should focus on the evaluation and implementation of this process for the large scale industrial production. Screening of biocatalysts that are more thermostable, active and economical would also be beneficial.

## **6. Materials and Methods**

### **6.1 Materials**

#### **6.1.1 Chemicals**

Unless otherwise specified, lab consumables and chemicals were purchased from Sigma-Aldrich Ltd. (Gillingham, UK), Acros Organics Ltd. (Geel, Belgium), Fisher Scientific Ltd. (Loughborough, UK), Bio-Rad Ltd. (Hemel Hempstead, UK), GE healthcare (Uppsala, Sweden) and Expedeon Ltd. (Babraham, UK). KREDs were gifts from Codexis (California, USA). Novozym<sup>®</sup> 435 and Lipzyme<sup>®</sup> CALB L were purchased from Novozymes Ltd. (Bagsværd, Denmark), and **100a** was a gift from Croda Ltd.

#### **6.1.2 Media**

##### **6.1.2.1 LB medium**

LB Broth (20 g) was dissolved in distilled water (dH<sub>2</sub>O, 1 L), and sterilised by autoclaving.

##### **6.1.2.2 LB agar:**

LB medium and agarose (15 g) were dissolved in d H<sub>2</sub>O (1 L) and sterilised by autoclaving (130 °C, 20 minutes). The LB/agar was melted in a microwave and cooled to 50 °C in a water bath prior to use.

### 6.1.3 Buffers and Solutions

#### 6.1.3.1 Stock NaPi buffer

Na<sub>2</sub>HPO<sub>4</sub> (1 M) solution was prepared by dissolving 17.8 g in dH<sub>2</sub>O (90 mL) and NaH<sub>2</sub>PO<sub>4</sub> (1 M) solution was prepared by dissolving 15.6 g in dH<sub>2</sub>O (90 mL). NaPi buffer (1 M, pH 7.0) was obtained by mixing Na<sub>2</sub>HPO<sub>4</sub> (57.7 mL, 1 M) and NaH<sub>2</sub>PO<sub>4</sub> (42.3 mL, 1 M).

#### 6.1.3.2 GOase purification buffers

A series of buffers with various imidazole concentrations (30, 100, 200 and 400 mM and 1 M) were required. Listed are the composition of each buffer employed in the purification.

**Buffer A:** NaPi 20 mM, NaCl 500 mM, PMSF 1 mM

**Buffer B:** NaPi 20 mM, NaCl 500 mM, PMSF 1 mM, 1 M imidazole

The following buffers were then made up by mixing **Buffer A** and **Buffer B**:

**Buffer 30:** NaPi 20 mM, NaCl 500 mM, PMSF 1 mM, 30 mM imidazole

**Buffer 100:** NaPi 20 mM, NaCl 500 mM, PMSF 1 mM, 100 mM imidazole

**Buffer 200:** NaPi 20 mM, NaCl 500 mM, PMSF 1 mM, 200 mM imidazole

**Buffer 400:** NaPi 20 mM, NaCl 500 mM, PMSF 1 mM, 400 mM imidazole

The final pH value was adjusted to 7.4 for all the listed buffers.

#### 6.1.3.3 Lysozyme solution

The lysozyme solution was prepared prior to use at a concentration of 10 mg/mL.

#### 6.1.3.4 Ampicillin solution

Ampicillin was prepared as a stock solution at a concentration of 100 g/L in dH<sub>2</sub>O, filter sterilised using 0.22 µm filters (Millipore) and stored at -20 °C.

The Ampicillin stock solution was used at a final concentration of 0.1 g/L.

## **6.2 Methods**

### **6.2.1 Protein preparation**

#### **6.2.1.1 Procedures for transformation by electroporation**

To BL21 star cells (40  $\mu$ L) added the DNA (10 ng) and the mixture was left on ice for 1 min. Electroporation was then performed by adding the mixture to an electroporation cuvette from Bio-Rad and pulsed at 200  $\Omega$ , 2.5 kV and 25 $\mu$ F. SOC medium (500  $\mu$ L) was pre-warmed at 42 °C and added immediately after the electroporation. The mixture was then incubated at 37 °C, 250 rpm for 1 h. The transformation reaction mixture (15  $\mu$ L) was then plated on an LB-agar plate supplemented with ampicillin. The plate was incubated in the static incubator at 37 °C overnight.

#### **6.2.1.2 Growth and expression of cultures**

Day one: a starting culture was prepared using a single colony transformant (§6.2.1.1) to inoculate LB medium (5 mL) supplemented with ampicillin (0.1 g/L). The starting culture was then incubated at 37 °C, 250 rpm until an OD<sub>600</sub> of 0.5-0.6 was reached. 5 mL of the starting culture was subsequently added to each conical flask (2 L) containing LB medium (600 mL) and then incubated overnight at 26 °C.

Day two: The cells were harvested by centrifuging at 6000 rpm for 30 min at 4 °C. The supernatant was discarded and the cells were lysed as follows:

- (1) the pellet was resuspended with **Buffer A**(12 mL).
- (2) fresh lysozyme solution was added and incubated at 37 °C for 30 min.
- (3) the cells were lysed by 15 bursts of sonication of 30 second each.

Lysis suspension was centrifuged at 6000 rpm for 30 min at 4 °C and the



supernatant was collected as CFE. The cell lysis process was repeated twice and the three CFEs and pellets were stored at 4 °C.

### 6.2.1.3 Protein purification

#### (1) Hi Trap<sup>TM</sup> chelating column chromatography

A Ni<sup>2+</sup> loaded 5 mL Hi Trap<sup>TM</sup> chelating column from GE healthcare was employed for the purification of the protein. All buffers were filtered through 0.45 µm syringe filters before being applied to the columns. The purification was performed as follows:

The column was washed with dH<sub>2</sub>O (25 mL) and equilibrated as follows:

- 2.5 mL NiSO<sub>4</sub> (0.1 M);
- 25 mL dH<sub>2</sub>O;
- 25 mL **Buffer 30**.

The CFE was centrifuged and the pellet discarded. The volume of the supernatant was measured and **Buffer B** was added to obtain a final concentration of 30 mM imidazole.

The sample was filtered and loaded onto the column. The target protein was then eluted and the fractions collected as follows:

- 25 mL **Buffer 30**: → E0 (wash) fraction (25 mL);
- 10 mL **Buffer 100**: → E1 fraction (10 mL);
- 20 mL **Buffer 200**: → E2 to E5 fractions (5 mL each);
- 15 mL **Buffer 400**: → E6 fraction (15 mL);
- 15 mL **Buffer B**: → E7 fraction (15 mL).

The column was then washed for storage as follows:

- 25 mL **Buffer 30** with 50 mM EDTA, pH 7.4;
- 25 mL dH<sub>2</sub>O;
- 25 mL 70 % ethanol.

The column was stored at 4 °C and the fractions were analyzed using SDS-PAGE electrophoresis.

**(2) Imidazole removal and protein concentration**

Pure fractions were collected as observed from sample electrophoresis. Imidazole was removed using an Amicon Ultra-15 centrifugal filter unit with ultracel-30 membrane (30000 MWCO, hereafter referred as Amicon filter tube). Combined fractions were aliquoted into one Amicon filter tube, then diluted with NaPi buffer (100 mM pH 7.0) till 15 mL. The Amicon filter tube containing the fractions were centrifuged at 4000 rpm and concentrated to a volume between 0.25 mL and 1 mL. Cycles of dilution/concentration were carried out till the imidazole concentration in the sample was between 1 and 5 nM.

Concentrated samples were combined and the solution was further centrifuged again in order to remove any precipitate.

**(3) Copper-loading of the protein**

Six molar eq. of  $\text{CuSO}_4$  (relative to the protein) was added to the sample. It was then incubated in the fridge overnight at 4 °C. Excess copper was removed by using the Amicon filter tubes with NaPi buffer (100 mM pH 7.0).

Concentrated sample were frozen in liquid nitrogen, and stored at -80 °C.

**6.2.1.4 Protein analysis**

LaemmLi dye (5 µL) was added to each sample (25 µL), and the protein was denatured at 95 °C for 5 min.

The samples were loaded onto ready prepared Bio-Rad Criterion™ Precast gels. Pre-stained broad range protein marker was also loaded as a reference. The gel was run at a voltage of 150 V using SDS gel electrophoresis buffer (TGS buffer, BIO-RAD). The protein bands were visualised by staining the gel with Instant Blue (Novexin).

Samples for purification fractions analysed by SDS-PAGE can be visualised as shown in Figure 94.

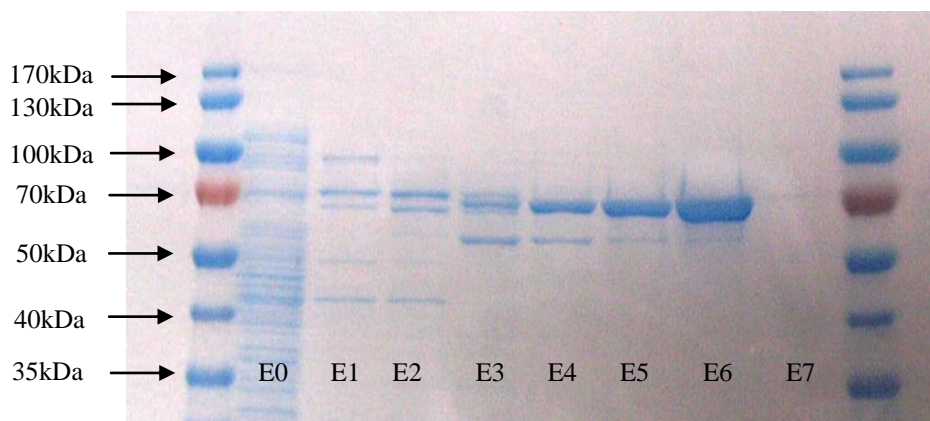


Figure 94. SDS-PAGE for fractions from protein purification.

## 6.2.2 Procedures for production of single atropisomers

### 6.2.2.1 Desymmetrisation of the diols of diaryl ethers and biaryls

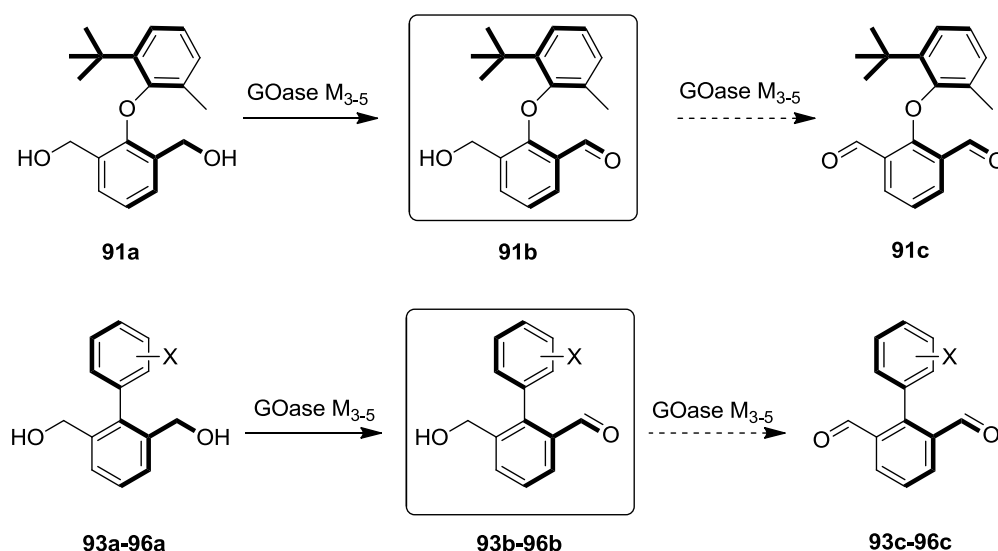


Figure 95. Desymmetrisation of proatropisomeric diols.

Desymmetrisation of diols of diaryl ethers and biaryls were conducted at 0.5 mL scale according to the scheme outlined in Figure 95.

The substrates were dissolved in DMSO at a concentration of 10 g/L. Horse radish peroxidase (HRP) and catalase from bovine liver were dissolved in dH<sub>2</sub>O at a 10 g/L concentration.

The reaction mixture was placed in a glass tube, and ran under the following conditions and concentrations: 10 mM substrates, DMSO (30%,

v/v) HRP (1 g/L) and catalase (0.1 g/L) in NaPi buffer (100 mM, pH 7.0) at 30 °C and 250 rpm. Oxygen was bubbled through for 5 min in the solution prior to addition of the enzyme. Then the reaction mixture was purged with oxygen again after enzyme addition. Parafilm<sup>®</sup> was used to wrap the rubber cap of the tube in order to reduce leakage of oxygen. Oxygen purging was performed each time after sampling.

#### 6.2.2.2 Kinetic resolution of the monoaldehydes of diaryl ethers and biaryls

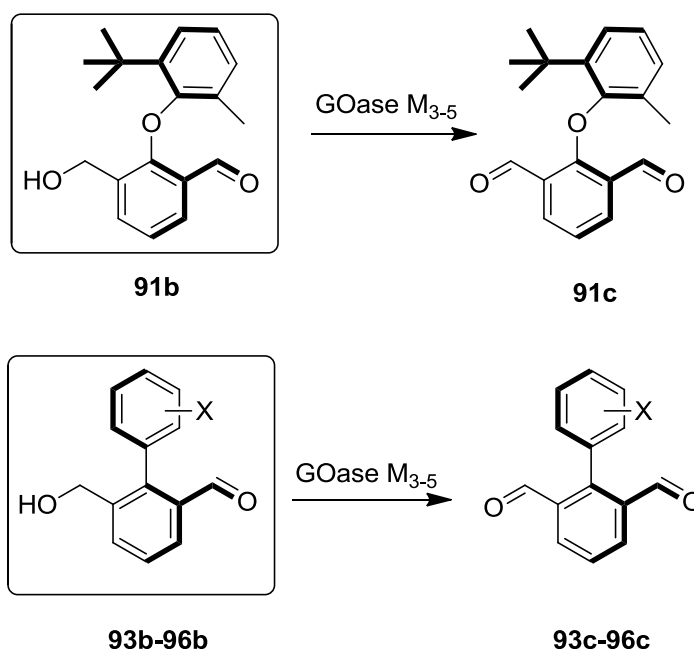


Figure 96. Kinetic resolution of monoaldehyde of diaryl ethers.

Kinetic resolution of monoaldehydes of diaryl ethers and biaryls were conducted at 0.5 mL scale according to the scheme outlined in Figure 96. The substrates were dissolved in DMSO at a concentration of 10 g/L. HRP and catalase from bovine liver were dissolved in deionised water at 10 g/L concentration.

The reaction mixture was placed in a glass tube and run under the following conditions and concentrations: 10 mM substrates, DMSO (30%, v/v), HRP (1 g/L) and catalase (0.1 g/L) in dH<sub>2</sub>O at 30 °C and 250 rpm. Oxygen

was bubbled through for 5 min in the solution prior to addition of the enzyme. Then the reaction mixture was purged with oxygen again after enzyme addition. Parafilm<sup>®</sup> was used to wrap the rubber cap of the tube in order to reduce leakage of oxygen. Oxygen purging was performed each time after sampling.

### 6.2.2.3 Reduction of the dialdehydes of diaryl ethers and biaryls

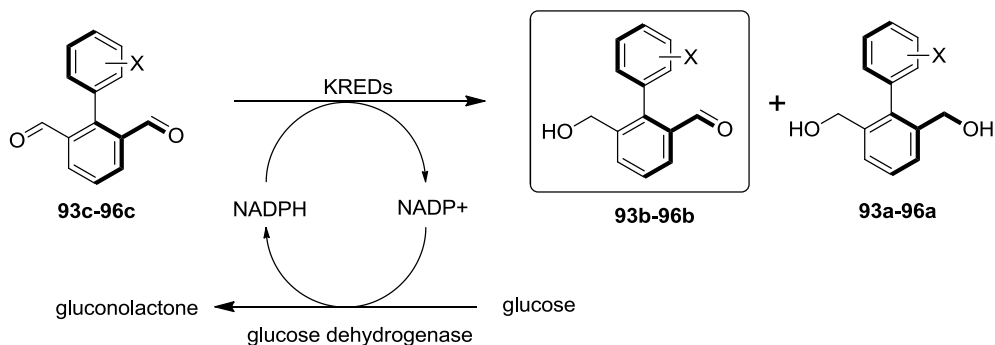


Figure 97. Reduction of dialdehydes of diaryl ethers and biaryls.

Reduction of dialdehydes of diaryl ethers and biaryls were conducted at 1 mL scale according to the scheme outlined in Figure 97. A stock substrate solution of 50 g/L in DMSO was prepared. Next, a reaction solution containing NADP<sup>+</sup> (1 g/L), glucose dehydrogenase (1 g/L, Codexis<sup>®</sup> CDX-901) and glucose (3.8 g/L) was prepared in KPi buffer (100 mM, pH 7.0). 950  $\mu$ L of this reaction solution was added to each glass tube containing each KRED enzyme (5 mg). Finally, 50  $\mu$ L of the substrate solution was added to each reaction vial. The reactions were placed in incubator and run at 30  $^{\circ}$ C with a mixing rate of 250 rpm.

### 6.2.3 Procedures for the deracemisation of secondary alcohols

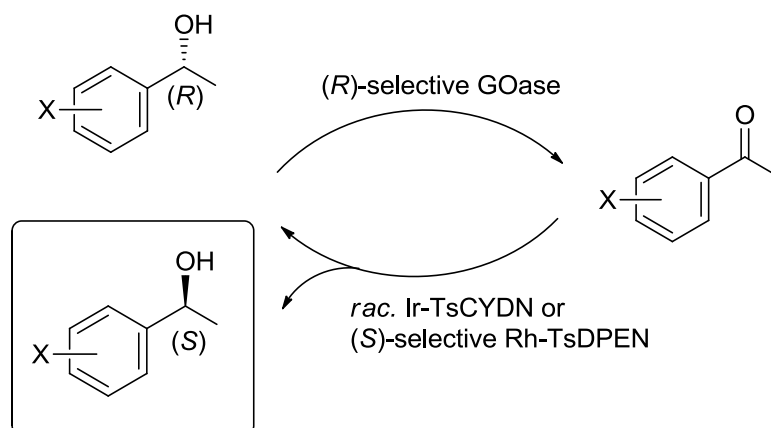


Figure 98. Deracemisation of secondary alcohols.

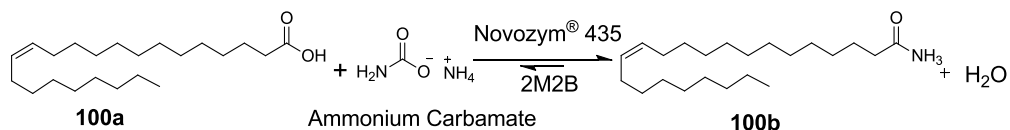
Deracemisation of secondary alcohols were conducted in 2 steps. The reduction step involved the synthesis of the metal precatalysts and reduction of the acetophenone substrate. The oxidation step involved the oxidation of the alcohols by GOase M<sub>3-5</sub>.

The synthesis of the metal precatalysts was conducted by dissolving [Cp\*RhCl<sub>2</sub>]<sub>2</sub> or [Cp\*IrCl<sub>2</sub>]<sub>2</sub> and 1.2 eq. of the ligand TsDPEN or TsCYDN in water (2 mL). The solution was placed in a 25 mL round bottom flask and stirred at 40 °C for 1 h. The suspension was directly used for reduction of acetophenone substrates.

Reduction of acetophenone was performed at 0.5 mL scale with 25 mM substrate, HCOONa (various eq.) and the precatalyst (various S/C ratios). The reaction solution was placed in a 1.5 mL eppendorf tube and shaken in the Thermomixer<sup>®</sup> at 37 °C, 900 rpm.

The oxidation step of deracemisation reactions was performed at 0.5 mL scale. HRP (1 g/L) and catalase (0.1 g/L) were added to the reaction mixture. Aliquots of GOase M<sub>3-5</sub> were defrosted and added as a solution. The reaction mixture was placed in an eppendorf tube (1.5 mL) and shaken in the Thermomixer<sup>®</sup> at 37 °C, 900 rpm.

## 6.2.4 Procedures for the lipase catalysed solvent-free amidation



Lipase catalysed amidation of **100a** in organic solvents was performed at 5 mL scale. **100a** (100 mM) was dissolved in 2M2B (5 mL) and placed in a 2-neck 50 mL round bottom flask equipped with a quick-fit temperature probe. 0.5 eq. of ammonium carbamate and CALB (30 wt%) was then added and the reaction mixture was stirred with a magnetic stirrer bar at 60 °C.

Solvent-free lipase catalysed amidation of fatty acids was performed with **100a** (20-50 g), various eq. of ammonium carbamate and Novozym<sup>®</sup> 435 (1.5 - 3 wt%). **100a** was first placed in a 2-neck 50 mL round bottom flask equipped with a quick-fit temperature probe and the temperature was brought to 90 °C. A hot-plate with magnetic stirring and an oil bath was used to control the temperature and mixing of the reaction. Then CALB and ammonium carbamate were added and the flask was capped with a rubber septum with a needle penetrating through to release pressure.

## 6.2.5 Analytical techniques

Normal phase chiral HPLC was performed on an Agilent system equipped with a G1379A degasser, G1312A binary pump, a G1329A autosampler unit, a G1367A diode array detector and a G1316A temperature controlled column compartment; columns and conditions were indicated for each compound separately. Columns used were CHIRALCEL<sup>®</sup> OD-H, CHIRALCEL<sup>®</sup> OJ-H, CHIRALCEL<sup>®</sup> AD-H, CHIRALCEL<sup>®</sup> AS-H analytical columns.

GC-FID was performed on an Agilent 6850 Network GC system equipped with a GERSTEL<sup>®</sup> autosampler. Columns used were Agilent<sup>®</sup> HP-1 for determination of conversions and CHIRALSIL<sup>®</sup>-DEX CB for determination of *ee*.

The *ee* was calculated using the area for the peaks of (*S*)-enantiomer ( $A_S$ ) and (*R*)-enantiomer ( $A_R$ ) with equation (1):

$$ee [\%] = \frac{A_S - A_R}{A_S + A_R} \times 100 \quad (A_S > A_R) \quad (1)$$

Conversions were calculated based on the ratio between the normalised areas of the starting material ( $A_{ST}$ ) and product ( $A_P$ ) with equation (2):

$$Conversion [\%] = \frac{A_P}{A_{ST} + A_P} \times 100 \quad (2)$$

E values can be calculated based on the *ee* of either the substrate of the product, and conversions with equations (3) and (4):

$$E = \frac{\ln\{1 - c[1 + ee(P)]\}}{\ln\{1 - c[1 - ee(P)]\}} \quad (3)$$

$$E = \frac{\ln\{(1 - c)[1 - ee(S)]\}}{\ln\{(1 - c)[1 + ee(S)]\}} \quad (4)$$

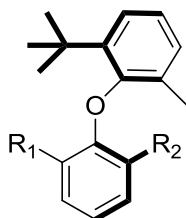
#### 6.2.5.1 HPLC analysis of diaryl ethers and biaryls for asymmetric synthesis of atropisomers

Sample (50  $\mu$ L) was taken for HPLC analysis of diaryl ethers **91a-c**, naphthyl substituted biaryls **93a-c**, halo substituted biaryls **95a-c** and **96a-c**. MTBE (200  $\mu$ L) was added, the sample was then thoroughly mixed in an eppendorf tube (1.5 mL) and the upper-layer was transferred to another eppendorf tube (1.5 mL). Volatiles were removed under reduced pressure and ethanol (100  $\mu$ L) was added.

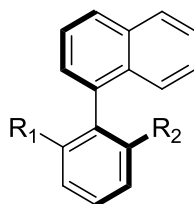
Sample (50  $\mu$ L) was taken and chloroform ( $3 \times 500$   $\mu$ L) was used for the extraction of phenanthryl substituted biaryls **94a-c**. The sample was then thoroughly mixed in an eppendorf tube and the upper-layer was transferred to another eppendorf tube. The organic phase was combined and volatiles were removed under reduced pressure and MTBE (100  $\mu$ L) was added.



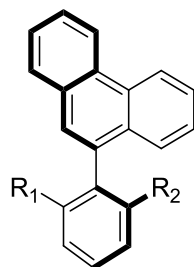
The solution containing the substrates was then transferred into a 2 mL HPLC vial with a 0.2 mL insert and analysed by normal phase HPLC for both conversions and *ee*. The peak elution times and chiral analysis methods for each substrate are listed below.



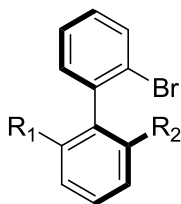
1. Diol **91a** ( $R_1 = R_2 = \text{CH}_2\text{OH}$ ) = 33.9 min; monoaldehyde **91b** ( $R_1 = \text{CHO}$ ,  $R_2 = \text{CH}_2\text{OH}$ ) = 17.3 min ((*M*)-**91b**), 18.5 min ((*P*)-**91b**); dialdehyde **91c** ( $R_1 = R_2 = \text{CHO}$ ) = 10.7 min. [Chiralcel<sup>®</sup> ASH: isohexane: IPA = 93:7 at 254 nm, flow rate: 1 mL/min]



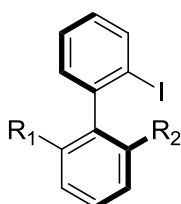
2. Diol **93a** ( $R_1 = R_2 = \text{CH}_2\text{OH}$ ) = 32.9 min; monoaldehyde **93b** ( $R_1 = \text{CHO}$ ,  $R_2 = \text{CH}_2\text{OH}$ ) = 11.3 min ((*M*)-**93b**), 11.9 min ((*P*)-**93b**); dialdehyde **93c** ( $R_1 = R_2 = \text{CHO}$ ) = 6.9 min. [Chiralcel<sup>®</sup> ADH: isohexane: IPA = 88:12 at 254 nm, flow rate: 1 mL/min]



3. Diol **94a** ( $R_1 = R_2 = \text{CH}_2\text{OH}$ ) = 39.5 min; monoaldehyde **94b** ( $R_1 = \text{CHO}$ ,  $R_2 = \text{CH}_2\text{OH}$ ) = 12.4 min ((*M*)-**94b**), 13.5 min ((*P*)-**94b**); dialdehyde **94c** ( $R_1 = R_2 = \text{CHO}$ ) = 9.9 min. [Chiralcel<sup>®</sup> ADH: isohexane: IPA = 85:15 at 254 nm, flow rate: 1 mL/min]



4. Diol **95a** ( $R_1 = R_2 = \text{CH}_2\text{OH}$ ) = 33.7 min; monoaldehyde **95b** ( $R_1 = \text{CHO}$ ,  $R_2 = \text{CH}_2\text{OH}$ ) = 28.9 min ((*P*)-**95b**), 31.1 min ((*M*)-**95b**); dialdehyde **95c** ( $R_1 = R_2 = \text{CHO}$ ) = 13.2 min. [Chiralcel<sup>®</sup> ADH: n-heptane: ethanol = 95:5 at 210 nm, flow rate: 0.8 mL/min]

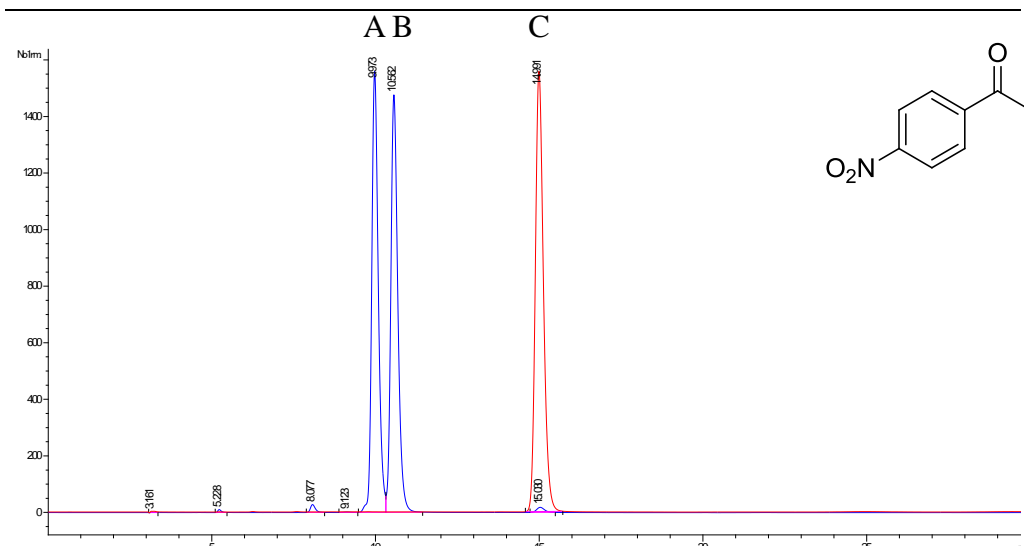


5. Diol **96a** ( $R_1 = R_2 = \text{CH}_2\text{OH}$ ) = 27.7 min; monoaldehyde **96b** ( $R_1 = \text{CHO}$ ,  $R_2 = \text{CH}_2\text{OH}$ ) = 10.9 min ((*P*)-**96b**), 12.1 min ((*M*)-**96b**); dialdehyde **96c** ( $R_1 = R_2 = \text{CHO}$ ) = 7.9 min. [Chiralcel<sup>®</sup> ADH: isohexane: IPA = 88:12 at 254 nm, flow rate: 1 mL/min]

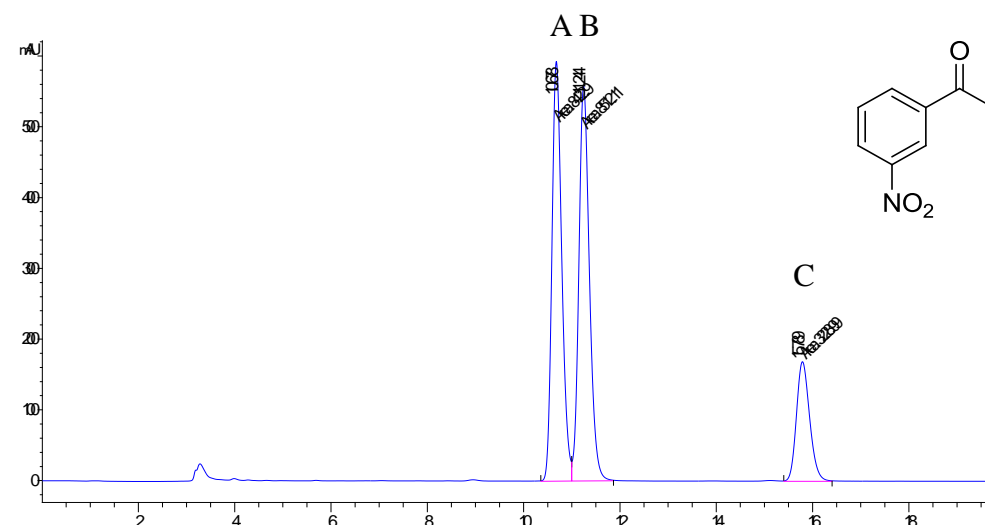
#### 6.2.5.2 HPLC and GC analysis of secondary alcohols and ketones for deracemisations

Sample (50  $\mu\text{L}$ ) was taken for HPLC analysis and dichloromethane (DCM,  $3 \times 500 \mu\text{L}$ ) was added. The sample was then thoroughly mixed in an eppendorf tube (1.5 mL) and the upper-layer was transferred into another eppendorf tube (2 mL). The organic phase was combined and then passed through a short silica column. Diethyl ether was used to flush the column. The volatiles were removed under reduced pressure. Ethanol (100  $\mu\text{L}$ ) was added and then transferred into a HPLC vial (2 mL) with 0.2 mL insert and analysed by normal phase HPLC for both conversions and *ee*.

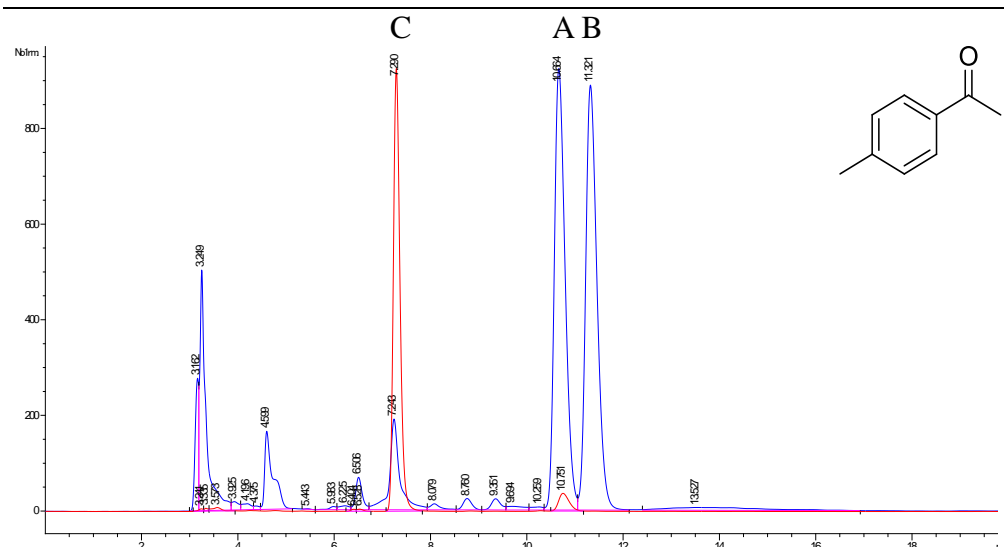
For chiral GC analysis, the same sampling method was employed.



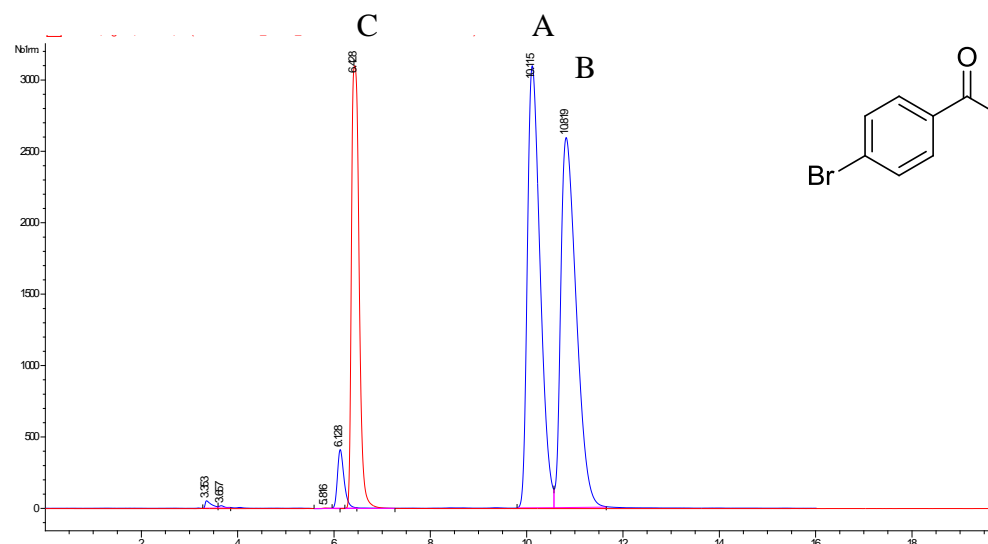
1. A, B = 4'-nitro-1-phenylethanol = 9.9, 10.6 min; C = 4'-nitroacetophenone = 14.9 min [Chiralcel<sup>®</sup> ADH: isohexane: ethanol = 90:10 at 254 nm, flow rate: 1 mL/min]



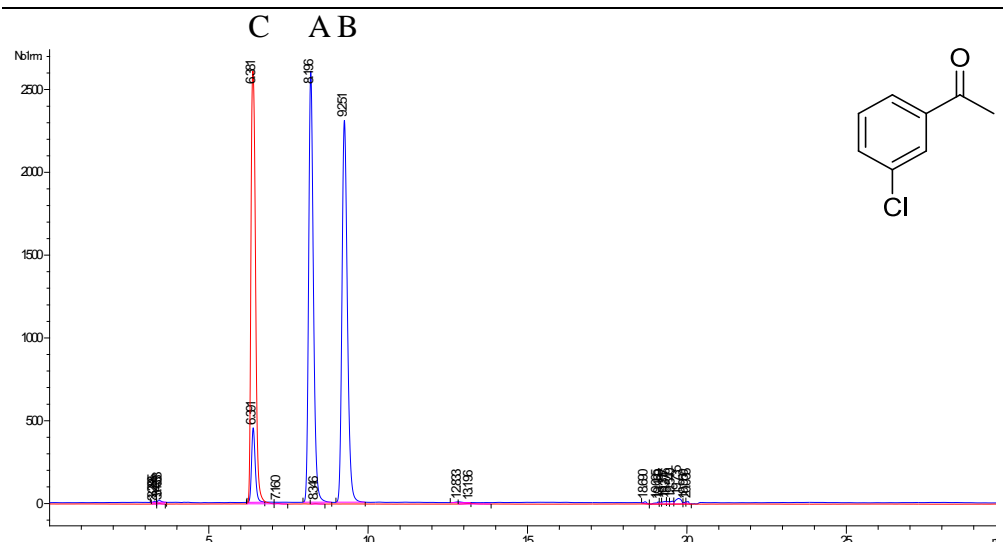
2. A, B = 3'-nitro-1-phenylethanol = 10.7, 11.2 min; C = 3'-nitroacetophenone = 15.8 min [Chiralcel<sup>®</sup> OJH: isohexane: ethanol = 90:10 at 254 nm, flow rate: 1 mL/min]



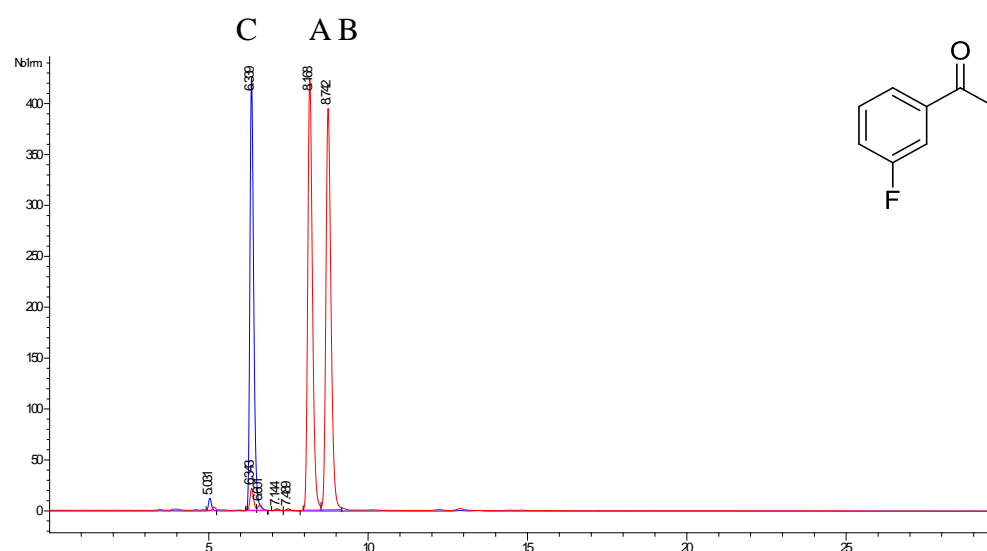
3. A, B = 4'-methyl-1-phenylethanol = 10.9, 11.3 min; C = 4'-methylacetophenone = 7.3 min [Chiralcel<sup>®</sup> OJH: isohexane: ethanol = 95:5 at 254 nm, flow rate: 1 mL/min]



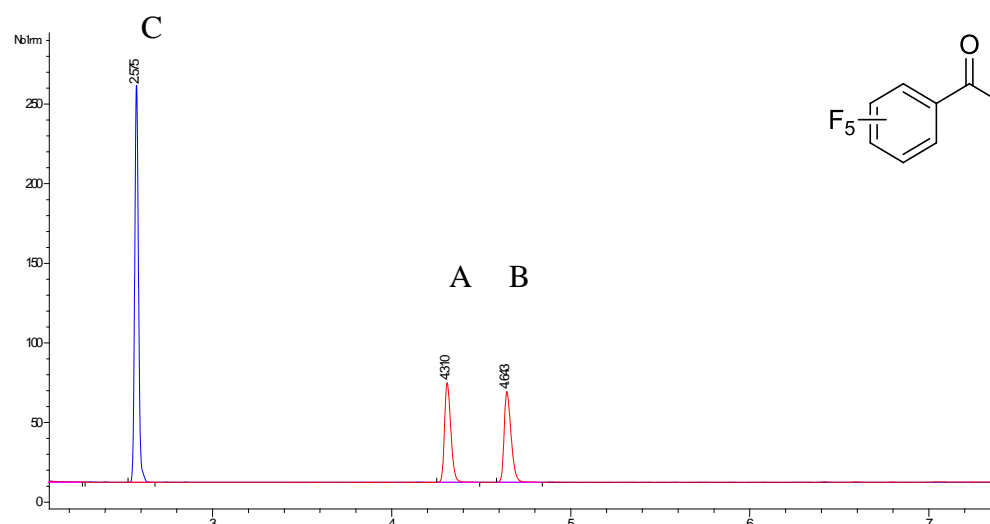
4. A, B = 4'-bromo-1-phenylethanol = 10.1, 10.8 min; C = 4'-bromoacetophenone = 6.1 min [Chiralcel<sup>®</sup> ODH: isohexane: ethanol = 97:3 at 254 nm, flow rate: 1 mL/min]



5. A, B = 3'-chloro-1-phenylethanol = 8.2, 9.3 min; C = 3'-chloroacetophenone = 6.4 min [Chiralcel<sup>®</sup> OJH: isohexane: ethanol = 95:5 at 210 nm, flow rate: 1 mL/min]



6. A, B = 3'-fluoro-1-phenylethanol = 8.2, 8.7 min; C = 3'-fluoroacetophenone = 6.3 min [Chiralcel<sup>®</sup> OJH: isohexane: ethanol = 95:5 at 254 nm, flow rate: 1 mL/min]



7. A, B = pentafluoro-1-phenylethanol = 4.3, 4.6 min; C = pentafluoroacetophenone = 2.6 min [CHIRALSIL<sup>®</sup>-DEX CB, flow rate: 1.7ml/min, 250 °C injector temperature, 100:1 split. Oven: 160 °C 2 min, Ramp: 10 °C/min, 200 °C 5min. Total time: 11 min.]

#### 6.2.5.3 GC and acid value analysis of 100a and 100b for lipase catalysed amidation of 100a

For determination of reaction conversions by GC, to a glass tube added 500 µL of sample in 1 mL of the solvent mixture with a ratio of methanol : toluene = 2:1. Subsequently, trimethylsilyldiazomethane (TMS-DM) (50 µL, 2.0 M in isohexane) was added and the sample was stirred at 40 °C for 20 minutes. The solvents were then evaporated under reduced pressure and isohexane was added to dissolve the erucic acid methyl ester. The solution was then subjected to GC analysis.

The GC column CHIRALSIL<sup>®</sup> HP-1 was used with 1.7 mL/min flow rate, 250 °C injector temperature, 100:1 split. The oven temperature was programmed as the following: 160 °C 2 min, Ramp: 5 °C/min, 300 °C 5 min. Total time: 33 min.

The reaction conversions were also determined by acid value. W g (*ca.* 2 g) of sample was taken and dissolved in ethanol (50 mL) at 70 °C. To the solution phenolphthalein (0.5 mL, 0.1 %) was added. Next, the solution was

titrated by V mL of 0.1 N or 0.5 N KOH and the acid value was calculated according to equation (5):

$$\text{Acid value} = \frac{V \times N \times 56.1}{W} \quad (5)$$

where: A – mL of 0.1 N or 0.5 N KOH consumed for sample.

N – Normality of KOH

W – Weight in grams of the sample.

#### 6.2.5.4 Standard curves of substrates and products

Both conversions and *ee* were determined employing normal phase HPLC (see §6.2.5) unless otherwise specified. The calculations of conversions were calibrated by standard curves and gradient (m) of the best fit trend line of equations of standard curves for all the substrates and products employed in biotransformations are listed in Table 24.

Table 24. Slope of the best fit trend line of equations of standard curves ( $y = mx$ ) of substrates and products of biotransformations.

Compounds	No.	254nm	210nm
4'-nitro-1-phenylalcohol	<b>62</b>	374.8	427
4'-nitroacetophenone	<b>63</b>	616.4	373.5
3'-nitro-1-phenylalcohol		2097.8	3824.9
3'-nitroacetophenone	<b>70</b>	2160.6	3923.2
3'-fluoro-1-phenylalcohol		108.9	1219
4'-methyl-1-phenylalcohol		51.1	2363.8
4'-methylacetophenone	<b>71</b>	3378.1	2947.6
4'-bromo-1-phenylalcohol		68.4	2533.3
4'-bromoacetophenone	<b>72</b>	5502.1	3840
3'-chloro-1-phenylalcohol		37.8	2538.8
3'- chloroacetophenone	<b>73</b>	646.2	4417.8
3'-fluoroacetophenone	<b>74</b>	266.9	762.3

Table continued

methyl <i>tert</i> -butyl diaryl ether diol	<b>91a</b>	87.3 <sup>[a]</sup>	N.D <sup>[b]</sup>
methyl <i>tert</i> -butyl diaryl ether monoaldehyde	<b>91b</b>	396.7 <sup>[a]</sup>	N.D <sup>[b]</sup>
methyl <i>tert</i> -butyl diaryl ether dialdehyde	<b>91c</b>	4321.8 <sup>[a]</sup>	N.D <sup>[b]</sup>
naphthyl biaryl diol	<b>93a</b>	711.5	N.D <sup>[b]</sup>
naphthyl biaryl monoaldehyde	<b>93b</b>	1692.8	N.D <sup>[b]</sup>
naphthyl biaryl dialdehyde	<b>93c</b>	4385.8	N.D <sup>[b]</sup>
phenanthryl biaryl diol	<b>94a</b>	16632.4	N.D <sup>[b]</sup>
phenanthryl biaryl monoaldehyde	<b>94b</b>	7190.2	N.D <sup>[b]</sup>
phenanthryl biaryl dialdehyde	<b>94c</b>	15125.5	N.D <sup>[b]</sup>
bromo biaryl diol	<b>95a</b>	206.8	N.D <sup>[b]</sup>
bromo biaryl monoaldehyde	<b>95b</b>	2623.0	N.D <sup>[b]</sup>
bromo biaryl dialdehyde	<b>95c</b>	1977.6	N.D <sup>[b]</sup>
iodo biaryl diol	<b>96a</b>	371.7	N.D <sup>[b]</sup>
iodo biaryl monoaldehyde	<b>96b</b>	2863.1	N.D <sup>[b]</sup>
iodo biaryl dialdehyde	<b>96c</b>	20907.4	N.D <sup>[b]</sup>

[a] standard curves were measured by reverse phase HPLC (Zobax XDB C-18). [b] N.D. = not determined.



## Appendix 1: IUPAC three and one letter code for amino acids

Letter	Code	Amino acid	Letter	Code	Amino acid
<b>A</b>	Ala	Alanine	<b>M</b>	Met	Methionine
<b>C</b>	Cys	Cysteine	<b>N</b>	Asn	Asparagine
<b>D</b>	Asp	Aspartic acid	<b>P</b>	Pro	Proline
<b>E</b>	Glu	Glutamic acid	<b>Q</b>	Gln	Glutamine
<b>F</b>	Phe	Phenylalanine	<b>R</b>	Arg	Arginine
<b>G</b>	Gly	Glycine	<b>S</b>	Ser	Serine
<b>H</b>	His	Histidine	<b>T</b>	Thr	Threonine
<b>I</b>	Ile	Isoleucine	<b>V</b>	Val	Valine
<b>K</b>	Lys	Lysine	<b>W</b>	Trp	Tryptophan
<b>L</b>	Leu	Leucine	<b>Y</b>	Tyr	Tyrosine

## Appendix 2: Biocatalytic Desymmetrisation of an Atropisomer with both an Enantioselective Oxidase and Ketoreductases

### Communications

#### Atroposelectivity

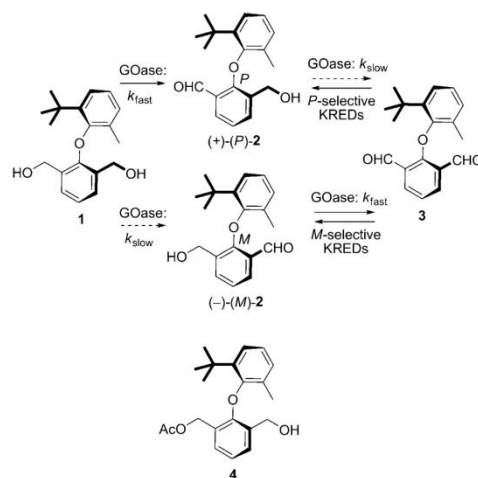
DOI: 10.1002/anie.201002580

### Biocatalytic Desymmetrization of an Atropisomer with both an Enantioselective Oxidase and Ketoreductases\*\*

Bo Yuan, Abigail Page, Christopher P. Worrall, Franck Escalettes, Simon C. Willies, Joseph J. W. McDouall, Nicholas J. Turner,\* and Jonathan Clayden\*

Atropisomeric ligands have found numerous powerful applications in catalysis,<sup>[1]</sup> and the atropisomeric biaryl bisphosphine binap played an important role in the award of a Nobel Prize to Noyori in 2001.<sup>[2]</sup> Enantiomerically pure atropisomers commonly employed as chiral ligands are generally made by resolution: there are still relatively few effective methods for direct asymmetric coupling to form single enantiomers.<sup>[3]</sup> Kinetic resolution<sup>[4]</sup> and dynamic resolution<sup>[5]</sup> under kinetic<sup>[5a]</sup> or thermodynamic<sup>[5b]</sup> control are particularly appealing given the possibility offered by atropisomerism for thermal racemization of the less reactive enantiomer. The use of desymmetrization for the synthesis of single atropisomers is rare.<sup>[6]</sup> Following the early example of enantioselective lithiation reported by Raston and co-workers,<sup>[6b]</sup> the research groups of Hayashi<sup>[6c]</sup> and Harada<sup>[6d]</sup> also reported chemical methods for desymmetrizing biphenyl compounds. A single example of the enzymatic desymmetrization of a biaryl compound with a lipase was reported by Matsumoto et al.<sup>[6e]</sup>

Herein, we report two novel and complementary biocatalytic approaches to the enantioselective synthesis of atropisomers by the desymmetrization of appropriate achiral substrates containing a pair of enantiotopic functional groups. The atropisomer in question is the diaryl ether **2**, which may be formed either by enantioselective oxidation of the symmetrical diol **1** or by the corresponding reduction of the symmetrical dialdehyde **3** (Scheme 1). The enzymes we employed for these transformations were 1) a variant of galactose oxidase (GOase) which had been previously evolved to accept chiral benzylic alcohols as substrates with high enantioselectivity (**1**→**2**)<sup>[7]</sup> and 2) a family of ketoreductases that are known to possess good activity and enantioselectivity for the asymmetric reduction of benzylic ketones (**3**→**2**).<sup>[8]</sup>



**Scheme 1.** Enantioselective transformations of atropisomeric and pro-atropisomeric diaryl ethers. GOase = galactose oxidase. KRED = ketoreductase.

Atropisomeric diaryl ethers<sup>[9]</sup> form part of the structure of vancomycin<sup>[10]</sup> and are promising scaffolds for the construction of new chiral ligands.<sup>[11]</sup> Dialdehyde **3** and diol **1** were made by our published route.<sup>[9]</sup> In an initial screen, we attempted enantioselective acetylation by incubating diol **1** with *Candida antarctica* lipase B and vinyl acetate. Slow acylation of **1** was observed with approximately 50% conversion after 24 h to the monoacetate **4** and modest enantioselectivity (60% ee). In contrast, when diol **1** was incubated with the previously reported M<sub>3.5</sub> variant of GOase,<sup>[7]</sup> rapid oxidation to the monoaldehyde (*P*)-**2** resulted in 80% conversion after 24 h to material with 94% ee.

During the oxidation of **1** to **2**, rapid formation of the product (*P*)-**2** with approximately 88% ee (see below for assignment of the absolute configuration) was observed after 1 h, followed by a slower increase in enantiomeric purity to a maximum ee value of 94% (Figure 1). This increase in the ee value, along with the formation of the dialdehyde **3** (14% after 24 h), suggested that the minor enantiomer (*M*)-**2** produced in the enantioselective oxidation of **1** was removed preferentially by a secondary oxidation process to the dialdehyde **3**. Thus, the final enantiomeric purity of (*P*)-**2** resulted from a combination of enantioselective desymmet-

[\*] B. Yuan, Dr. F. Escalettes, Dr. S. C. Willies, Prof. N. J. Turner  
School of Chemistry, University of Manchester  
Manchester Interdisciplinary Biocentre  
131 Princess Street, Manchester M1 7DN (UK)  
Fax: (+44) 161-275-1311  
E-mail: nicholas.turner@manchester.ac.uk

A. Page, C. P. Worrall, Dr. J. J. W. McDouall, Prof. J. Clayden  
School of Chemistry, University of Manchester  
Oxford Road, Manchester M13 9PL (UK)  
E-mail: clayden@man.ac.uk

[\*\*] We are grateful to GlaxoSmithKline and the EPSRC for an Industrial CASE studentship (to A.P.) and to Croda for a Dorothy Hodgkin Award (to B.Y.). We thank Dr. James Raftery for the X-ray data on **3**.

Supporting information for this article is available on the WWW under <http://dx.doi.org/10.1002/anie.201002580>.

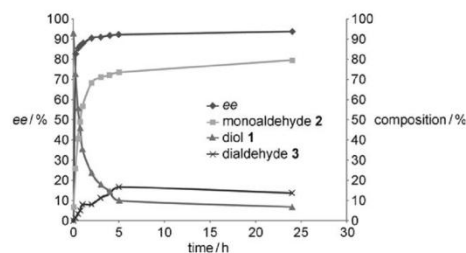


**Figure 1.** Enantioselective desymmetrization of diol **1** with the GOase  $M_{3.5}$  variant. Composition:  $\blacktriangle$  diol **1**,  $\blacksquare$  monoaldehyde **2**,  $\times$  dialdehyde **3**;  $\blacklozenge$  *ee* value of **2**.

rization and kinetic resolution, as has been noted before for other systems.<sup>[6a]</sup>

To investigate the enantioselectivity of the kinetic resolution process, we incubated racemic ( $\pm$ )-**2** with the GOase  $M_{3.5}$  variant. We observed 89% conversion after 24 h (Figure 2). As expected, the remaining atropisomer was of

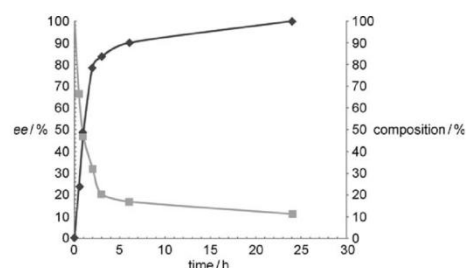


**Figure 2.** Kinetic resolution of ( $\pm$ )-**2** with the GOase  $M_{3.5}$  variant. Composition:  $\blacksquare$  monoaldehyde **2**;  $\blacklozenge$  *ee* value of **2**.

*P* configuration with an *ee* value of 99%. The resolution process proceeds more slowly than the desymmetrization reaction. The kinetic resolution under these conditions had a selectivity (*E*) value of approximately 4.<sup>[12,13]</sup>

The configurational stability of the sample of enantiomerically enriched **2** obtained by kinetic resolution was established by incubation in heptane at 90 °C. A slow first-order decay in the *ee* value from 62 to 34% was observed over a period of several days (see the Supporting Information). From this result, we deduced the half-life for racemization at this temperature to be 120 h, and estimated the barrier to enantiomerization to be greater than 130 kJ mol<sup>-1</sup> at 90 °C.<sup>[14]</sup>

The absolute sense of the enantioselective oxidation was established by comparison of experimental and modeled circular dichroism spectra of the starting material remaining after kinetic resolution, (+)-(*P*)-**2** (see the Supporting Information). The modeled spectrum (Figure 3, dotted line) matches closely the experimental CD spectrum (Figure 3, continuous line), with positive maxima aligning at 234 (observed) and 235 nm (modeled) and at 348 (observed)

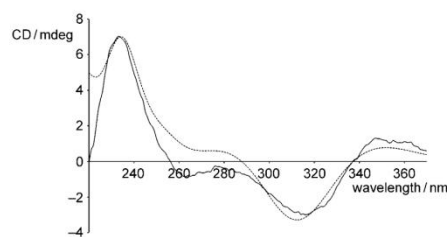


**Figure 3.** CD spectra of **2**. Solid line: spectrum observed for the less reactive enantiomer of **2**; dashed line: spectrum modeled for the lowest-energy conformer of (*P*)-**2**.

and 353 nm (modeled), a negative maximum at 316 (observed) and 313 nm (modeled), and a shoulder in both observed and modeled spectra at 280 nm. The match confirms that the slower-reacting enantiomer of **2**, and hence also the product of the desymmetrization of **1**, has the *P* configuration (Scheme 1).

The active site of GOase is characterized by a bowl-shaped cleft near the surface of the protein.<sup>[15]</sup> Modeling of the two enantiomers of **2** into the binding site of GOase revealed that the bulky *tert*-butyl group of the substrate is forced to occupy a position in which it is pointing away from the cleft and towards the surface of the protein. In such a binding mode, the hydroxymethyl group of (*M*)-**2** is placed close to the copper-containing reactive center and poised for oxidation to the aldehyde (Figure 4). This model therefore

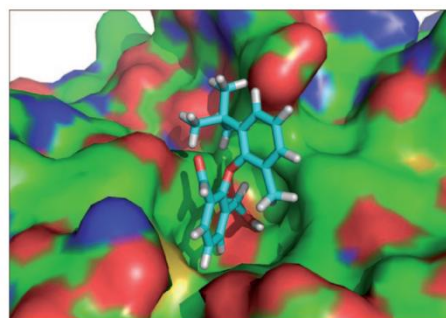


**Figure 4.** Model of the more reactive enantiomer (*M*)-**2** in the active site of galactose oxidase.

predicts that (*M*)-**2** is the faster-reacting enantiomer in the kinetic resolution process, an observation which is in agreement with the assignment of absolute configuration on the basis of circular dichroism.

We also examined an alternative approach for the synthesis of enantiomerically enriched monoaldehyde **2**: asymmetric reduction of the symmetrical dialdehyde **3** with ketoreductases (KREDs). KREDs have been widely applied to the asymmetric reduction of ketones, particularly benzylic



# Communications

ketones,<sup>[16]</sup> but to our knowledge have not previously been used for the desymmetrization of pro-atropisomeric substrates. We screened 17 different KREDs<sup>[17]</sup> and determined the conversion and *ee* value of the product after 24 h (Table 1). All enzymes were active, and many showed high

**Table 1:** Reduction of **3** with ketoreductases (KREDs).

Entry	Enzyme <sup>[a]</sup>	Conversion <sup>[b]</sup> [%]	<i>ee</i> [%]	Configuration <sup>[c]</sup>
1	KRED101 ( <i>R</i> )	53	24	<i>P</i>
2	KRED103	6	22	<i>P</i>
3	KRED104	3	75	<i>M</i>
4	KRED105	2	99	<i>M</i>
5	KRED106	3	11	<i>P</i>
6	KRED108 ( <i>S</i> )	39	78	<i>M</i>
7	KRED109	3	54	<i>M</i>
8	KRED110	1	99	<i>M</i>
9	KRED114	95	40	<i>M</i>
10	KRED115 ( <i>R</i> )	33	9	<i>M</i>
11	KRED116	23	79	<i>M</i>
12	KRED117	7	79	<i>M</i>
13	KRED118 ( <i>S</i> )	91	77	<i>P</i>
14	KRED119 ( <i>S</i> )	99	71	<i>P</i>
15	KRED120 ( <i>S</i> )	22	87	<i>M</i>
16	KRED121 ( <i>R</i> )	84	61	<i>M</i>
17	KRED124 ( <i>R</i> )	3	99	<i>M</i>

[a] The typical selectivity of the KRED in the reduction of nonsymmetrical diaryl ketones is shown in parentheses (when known).<sup>[16]</sup> [b] Conversion after 24 h. [c] Major enantiomer produced by reduction.

enantioselectivity (Table 1, entries 4, 8, and 17); however, conversion was often low. Notable success was achieved with KRED118 (91 % conversion, 77 % *ee* (*P* enantiomer)) and KRED121 (84 % conversion, 61 % *ee* (*M* enantiomer); Table 1, entries 13 and 16). These KREDs were previously classified as either *S*- or *R*-selective on the basis of their stereoselectivity in the reduction of nonsymmetrical diaryl ketones.<sup>[16]</sup> Interestingly, this trend was not always followed for the reduction of **3**; that is, enantiomerically enriched (*P*)-**2** was obtained from both *R*-selective KRED101 and *S*-selective KRED118 (Table 1, entries 1 and 13). Similarly, (*M*)-**2** was obtained from both *R*- (KRED121) and *S*-selective (KRED108) enzymes (Table 1, entries 16 and 6). These results suggest that dialdehyde **3** binds at the active site of the ketoreductases in a different mode to that adopted by more conventional benzylic ketones.

Our results suggest that biocatalytic redox reactions may be more widely applicable to the asymmetric synthesis of atropisomers by desymmetrization. We are currently exploring further opportunities in this area.

Received: April 29, 2010

Published online: August 16, 2010

**Keywords:** asymmetric synthesis · atropisomerism · biocatalysis · diaryl ethers · enzymes

- [1] R. Noyori, *Asymmetric Catalysis in Organic Synthesis*, Wiley, New York, 1994; Y.-M. Li, F.-Y. Kwong, W.-Y. Yu, A. S. C. Chan, *Coord. Chem. Rev.* **2007**, *251*, 2119; M. Berthod, G. Mignani, G. Woodward, M. Lemaire, *Chem. Rev.* **2005**, *105*, 1801.
- [2] R. Noyori, *Angew. Chem.* **2002**, *114*, 2108; *Angew. Chem. Int. Ed.* **2002**, *41*, 2008; binap = 2,2'-bis(diphenylphosphanyl)-1,1'-binaphthyl.
- [3] a) G. Bringmann, A. J. P. Mortimer, P. A. Keller, M. J. Gresser, J. Garner, M. Breuning, *Angew. Chem.* **2005**, *117*, 5518; *Angew. Chem. Int. Ed.* **2005**, *44*, 5384; b) A. N. Cammidge, K. V. L. Crépy, *Chem. Commun.* **2000**, 1723; J. Yin, S. L. Buchwald, *J. Am. Chem. Soc.* **2000**, *122*, 12051.
- [4] T. Itoh, *J. Org. Chem.* **1995**, *60*, 4968; O. Kitagawa, M. Fujita, M. Kohriya, H. Hasegawa, T. Taguchi, *Tetrahedron Lett.* **2000**, *41*, 8539; T. Watanabe, K. Kamikawa, M. Uemura, *Tetrahedron Lett.* **1995**, *36*, 6695; R. Rios, C. Jimeno, P. J. Carroll, P. J. Walsh, *J. Am. Chem. Soc.* **2002**, *124*, 10272; J. Clayden, H. Turner, *Tetrahedron Lett.* **2009**, *50*, 3216; D. Pamperin, H. Hopf, C. Sydlatk, M. Pietzsch, *Tetrahedron: Asymmetry* **1997**, *8*, 319; D. Pamperin, C. Schulz, H. Hopf, C. Sydlatk, M. Pietzsch, *Eur. J. Org. Chem.* **1998**, 1441.
- [5] a) G. Bringmann, R.-M. Pfeifer, P. Schreiber, K. Hartner, M. Schraut, M. Breuning, *Tetrahedron* **2004**, *60*, 4349; G. Bringmann, D. Menche, *Acc. Chem. Res.* **2001**, *34*, 615; G. Bringmann, J. Hinrichs, T. Pabst, P. Henschel, K. Peters, E.-M. Peters, *Synthesis* **2001**, 155; A. Bracegirdle, J. Clayden, L. W. Lai, *Beilstein J. Org. Chem.* **2008**, *4*, 47; b) J. Clayden, P. Johnson, J. H. Pink, M. Helliwell, *J. Org. Chem.* **2000**, *65*, 7033; J. Clayden, D. Mitjans, L. H. Youssef, *J. Am. Chem. Soc.* **2002**, *124*, 5266; J. Clayden, L. W. Lai, M. Helliwell, *Tetrahedron* **2004**, *60*, 4399; J. Clayden, C. P. Worrall, W. Moran, M. Helliwell, *Angew. Chem.* **2008**, *120*, 3278; *Angew. Chem. Int. Ed.* **2008**, *47*, 3234; J. Clayden, J. Senior, M. Helliwell, *Angew. Chem.* **2009**, *121*, 6388; *Angew. Chem. Int. Ed.* **2009**, *48*, 6270; J. Clayden, S. P. Fletcher, J. J. W. McDouall, S. J. M. Rowbottom, *J. Am. Chem. Soc.* **2009**, *131*, 5331.
- [6] a) E. García-Urdiales, I. Alfonso, V. Gotor, *Chem. Rev.* **2005**, *105*, 313; b) L. M. Engelhardt, W.-P. Leung, C. L. Raston, G. Salem, P. Twiss, A. H. White, *J. Chem. Soc. Dalton Trans.* **1988**, 2403; c) T. Hayashi, S. Niizuma, T. Kamikawa, N. Suzuki, Y. Uozumi, *J. Am. Chem. Soc.* **1995**, *117*, 9101; T. Kamikawa, Y. Uozumi, T. Hayashi, *Tetrahedron Lett.* **1996**, *37*, 3161; d) T. M. T. Tuyet, T. Harada, K. Hashimoto, M. Hatsuta, A. Oku, *J. Org. Chem.* **2000**, *65*, 1335; T. Harada, T. M. T. Tuyet, A. Oku, *Org. Lett.* **2000**, *2*, 1319; e) T. Matsumoto, T. Konegawa, T. Nakamura, K. Suzuki, *Synlett* **2002**, 122.
- [7] F. Escalantes, N. J. Turner, *ChemBioChem* **2008**, *9*, 857–860; M. D. Truppo, F. Escalantes, N. J. Turner, *Angew. Chem.* **2008**, *120*, 2679–2681; *Angew. Chem. Int. Ed.* **2008**, *47*, 2639–2641.
- [8] G. W. Huisman, J. Liang, A. Krebber, *Curr. Opin. Chem. Biol.* **2010**, *14*, 122–129.
- [9] M. S. Betson, J. Clayden, C. P. Worrall, S. Peace, *Angew. Chem.* **2006**, *118*, 5935; *Angew. Chem. Int. Ed.* **2006**, *45*, 5803.
- [10] K. C. Nicolaou, C. N. C. Boddy, S. Bräse, N. Winssinger, *Angew. Chem.* **1999**, *111*, 2230; *Angew. Chem. Int. Ed.* **1999**, *38*, 2096.
- [11] For uses of non-biaryl atropisomers in catalysis, see: A. Honda, K. M. Waltz, P. J. Carroll, P. J. Walsh, *Chirality* **2003**, *15*, 615; W.-M. Dai, K. K. Y. Yeung, J.-T. Liu, Y. Zhang, I. D. Williams, *Org. Lett.* **2002**, *4*, 1615; W.-M. Dai, K. K. Y. Yeung, Y. Wang, *Tetrahedron* **2004**, *60*, 4425; W.-M. Dai, Y. Li, Y. Zhang, Z. Yue, J. H. Wu, *Chem. Eur. J.* **2008**, *14*, 5538; S. Brandes, B. Niess, M. Bella, A. Prieto, J. Overgaard, K. A. Jørgensen, *Chem. Eur. J.* **2006**, *12*, 6039.
- [12] W. Kroutil, A. Kleewein, K. Faber, *Tetrahedron: Asymmetry* **1997**, *8*, 3263–3274.

- [13] Attempted kinetic resolution with GOase of a less hindered compound with an isopropyl group in place of the *tert*-butyl group gave the racemic compound, probably as a result of racemization on the timescale of the reaction: compound **2** is resolvable by HPLC, but related compounds have low barriers to racemization (see Ref. [9]).
- [14] See: A. Ahmed, R. A. Bragg, J. Clayden, L. W. Lai, C. McCarthy, J. H. Pink, N. Westlund, S. A. Yasin, *Tetrahedron* **1998**, *54*, 13277.
- [15] S. J. Firbank, M. S. Rogers, C. M. Wilmot, D. M. Dooley, M. A. Halcrow, P. F. Knowles, M. J. McPherson, S. E. Phillips, *Proc. Natl. Acad. Sci. USA* **2001**, *98*, 12932.
- [16] M. D. Truppo, D. Pollard, P. Devine, *Org. Lett.* **2007**, *9*, 335–338.
- [17] All ketoreductases (KREDs) were obtained from Codexis Inc., 200 Penobscot Drive, Redwood City, CA 94063, USA.

---

## References

- [1] Escalettes, F.; Turner, N. J. *ChemBioChem* **2008**, *9*, 857.
- [2] Cooper, J. A. D.; Smith, W.; Bacila, M.; Medina, H. *J. Biol. Chem.* **1958**, *234*, 445.
- [3] Ito, N.; Phillips, S. E. V.; Stevens, C.; Ogel, Z. B.; McPherson, M. J.; Keen, J. N.; Yadav, K. D. S.; Knowles, P. F. *Nature* **1991**, *350*, 87.
- [4] McPherson, M. J.; Ogel, Z. B.; Stevens, C.; Yadav, K. D.; Keen, J. N.; Knowles, P. F. *J. Biol. Chem.* **1992**, *267*, 8146.
- [5] McPherson, M. J.; Stevens, C.; Baron, A. J.; Ogel, Z. B.; Seneviratne, K.; Wilmot, C.; Ito, N.; Brocklebank, I.; Phillips, S. E.; Knowles, P. F. *Biochem. Soc. Trans.* **1993**, *21* ( Pt 3), 752.
- [6] Turner, N. J. *Chem. Rev.* **2011**, *111*, 4073.
- [7] Siebum, A.; van Wijk, A.; Schoevaart, R.; Kieboom, T. *J. Mol. Cat. B Enz.* **2006**, *41*, 141.
- [8] Mendonca, M. H.; Zancan, G. T. *Arch. Biochem. Biophys.* **1987**, *252*, 507.
- [9] Rogers, M. S.; Baron, A. J.; McPherson, M. J.; Knowles, P. F.; Dooley, D. M. *J. Am. Chem. Soc.* **2000**, *122*, 990.
- [10] Firbank, S. J.; Rogers, M. S.; Wilmot, C. M.; Dooley, D. M.; Halcrow, M. A.; Knowles, P. F.; McPherson, M. J.; Phillips, S. E. V. *Proc. Natl. Acad. Sci. U. S. A.* **2001**, *98*, 12932.
- [11] Firbank, S.; Rogers, M.; Guerrero, R. H.; Dooley, D. M.; Halcrow, M. A.; Phillips, S. E.; Knowles, P. F.; McPherson, M. J. *Biochem. Soc. Symp.* **2004**, *15*.
- [12] Rogers, M. S.; Hurtado-Guerrero, R.; Firbank, S. J.; Halcrow, M. A.; Dooley, D. M.; Phillips, S. E.; Knowles, P. F.; McPherson, M. J. *Biochemistry* **2008**, *47*, 10428.
- [13] Wilkinson, D.; Akumanyi, N.; Hurtado-Guerrero, R.; Dawkes, H.; Knowles, P. F.; Phillips, S. E. V.; McPherson, M. J. *Protein Eng. Des. Sel.* **2004**, *17*, 141.
- [14] Rogers, M. S.; Tyler, E. M.; Akyumani, N.; Kurtis, C. R.; Spooner, R. K.; Deacon, S. E.; Tamber, S.; Firbank, S. J.; Mahmoud, K.; Knowles, P. F.; Phillips, S. E. V.; McPherson, M. J.; Dooley, D. M. *Biochemistry* **2007**, *46*, 4606.
- [15] Whittaker, M. M.; Ballou, D. P.; Whittaker, J. W. *Biochemistry* **1998**, *37*, 8426.
- [16] Whittaker, J. W. *Chem. Rev.* **2003**, *103*, 2347.
- [17] Minasian, S. G.; Whittaker, M. M.; Whittaker, J. W. *Biochemistry* **2004**, *43*, 13683.
- [18] Whittaker, J. W. *Arch. Biochem. Biophys.* **2005**, *433*, 227.
- [19] Wachter, R. M.; MontagueSmith, M. P.; Branchaud, B. P. *J. Am. Chem. Soc.* **1997**, *119*, 7743.
- [20] Wright, C.; Sykes, A. G. *J. Inorg. Biochem.* **2001**, *85*, 237.
- [21] Thomas, F. *Eur. J. Inorg. Chem.* **2007**, 2379.
- [22] Humphreys, K. J.; Mirica, L. M.; Wang, Y.; Klinman, J. P. *J. Am. Chem. Soc.* **2009**, *131*, 4657.
- [23] Deacon, S. E.; Mahmoud, K.; Spooner, R. K.; Firbank, S. J.; Knowles, P. F.; Phillips, S. E. V.; McPherson, M. J. *Chembiochem* **2004**, *5*, 972.
- [24] Wachter, R. M.; Branchaud, B. P. *J. Am. Chem. Soc.* **1996**, *118*, 2782.
- [25] Zhao, H. M.; Giver, L.; Shao, Z. X.; Affholter, J. A.; Arnold, F. H. *Nat. Biotechnol.* **1998**, *16*, 258.
- [26] Sun, L. H.; Petrounia, I. P.; Yagasaki, M.; Bandara, G.; Arnold, F. H. *Protein Eng.* **2001**,

- 14, 699.
- [27] Avigad, G.; Amaral, D.; Asensio, C.; Horecker, B. L. *J. Biol. Chem.* **1962**, 237, 2736.
- [28] Sun, L. H.; Bulter, T.; Alcalde, M.; Petrounia, I. P.; Arnold, F. H. *ChemBioChem* **2002**, 3, 781.
- [29] Baron, A. J.; Stevens, C.; Wilmot, C.; Seneviratne, K. D.; Blakeley, V.; Dooley, D. M.; Phillips, S. E. V.; Knowles, P. F.; McPherson, M. J. *J. Biol. Chem.* **1994**, 269, 25095.
- [30] Delagrave, S.; Murphy, D. J.; Pruss, J. L. R.; Maffia, A. M.; Marrs, B. L.; Bylina, E. J.; Coleman, W. J.; Grek, C. L.; Dilworth, M. R.; Yang, M. M.; Youvan, D. C. *Protein Eng.* **2001**, 14, 261.
- [31] Rannes, J. B.; Ioannou, A.; Willies, S. C.; Grogan, G.; Behrens, C.; Flitsch, S. L.; Turner, N. J. *J. Am. Chem. Soc.* **2011**, 133, 8436.
- [32] Reetz, M. T.; Bocola, M.; Carballeira, J. D.; Zha, D. X.; Vogel, A. *Angew. Chem., Int. Ed.* **2005**, 44, 4192.
- [33] Jeon, S. I.; Hong, J. W.; Yoon, H. C. *Biotechnol Lett* **2006**, 28, 1401.
- [34] Carter, J. H.; Deddens, J. A.; Pullman, J. L.; Colligan, B. M.; Whiteley, L. O.; Carter, H. W. *Clin. Cancer Res.* **1997**, 3, 1479.
- [35] Bulter, T.; Schumacher, T.; Namdjou, D. J.; Gutierrez Gallego, R.; Clausen, H.; Elling, L. *ChemBioChem* **2001**, 2, 884.
- [36] Garcia-Urdiales, E.; Alfonso, I.; Gotor, V. *Chem. Rev.* **2005**, 105, 313.
- [37] BCC, I. "Opportunities in chiral technology," 2009, <http://www.bccresearch.com/report/BIO012D.html>, accessed 11-09-2011.
- [38] Gruber, C. C.; Lavandera, I.; Faber, K.; Kroutil, W. *Advanced Synthesis & Catalysis* **2006**, 348, 1789.
- [39] Azerad, R.; Buisson, D. *Curr. Opin. Biotechnol.* **2000**, 11, 565.
- [40] Straathof, A. J. J.; Jongejan, J. A. *Enzyme Microb. Technol.* **1997**, 21, 559.
- [41] Eliel, E. L.; Wilen, S. H. *Stereochemistry of organic compounds*; Wiley: New York, p1142-1148, 1994.
- [42] Mannam, S.; Sekar, G. *Tetrahedron-Asymmetry* **2009**, 20, 497.
- [43] Gamez, P.; Arends, I.; Reedijk, J.; Sheldon, R. A. *Chem. Commun.* **2003**, 2414.
- [44] Pellissier, H. *Tetrahedron* **2011**, 67, 3769.
- [45] Kim, M. J.; Ahn, Y.; Park, J. *Curr. Opin. Biotechnol.* **2002**, 13, 578.
- [46] Lee, J. H.; Han, K.; Kim, M.-J.; Park, J. *Eur. J. Org. Chem.* **2010**, 999.
- [47] Turner, N. J. *Curr. Opin. Chem. Biol.* **2010**, 14, 115.
- [48] Kim, Y.; Park, J.; Kim, M.-J. *Chemcatchem* **2011**, 3, 271.
- [49] Pellissier, H. *Tetrahedron* **2008**, 64, 1563.
- [50] Allen, J. V.; Williams, J. M. J. *Tetrahedron Lett.* **1996**, 37, 1859.
- [51] Dinh, P. M.; Howarth, J. A.; Hudnott, A. R.; Williams, J. M. J.; Harris, W. *Tetrahedron Lett.* **1996**, 37, 7623.
- [52] Engstrom, K.; Vallin, M.; Syren, P. O.; Hult, K.; Backvall, J. E. *Org. Biomol. Chem.* **2011**, 9, 81.
- [53] Haak, R. M.; Berthiol, F.; Jerphagnon, T.; Gayet, A. J. A.; Tarabiono, C.; Postema, C. P.; Ritleng, V.; Pfeffer, M.; Janssen, D. B.; Minnaard, A. J.; Feringa, B. L.; de Vries, J. G. *J. Am. Chem. Soc.* **2008**, 130, 13508.
- [54] Persson, B. A.; Larsson, A. L. E.; Le Ray, M.; Backvall, J. E. *J. Am. Chem. Soc.* **1999**, 121,

- 1645.
- [55] Larsson, A. L. E.; Persson, B. A.; Backvall, J. E. *Angew. Chem., Int. Ed. Engl.* **1997**, *36*, 1211.
- [56] Choi, J. H.; Kim, Y. H.; Nam, S. H.; Shin, S. T.; Kim, M. J.; Park, J. *Angew. Chem., Int. Ed.* **2002**, *41*, 2373.
- [57] Choi, J. H.; Choi, Y. K.; Kim, Y. H.; Park, E. S.; Kim, E. J.; Kim, M. J.; Park, J. W. *J. Org. Chem.* **2004**, *69*, 1972.
- [58] Shakeri, M.; Engstrom, K.; Sandstrom, A. G.; Backvall, J.-E. *Chemcatchem* **2010**, *2*, 534.
- [59] Traff, A.; Lihammar, R.; Backvall, J. E. *J. Org. Chem.* **2011**, *76*, 3917.
- [60] Kim, Y.; Park, J.; Kim, M.-J. *Tetrahedron Lett.* **2010**, *51*, 5581.
- [61] Shvo, Y.; Czarkie, D.; Rahamim, Y.; Chodosh, D. F. *J. Am. Chem. Soc.* **1986**, *108*, 7400.
- [62] Reetz, M. T.; Schimossek, K. *Chimia* **1996**, *50*, 668.
- [63] Paetzold, J.; Backvall, J. E. *J. Am. Chem. Soc.* **2005**, *127*, 17620.
- [64] Hoben, C. E.; Kanupp, L.; Backvall, J.-E. *Tetrahedron Lett.* **2008**, *49*, 977.
- [65] Thalen, L. K.; Zhao, D.; Sortais, J. B.; Paetzold, J.; Hoben, C.; Backvall, J. E. *Chemistry* **2009**, *15*, 3403.
- [66] Gustafson, J. L.; Lim, D.; Miller, S. J. *Science* **2010**, *328*, 1251.
- [67] Pietruszka, J.; Simon, R. C.; Kruska, F.; Braun, M. *Eur. J. Org. Chem.* **2009**, 6217.
- [68] Garcia-Urdiales, E.; Alfonso, I.; Gotor, V. *Chem. Rev.* **2011**, *111*, PR110.
- [69] Zhao, L. S.; Han, B.; Huang, Z. L.; Miller, M.; Huang, H. J.; Malashock, D. S.; Zhu, Z. L.; Milan, A.; Robertson, D. E.; Weiner, D. P.; Burk, M. J. *J. Am. Chem. Soc.* **2004**, *126*, 11156.
- [70] Koehler, V.; Bailey, K. R.; Znabet, A.; Raftery, J.; Helliwell, M.; Turner, N. J. *Angew. Chem., Int. Ed.* **2010**, *49*, 2182.
- [71] Oikawa, T.; Mukoyama, S.; Soda, K. *Biotechnol. Bioeng.* **2001**, *73*, 80.
- [72] Adair, G. R. A.; Williams, J. M. J. *Chem. Commun.* **2005**, 5578.
- [73] Adair, G. R. A.; Williams, J. M. J. *Chem. Commun.* **2007**, 2608.
- [74] Voss, C. V.; Gruber, C. C.; Kroutil, W. *Angew. Chem., Int. Ed.* **2008**, *47*, 741.
- [75] Voss, C. V.; Gruber, C. C.; Faber, K.; Knaus, T.; Macheroux, P.; Kroutil, W. *J. Am. Chem. Soc.* **2008**, *130*, 13969.
- [76] Mutti, F. G.; Orthaber, A.; Schrittwieser, J. H.; de Vries, J. G.; Pietschnig, R.; Kroutil, W. *Chem Commun (Camb)* **2010**, *46*, 8046.
- [77] Shimada, Y.; Miyake, Y.; Matsuzawa, H.; Nishibayashi, Y. *Chemistry-an Asian Journal* **2007**, *2*, 393.
- [78] Titu, D.; Chadha, A. *Tetrahedron-Asymmetry* **2008**, *19*, 1698.
- [79] Fotheringham, I.; Archer, I.; Carr, R.; Speight, R.; Turner, N. J. *Biochemical Society Transactions* **2006**, *34*, 287.
- [80] Beard, T. M.; Turner, N. J. *Chem. Commun.* **2002**, 246.
- [81] Alexandre, F. R.; Pantaleone, D. P.; Taylor, P. P.; Fotheringham, I. G.; Ager, D. J.; Turner, N. J. *Tetrahedron Lett.* **2002**, *43*, 707.
- [82] Carr, R.; Alexeeva, M.; Enright, A.; Eve, T. S. C.; Dawson, M. J.; Turner, N. J. *Angew. Chem., Int. Ed.* **2003**, *42*, 4807.
- [83] Alexeeva, M.; Enright, A.; Dawson, M. J.; Mahmoudian, M.; Turner, N. J. *Angew. Chem., Int. Ed.* **2002**, *41*, 3177.
- [84] Carr, R.; Alexeeva, M.; Dawson, M. J.; Gotor-Fernandez, V.; Humphrey, C. E.; Turner, N.



- J. ChemBioChem* **2005**, *6*, 637.
- [85] Dunsmore, C. J.; Carr, R.; Fleming, T.; Turner, N. J. *J. Am. Chem. Soc.* **2006**, *128*, 2224.
- [86] Atkin, K. E.; Reiss, R.; Turner, N. J.; Brzozowski, A. M.; Grogan, G. *Acta. Crystallogr. F* **2008**, *64*, 182.
- [87] Atkin, K. E.; Reiss, R.; Koehler, V.; Bailey, K. R.; Hart, S.; Turkenburg, J. P.; Turner, N. J.; Brzozowski, A. M.; Grogan, G. *J. Mol. Biol.* **2008**, *384*, 1218.
- [88] Bailey, K. R.; Ellis, A. J.; Reiss, R.; Snape, T. J.; Turner, N. J. *Chem. Commun.* **2007**, 3640.
- [89] Eve, T. S. C.; Wells, A.; Turner, N. J. *Chem. Commun.* **2007**, 1530.
- [90] Wu, X. F.; Wang, C.; Xiao, J. L. *Platinum Met. Rev.* **2010**, *54*, 3.
- [91] Wu, X. F.; Li, X. H.; Zanotti-Gerosa, A.; Pettman, A.; Liu, J. K.; Mills, A. J.; Xiao, J. L. *Chem.-Eur. J.* **2008**, *14*, 2209.
- [92] Wu, X. F.; Vinci, D.; Ikariya, T.; Xiao, J. L. *Chem. Commun.* **2005**, 4447.
- [93] Hashiguchi, S.; Fujii, A.; Takehara, J.; Ikariya, T.; Noyori, R. *J. Am. Chem. Soc.* **1995**, *117*, 7562.
- [94] Fujii, A.; Hashiguchi, S.; Uematsu, N.; Ikariya, T.; Noyori, R. *J. Am. Chem. Soc.* **1996**, *118*, 2521.
- [95] Wu, X. F.; Liu, J. K.; Li, X. H.; Zanotti-Gerosa, A.; Hancock, F.; Vinci, D.; Ruan, J. W.; Xiao, J. L. *Angew. Chem., Int. Ed.* **2006**, *45*, 6718.
- [96] Wu, X. F.; Li, X. G.; King, F.; Xiao, J. L. *Angew. Chem., Int. Ed.* **2005**, *44*, 3407.
- [97] Li, X. G.; Wu, X. F.; Chen, W. P.; Hancock, F. E.; King, F.; Xiao, J. L. *Org. Lett.* **2004**, *6*, 3321.
- [98] Wu, X. F.; Li, X. G.; Hems, W.; King, F.; Xiao, J. L. *Org. Biomol. Chem.* **2004**, *2*, 1818.
- [99] Wu, X. F.; Xiao, J. L. *Chem. Commun.* **2007**, 2449.
- [100] Wu, X. F.; Liu, J. K.; Di Tommaso, D.; Iggo, J. A.; Catlow, C. R. A.; Bacsá, J.; Xiao, J. L. *Chem. Eur. J.* **2008**, *14*, 7699.
- [101] Haack, K. J.; Hashiguchi, S.; Fujii, A.; Ikariya, T.; Noyori, R. *Angew. Chem., Int. Ed. Engl.* **1997**, *36*, 285.
- [102] Heiden, Z. M.; Rauchfuss, T. B. *J. Am. Chem. Soc.* **2007**, *129*, 14303.
- [103] Li, X.; Blacker, J.; Houson, I.; Wu, X.; Xiao, J. *Synlett* **2006**, 1155.
- [104] Bringmann, G.; Mortimer, A. J. P.; Keller, P. A.; Gresser, M. J.; Garner, J.; Breuning, M. *Angew. Chem.-Int. Edit.* **2005**, *44*, 5384.
- [105] Eliel, E. L., Wilen, S. H. *In Stereochemistry of organic compounds*; Wiley: New York, p1142-1148, 1994.
- [106] Bringmann, G.; Gulder, T.; Gulder, T. A. M.; Breuning, M. *Chem. Rev.* **2011**, *111*, 563.
- [107] Kozłowski, M. C.; Morgan, B. J.; Linton, E. C. *Chem. Soc. Rev.* **2009**, *38*, 3193.
- [108] Bringmann, G.; Menche, D. *Acc. Chem. Res.* **2001**, *34*, 615.
- [109] Hassan, J.; Sevignon, M.; Gozzi, C.; Schulz, E.; Lemaire, M. *Chem. Rev.* **2002**, *102*, 1359.
- [110] Cozzi, P. G.; Emer, E.; Gualandi, A. *Angew. Chem., Int. Ed.* **2011**, *50*, 3847.
- [111] Clayden, J.; Lai, L. W. *Angew. Chem., Int. Ed.* **1999**, *38*, 2556.
- [112] Clayden, J.; Lai, L. W. *Tetrahedron Lett.* **2001**, *42*, 3163.
- [113] Clayden, J.; Lai, L. W.; Helliwell, M. *Tetrahedron* **2004**, *60*, 4399.

- [114] Clayden, J.; Mitjans, D.; Youssef, L. H. *J. Am. Chem. Soc.* **2002**, *124*, 5266.
- [115] Clayden, J.; Worrall, C. P.; Moran, W. J.; Helliwell, M. *Angew. Chem., Int. Ed.* **2008**, *47*, 3234.
- [116] Clayden, J.; Fletcher, S. P.; McDouall, J. J. W.; Rowbottom, S. J. M. *J. Am. Chem. Soc.* **2009**, *131*, 5331.
- [117] Clayden, J.; Senior, J.; Helliwell, M. *Angew. Chem., Int. Ed.* **2009**, *48*, 6270.
- [118] Betson, M. S.; Clayden, J.; Helliwell, M.; Mitjans, D. *Org. Biomol. Chem.* **2005**, *3*, 3898.
- [119] Thaler, T.; Geittner, F.; Knochel, P. *Synlett* **2007**, 2655.
- [120] Penhoat, M.; Levacher, V.; Dupas, G. *J. Org. Chem.* **2003**, *68*, 9517.
- [121] Bringmann, G.; Breuning, M.; Pfeifer, R. M.; Schenk, W. A.; Kamikawa, K.; Uemura, M. *J. Organomet. Chem.* **2002**, *661*, 31.
- [122] Miyano, S.; Tobita, M.; Nawa, M.; Sato, S.; Hashimoto, H. *Chem. Comm.* **1980**, 1233.
- [123] Lipshutz, B. H.; Kayser, F.; Liu, Z. P. *Angew. Chem., Int. Ed. Engl.* **1994**, *33*, 1842.
- [124] Spring, D. R.; Krishnan, S.; Blackwell, H. E.; Schreiber, S. L. *J. Am. Chem. Soc.* **2002**, *124*, 1354.
- [125] Feldman, K. S.; Sahasrabudhe, K. *J. Org. Chem.* **1999**, *64*, 209.
- [126] Nelson, T. D.; Meyers, A. I. *J. Org. Chem.* **1994**, *59*, 7184.
- [127] Cammidge, A. N.; Crepy, K. V. L. *Chem. Commun.* **2000**, 1723.
- [128] Baudoin, O. *Eur. J. Org. Chem.* **2005**, 4223.
- [129] Okuyama, K.; Shingubara, K.; Tsujiyama, S.; Suzuki, K.; Matsumoto, T. *Synlett* **2009**, 941.
- [130] Matsumoto, T.; Konegawa, T.; Nakamura, T.; Suzuki, K. *Synlett* **2002**, 122.
- [131] Taniguchi, T.; Fukuba, T. A.; Nakatsuka, S.; Hayase, S.; Kawatsura, M.; Uno, H.; Itoh, T. *J. Org. Chem.* **2008**, *73*, 3875.
- [132] Hudlicky, T.; Reed, J. W. *Chem. Soc. Rev.* **2009**, *38*, 3117.
- [133] Sridhar, M.; Vadivel, S. K.; Bhalerao, U. T. *Tetrahedron Lett.* **1997**, *38*, 5695.
- [134] Takemoto, M.; Suzuki, Y.; Tanaka, K. *Tetrahedron Lett.* **2002**, *43*, 8499.
- [135] Miyashita, A.; Yasuda, A.; Takaya, H.; Toriumi, K.; Ito, T.; Souchi, T.; Noyori, R. *J. Am. Chem. Soc.* **1980**, *102*, 7932.
- [136] Nicolaou, K. C.; Mitchell, H. J.; Jain, N. F.; Winssinger, N.; Hughes, R.; Bando, T. *Angewandte Chemie-International Edition* **1999**, *38*, 240.
- [137] Bringmann, G.; Gotz, R.; Keller, P. A.; Walter, R.; Boyd, M. R.; Lang, F. R.; Garcia, A.; Walsh, J. J.; Tellitu, I.; Bhaskar, K. V.; Kelly, T. R. *J. Org. Chem.* **1998**, *63*, 1090.
- [138] Alcock, N. W.; Brown, J. M.; Hulmes, D. I. *Tetrahedron-Asymmetry* **1993**, *4*, 743.
- [139] Truppo, M. D.; Escalettes, F.; Turner, N. J. *Angew. Chem., Int. Ed.* **2008**, *47*, 2639.
- [140] Betson, M. S.; Clayden, J.; Worrall, C. R.; Peace, S. *Angew. Chem., Int. Ed.* **2006**, *45*, 5803.
- [141] Truppo, M. D.; Pollard, D.; Devine, P. *Org. Lett.* **2007**, *9*, 335.
- [142] Martin, R. H. *Angew. Chem., Int. Ed. Engl.* **1974**, *13*, 649.
- [143] Urbano, A. *Angew. Chem., Int. Ed.* **2003**, *42*, 3986.
- [144] Amemiya, R.; Yamaguchi, M. *Chem. Rec.* **2008**, *8*, 116.
- [145] Cravatt, B. F.; Prosperogarcia, O.; Siuzdak, G.; Gilula, N. B.; Henriksen, S. J.; Boger,

- D. L.; Lerner, R. A. *Science* **1995**, 268, 1506.
- [146] Wakamatsu, K.; Masaki, T.; Itoh, F.; Kondo, K.; Sudo, K. *Biochem. Biophys. Res. Commun.* **1990**, 168, 423.
- [147] Slotema, W. F.; Sandoval, G.; Guieysse, D.; Straathof, A. J. J.; Marty, A. *Biotechnol. Bioeng.* **2003**, 82, 664.
- [148] Litjens, M. J. J.; Straathof, A. J. J.; Jongejan, J. A.; Heijnen, J. J. *Tetrahedron* **1999**, 55, 12411.
- [149] Wikteliu, D. *Synlett* **2005**, 2113.
- [150] Jaeger, K. E.; Eggert, T. *Curr. Opin. Biotechnol.* **2002**, 13, 390.
- [151] Liese, A.; Villela, M. *Curr. Opin. Biotechnol.* **1999**, 10, 595.
- [152] Straathof, A. J.; Panke, S.; Schmid, A. *Curr. Opin. Biotechnol.* **2002**, 13, 548.
- [153] Schulze, B.; Wubbolts, M. G. *Curr. Opin. Biotechnol.* **1999**, 10, 609.
- [154] Patel, R. N. *Coord. Chem. Rev.* **2008**, 252, 659.
- [155] Gotor-Fernandez, V.; Busto, E.; Gotor, V. *Adv. Synth. Catal.* **2006**, 348, 797.
- [156] Anderson, E. M.; Karin, M.; Kirk, O. *Biocatal. Biotransform.* **1998**, 16, 181.
- [157] Ghanem, A.; Aboul-Enein, H. Y. *Tetrahedron-Asymmetry* **2004**, 15, 3331.
- [158] Bornscheuer, U. T.; Kazlauskas, R. J. *Angew. Chem. Int. Ed.* **2004**, 43, 6032.
- [159] Kazlauskas, R. J. *Curr. Opin. Chem. Biol.* **2005**, 9, 195.
- [160] Uppenberg, J.; Patkar, S.; Bergfors, T.; Jones, T. A. *J. Mol. Biol.* **1994**, 235, 790.
- [161] Uppenberg, J.; Hansen, M. T.; Patkar, S.; Jones, T. A. *Structure* **1994**, 2, 293.
- [162] Jochens, H.; Hesseler, M.; Stiba, K.; Padhi, S. K.; Kazlauskas, R. J.; Bornscheuer, U. T. *ChemBioChem* **2011**, 12, 1508.
- [163] Lutz, S. *Tetrahedron-Asymmetry* **2004**, 15, 2743.
- [164] Qian, Z.; Lutz, S. *J. Am. Chem. Soc.* **2005**, 127, 13466.
- [165] Svedendahl, M.; Hult, K.; Berglund, P. *J. Am. Chem. Soc.* **2005**, 127, 17988.
- [166] Litjens, M. J. J.; Straathof, A. J. J.; Jongejan, J. A.; Heijnen, J. J. *Chemical Communications* **1999**, 1255.
- [167] Prasad, A. K.; Husain, M.; Singh, B. K.; Gupta, R. K.; Manchanda, V. K.; Olsen, C. E.; Parmar, V. S. *Tetrahedron Lett.* **2005**, 46, 4511.
- [168] Tufvesson, P.; Annerling, A.; Hatti-Kaul, R.; Adlercreutz, D. *Biotechnol. Bioeng.* **2007**, 97, 447.
- [169] Levinson, W. E.; Kuo, T. M.; Kurtzman, C. P. *Enzyme and Microbial Technology* **2005**, 37, 126.
- [170] Brady, D.; Jordaan, J. *Biotechnol. Lett.* **2009**, 31, 1639.
- [171] Cao, L. Q. *Curr. Opin. Chem. Biol.* **2005**, 9, 217.
- [172] Sun, J. N.; Jiang, Y. J.; Zhou, L. Y.; Gao, J. *New Biotechnol.* **2010**, 27, 53.